ESTIMATION OF STABILITY AND CONTROL DERIVATIVES FROM FLIGHT DATA OF KIRAN AIRCRAFT USING FEED FORWARD NEURAL NETWORKS

by

Squadron Leader Aslam Shahzad Khan

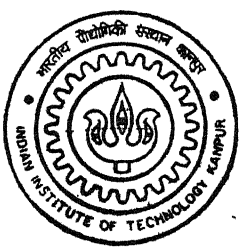

DEPARTMENT OF AEROSPACE ENGINEERING

INDIAN INSTITUTE OF TECHNOLOGY KANPUR

December, 2000

ESTIMATION OF STABILITY AND CONTROL DERIVATIVES FROM FLIGHT DATA OF KIRAN AIRCRAFT USING FEED FORWARD NEURAL NETWORKS

A Thesis Submitted
in Partial Fulfillment of the Requirements
for the Degree of

Master of Technology

by

Squadron Leader Aslam Shahzad Khan

to the

Department of Aerospace Engineering
Indian Institute of Technology, Kanpur

December, 2000

CERTIFICATE

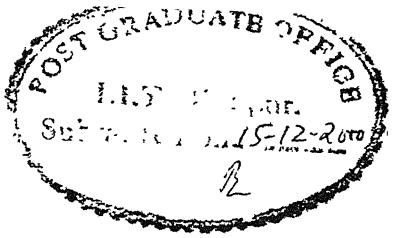

It is certified that the work contained in this thesis entitled, "Estimation of Stability and Control Derivatives from Flight Data of Kiran Aircraft using Feed Forward Neural Networks" by Sqn. Ldr. Aslam Shahzad Khan has been carried out under our supervision and that this work has not been submitted elsewhere for a degree.

(Dr. A. K. Ghosh)
Assistant Professor
Department of Aerospace Engineering
Indian Institute of Technology
Kanpur - 208016

(Gp. Capt. N. S. Athrey)
Co-Supervisor
ASTE, AF
Bangalore-560017

December, 2000

ABSTRACT

Recently, a new method based on Feed Forward Neural Networks (FFNNs), called the 'Delta' method, has been proposed for estimating the aircraft stability and control derivatives (parameters) from flight data. In the past, the Delta method has been validated on simulated data and a few limited set of real flight data only for lateral-directional motion. In the present work, the Delta method has been validated on extensive real flight test data, both for longitudinal and lateral-directional motion. The Delta method has been firstly used to estimate parameters from raw flight data that may contain bias, scale factor and measurement noise errors. Further, the Delta method has also been used to extract parameters from the corrected flight data (that is flight data obtained after applying data compatibility checks to raw flight data). The results of the Delta method show good consistency and low standard deviation. Further, the estimated aerodynamic coefficients and estimated response obtained from the estimates, compare very well with the respective measured quantities. Thus, the Delta method estimates are fairly accurate. The results show that the Delta method can be advantageously applied to estimate parameters from real flight data. The Delta method, unlike conventional methods, neither requires a priori fix of model nor involves integration of equations of motion of the system nor requires initial guess values of the aerodynamic parameters to be given. This is a distinct advantage of the Delta method. Further, the results show that the Delta method is capable of estimating parameters from the raw flight data using the measured values of the motion variables that are not corrected for bias and scale factor errors.

ACKNOWLEDGEMENTS

With a profound sense of gratitude, I express my sincere thanks to my esteemed teachers and thesis supervisors, Dr. A. K. Ghosh and Gp. Capt. N. S. Athrey for their invaluable guidance and encouragement throughout this work. I am indebted to them for providing me with all the required facilities and help in every possible way at IIT Kanpur and ASTE, AF, Bangalore. But for their untiring cooperation, time and patience, this work would not have seen the light of the day.

I take this opportunity to express my special thanks to Dr. S. C. Raisinghani, Professor, Aerospace Engineering Deptt., who was my guide for the initial period of the thesis. He always found the time for teaching me and giving me an unique insight into the area of Flight Mechanics.

I express my thanks to all the Officers and men of ASTE, AF, who helped me in every conceivable way and provided me with a warm hospitality during my stay with them for the thesis work.

I have no words to express my thanks to my parents and brothers, my wife Samira and son Arbaaz, who have been a constant source of moral encouragement and inspiration to me.

I wish to thank all my friends and well wishers who made my stay at IIT Kanpur, memorable and pleasant.

Sqn Ldr Aslam S. Khan

CONTENTS

LIST OF FIGURES

LIST OF TABLES

NOMENCLATURE

a_x , a_y , a_z	= Accelerations along x, y and z body axes, m/s^2
C_L , C_y	= Coefficient of lift force and side force
C_l , C_m , C_n	= Coefficients of rolling, pitching and yawing moment
C_x , C_y , C_z	= Coefficients of longitudinal, lateral and vertical force
C_{Lo}, C_{yo},	= Aerodynamic trim parameters
C_{lo}, C_{mo} , C_{no}	
c	= Mean aerodynamic chord, m
g	= Acceleration due to gravity, m/s^2
z_p	= Altitude, m
I_x, I_y , I_z	= Moments of Inertial about x, y and z axis, kgm^2
I_{xy}, I_{yz} , I_{zx}	= Cross products of inertia, kgm^2
K_β	= Scale factor for angle of sideslip
m	= Aircraft mass, kg
n	= Number of state variables
n_i	= Generalized coordinates
p, q, r	= Roll, pitch and yaw rates, rad/s
$\bar{q}$	= Dynamic Pressure, N/m^2
b	= Wing Span, m
s	= Half wing Span, m
S	= Reference Wing area, m^2
t	= Time, sec
u, v, w	= Velocity components along x, y and z body axes, m/s

W_{ij} = Connection weight

Xa, Ya, Za = Accelerometer offset distances relative to c.g., m

α = Angle of attack, rad

β = Angle of sideslip, rad

δa = Aileron deflection, rad

δr = Rudder deflection, rad

δe = Elevator deflection, rad

λ = Logistic gain factor

μ = Learning rate parameter

Ω = Momentum rate parameter

ρ = Density of air, Kg/m^3

Δt = Time interval, sec

Superscripts

-1 = Inverse

. = Derivative with respect to time

Subscripts

o = Initial conditions

i, j = General indices

m = Measured variables

Abbreviations and Acronyms

AOA = Angle of Attack

AOS = Angle of Sideslip

ASTE = Aircraft and Systems Testing Establishment, Bangalore

ANN = Artificial Neural Network

Act = Actual

Meas = Measured

Estm = Estimated

c g = Center of gravity

Delta-e = Elevator Deflection

Delta-a = Aileron Deflection

Delta-r = Rudder Deflection

FFNN = Feed Forward Neural Network

FLT = Flight Number

IAF = Indian Air Force

IAS = Indicated Airspeed

TAS = True Airspeed

TP = Test Point

ML = Maximum Likelihood

MLE = Maximum Likelihood Estimation algorithm

MSE = Mean Square Error

BPA = Back Propagation Algorithm

Stability and Control Derivatives

Longitudinal Derivatives

$C_{L\alpha} = \partial C_L / \partial \alpha, \quad C_{Lq} = \partial C_L / \partial (qc/2V), \quad C_{L\delta} = \partial C_L / \partial \delta$

$C_{m\alpha} = \partial C_m / \partial \alpha, \quad C_{mq} = \partial C_m / \partial (qc/2V), \quad C_{m\delta} = \partial C_m / \partial \delta$

$C_{m\dot{\alpha}} = \partial C_m / \partial (\dot{\alpha} c/2V)$

Lateral-Directional derivatives

$C_{lp} = \partial C_l / \partial(ps/2V)$, $C_{lr} = \partial C_l / \partial(rs/2V)$, $C_{l\beta} = \partial C_l / \partial\beta$

$C_{l\delta a} = \partial C_l / \partial\delta a$, $C_{l\delta r} = \partial C_l / \partial\delta r$

$C_{np} = \partial C_n / \partial(ps/2V)$, $C_{nr} = \partial C_n / \partial(rs/2V)$, $C_{n\beta} = \partial C_n / \partial\beta$

$C_{n\delta a} = \partial C_n / \partial\delta a$, $C_{n\delta r} = \partial C_n / \partial\delta r$ $C_{n\dot{\beta}} = \partial C_n / \partial(\dot{\beta}s/2V)$

$C_{yp} = \partial C_y / \partial(ps/2V)$, $C_{yr} = \partial C_y / \partial(rs/2V)$, $C_{y\beta} = \partial C_l / \partial\beta$

$C_{y\delta a} = \partial C_y / \partial\delta a$, $C_{y\delta r} = \partial C_y / \partial\delta r$

CHAPTER 1

INTRODUCTION

Airplane parameter estimation is the process of estimating numerical values of the aerodynamic stability and control derivatives from flight test data. Accurate values of these parameters are required in the mathematical model for description of the airplane dynamics. Such models are useful for specification of stability augmentation systems, flight simulators and for verification of theoretically predicted models.

There are three distinct approaches for estimating stability and control derivatives:

- Theoretical Methods
- Wind tunnel testing
- Flight Testing

At the preliminary design stage of an airplane, theoretical method[1,2,3] are useful in spite of their limited accuracy. The wind tunnel test improves the accuracy of estimation but it is a time consuming and expensive way of estimating stability and control derivatives. Precise simulation of control surfaces, power effects and flight conditions is difficult. The model tested in wind tunnel is generally slightly different from the actual airplane due to last minute configuration changes. Other reasons for discrepancies between flight and wind tunnel results are Reynolds number discrepancies and interference due to

support system. It is therefore desirable that the wind tunnel estimates be corroborated with the estimates from the actual flight test data.

The most commonly used methods for parameter estimation from flight data are broadly classified into the following categories.

- Equation error method
- Output error method (the maximum likelihood method being the most popular)

The principle of least squares is used in the equation error method wherein the error gets minimized with respect to the unknown parameter in each of the equations[4]. Its advantages include computation simplicity, non-iterative nature and applicability to both linear and non-linear models. In the output error method, the error between the measured and the model response produced by identical inputs is minimized. The method assumes that there exist no modeling errors. This method processes the measurement noise while assuming the model representation of the given system to be exact. The maximum likelihood (ML) estimator and its several variants have been the most successfully used methods for estimating parameters from flight data[5,6]. However, ML method and its variants need a priori fix of an aerodynamic model. Further, for highly maneuverable aircraft (unstable in open loop), ML method faces difficulties during integration of system equations and leads to diverging solutions[7].

The above mentioned methods require accurate measurement of input output variables. This requirement is difficult to meet in practice due to many types of measurement errors in flight data[8,9].

A few typical measurement errors present in data are: the bias (also called zero shift), scale factor, time shift and measurement noise. For conventional parameter estimation methods, it is, therefore, required that the data compatibility check (sometimes referred to as flight path reconstruction) be performed to get accurate results. Thus, the data compatibility check becomes an integral part of the process of parameter estimation.

The data compatibility is performed using the standard kinematic equations, and applying a ML algorithm[9]. The data compatibility check provides accurate information about the aircraft states, and also estimation of biases, scale factors and time shifts errors in the recorded data. Elimination of such errors from the flight measurements prior to estimation of parameters helps to improve the accuracy of the estimates. However, the process of data compatibility check for estimation of errors can itself be quite sensitive to the methodology employed, and at times, it may be as time consuming as the process of estimating parameters itself[7,8,9].

More recently, investigations have been carried out to explore the potential of Artificial Neural Networks (ANNs) for aircraft aerodynamic modeling and parameter estimation. ANNs are biologically inspired, massively parallel computational paradigms that mimic, to some degree, actual neurological systems. Historically, ANNs were developed out of continued interest in the constructional and functional details of the human brain, and the research there upon to understand its neurological capabilities such as its ability to learn, to retain and to recall information on demand. The ANNs have

been successfully used for modeling in various fields such as signal processing, pattern recognition, system identification and control, and so on.

A class of artificial neural networks called the 'feed forward neural networks' (FFNNs) are most widely used among all types of ANNs for aircraft modeling. As plenty of literature is available on FFNNs, here we present only a brief outline about them. The FFNNs have neurons arranged in layers like directed graphs, and these are static in nature. FFNNs lead to a black box model in which no physical significance can be assigned to either the network structure or to the network weights. FFNNs work as general function approximators, and are capable of approximating any continuous function to any desired accuracy by an appropriate network architecture[10]. A brief write up on the various aspects of FFNNs is presented in Appendix 'A'.

The ability of FFNNs has been utilized to model aircraft aerodynamics successfully[11,12,13,14]. Very recently, Raisinghani et al[15,16] have used FFNNs for modeling aircraft aerodynamics wherein the measured responses and control inputs are mapped to the aerodynamic coefficients; such a neural model is subsequently used to estimate aircraft parameters by the Delta method[15,17,18,19]. It is also mentioned that the FFNN modeling does not require any a priori postulation of the mathematical model for the aircraft aerodynamics. Applicability of the Delta method for estimation of lateral-directional parameters from simulated as well as limited real flight data has been demonstrated, respectively, by Ghosh et al[17,18] and Raisinghani et al[15,16]. Further, in Ref. 20, it was shown that the Delta method can be applied advantageously for extracting aircraft parameters from flight data containing unknown bias, scale factor and

measurement noise errors. The distinct advantage of using the Delta method as reported in the above reference, can be summarized as follows.

(a). The Delta method can be regarded as a non-parametric modeling method; both the structure and parameters need not be known a priori.

(b). The Delta method can be applied directly for extracting aerodynamic parameters from flight data containing unknown bias, scale factor and measurement noise errors.

(c) For the Delta method, there is no need to estimate the initial conditions of flight variables.

Raisinghani et al[15,16] have demonstrated the above advantages of the Delta method by applying it to a limited sets of real flight data (only for lateral-directional motion) which were obtained from abroad. The next obvious step was to further strengthen the efficacy and accuracy of these methods by validation on actual flight data for longitudinal motion. The Delta method was also required to be re-validated on sufficient sets of real flight data generated for lateral-directional motion by giving specific test inputs.

Thus the motivation for the present work was to carry out a well planned, comprehensive and exhaustive flight trial exercise to gather sufficient real flight test data for validating the Delta method with respect to the advantages mentioned in paragraphs (a), (b) and (c) above. Towards this end, a joint project was undertaken by IIT Kanpur and Aircraft and Systems on Testing Establishment (ASTE), Indian Airforce (IAF), Bangalore, such that the flight trials would be undertaken at ASTE and subsequent

analysis would take place at IIT Kanpur. Accordingly, Kiran MK IA aircraft, available with ASTE was chosen as the test aircraft.

It must be noted that such an exercise was undertaken for the first time in the country, wherein, we have designed our own experiments to gather exhaustive real flight test data for parameter estimation using the Delta method.

The accuracy and reliability of parameter estimates obtained via any of the estimation methods, depends heavily on the amount of information available in the flight data. In the seventies, Mehra, Gupta, et al[21,22,23] have significantly contributed to the optimal input design. Although sporadic developments on optimal input design have been reported since then, the 3-2-1-1 input (explained in subsequent chapter) remains to date as the one most accepted worldwide and utilized by the international flight test community.

Accordingly, the majority of the flight test data on the Kiran aircraft was generated using the 3-2-1-1 control input. Apart from this, other forms of inputs, such as doublet and pulse inputs, were also given to enable a study of effect of input form on parameter estimates. The flight data thus generated will necessarily have measurement errors like bias and scale factors etc. These sets of data are referred to as raw flight data for future reference. The next step was to correct the flight data by incorporating the appropriate values of bias and scale factors obtained though data compatibility check and these will be referred to as 'corrected data' in the thesis.

In the present work, the Delta method is used for extracting parameters from real flight data corresponding to longitudinal and lateral-directional dynamics. The Delta method is used for extracting parameters from raw as well as corrected flight data. The

results show that the Delta method can be advantageously applied to estimate parameters from real flight data. This method neither requires a priori fix of model nor involves integration of equations of motion of the system. Further, the results show that the Delta method is capable of estimating parameters from the raw flight data using the measured values of the motion variables that are not corrected for the bias and/or the scale factor errors.

The work carried out in this thesis is presented in four chapters. In Chapter 1, a brief introduction is given on the subject of aircraft parameter estimation. Additionally, the motivation for the present work is also discussed. Chapter 2 deals with the maneuvers used for generation of simulated and real flight data. Further, the details of the data compatibility checks and the Delta method of FFNN are outlined. Chapter 3 consists of the descriptive study of the results obtained. Finally, Chapter 4 gives the conclusions drawn from the present work and also the recommendations for future work.

CHAPTER 2

GENERATION OF FLIGHT DATA AND DATA COMPATIBILITY CHECK

2.1 GENERAL

This chapter describes the various types of simulated and real flight data generated for use in aerodynamic modeling and parameter estimation via the Delta method using FFNN. The procedure used for generating the simulated data is first explained in brief. Next, the work undertaken to generate real flight data in coordination with Indian Air Force (IAF) is described. The preprocessing procedure used for the real flight data is also discussed.

The symmetry about the X-Z plane of the aircraft and small angle approximations allow separation of the equations of motion into two largely independent sets describing the longitudinal and the lateral-directional motion of aircraft. The unknown parameters also separate into longitudinal and lateral-directional sets. We have assumed the separation of longitudinal and the lateral-directional dynamics in the present work. Accordingly, simulated data generation, aerodynamic modeling and parameter estimation are carried out separately for the longitudinal and the lateral-directional motions. For generating the simulated flight data, the equations of motion pertaining to longitudinal and lateral-directional dynamics were solved using fourth order Runga-Kutta method. At this stage, it must be emphasized that we need neither the equations of motion nor their solutions for the FFNN modeling and subsequent parameter estimation via the Delta

method . The procedure used for generation of simulated data is now discussed in the next paragraph.

2.2 SIMULATED FLIGHT DATA -LONGITUDINAL MOTION

As a first step, to check the proper working of all the FFNN programs written in MATLAB, it was decided to use simulated flight data initially. This would also increase the confidence level before working on real flight data. It would also provide a basis for comparison of the results as well as the effect of various variables when dealing with real flight data. The simulated flight data was obtained by solving following equations of motion corresponding to short period mode (u = constant)[24].

$$\dot{\alpha} - q = -[\rho uS/2m]C_L \tag{2.1}$$

$$\dot{q} = [\rho u^2 Sc/2I_y]C_m \tag{2.2}$$

where,

$$C_L = C_{Lo} + C_{L\alpha}\alpha + C_{Lq}\frac{qc}{2u} + C_{L\delta e}\delta e$$

$$C_m = C_{mo} + C_{m\alpha}\alpha + C_{mq}\frac{qc}{2u} + C_{m\delta e}\delta e$$

For generation of simulated flight data, the Kiran MK IA aircraft was chosen as the example aircraft. The flight conditions, mass, moment of inertia and geometric characteristics as given in Table 2.1 below were fed into the above equations along with the aerodynamic parameters.

Table 2.1 Flight Conditions, Mass, Moment of Inertia and Geometric Characteristics of Kiran Aircraft

True Air Speed	V =	103.2157 m/sec
Mass	m =	3442.5 Kg
Density	ρ =	0.7 Kg/m^3
Wing Area	S =	19 m^2
Mean Aerodynamic chord	c =	1.891 m
Wing span	b =	10.7 m
Half wing span	s=b/2 =	5.35 m
Moment of Inertia	Ix =	4332.084 Kg-m^2
	Iy =	15132.802 Kg-m^2
	Iz =	18548.354 Kg-m^2
	Ixy =	20.517 Kg-m^2

The longitudinal aerodynamic parameters were taken from Ref. 25, and are as shown in Table 2.2 below. These values will be henceforth referred to as true values for the longitudinal stability and control derivatives. The values of the parameters C_{Lo} and C_{mo} were not available and hence they were assumed to be zero.

Table 2.2 Aerodynamic characteristic of Kiran MK 1A Aircraft - Longitudinal Motion

Sl. No.	**Parameter**	**Value used (per radian)**
1.	$C_{L\alpha}$	4.9
2.	C_{Lq}	10.0
3.	$C_{L\delta e}$	0.4
4.	$C_{m\alpha}$	-0.60
5.	C_{mq}	-13.0
6.	$C_{m\delta e}$	-0.68

The control input form used to generate the simulated data for longitudinal motion was the flight 3-2-1-1 δe input with an amplitude of 0.1 radian and time period of seven seconds as given in Fig. 2.1 a.

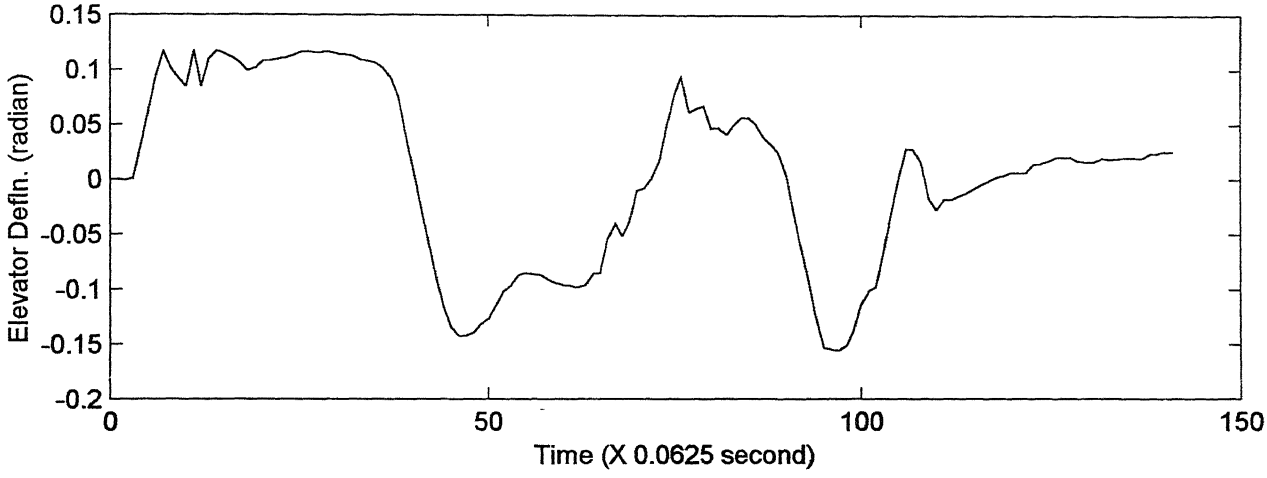

Fig. 2.1a Plot of Flight 3-2-1-1 Elevator Input Used For Generation Of Simulated Data

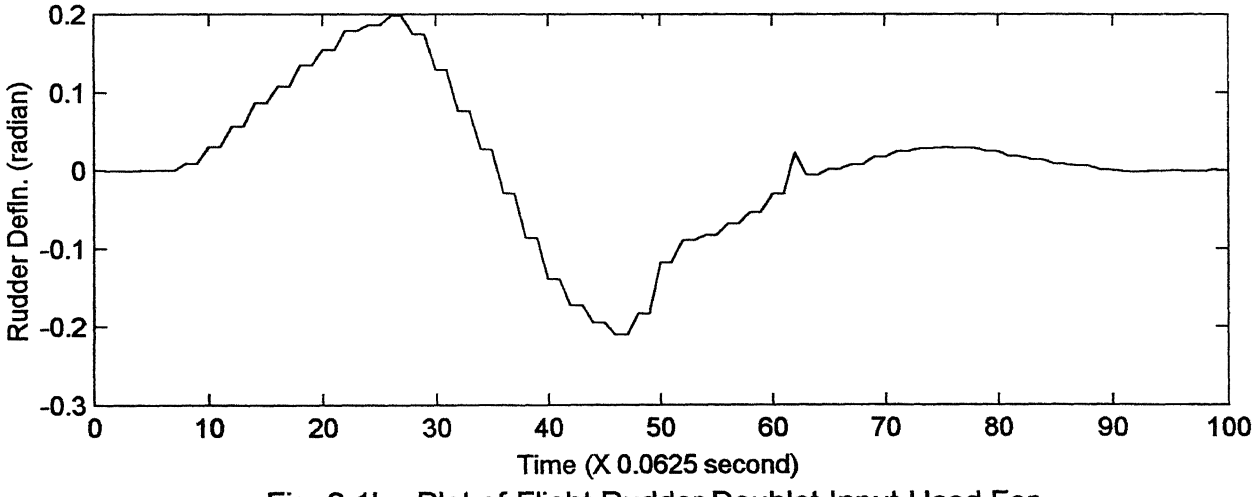

Fig. 2.1b Plot of Flight Rudder Doublet Input Used For Generation Of Simulated Data

2.3 SIMULATED FLIGHT DATA - LATERAL DIRECTIONAL MOTION

The simplified equations of motion used for generating the lateral-directional simulated flight data are as follows[18]:

$$\dot{\beta} = -r + (g/V)\sin\phi + (\bar{q}S/mV)C_y \tag{2.3}$$

$$\dot{p} = \{1/(I_x I_z - I^2_{xz})\}\{\bar{q}Ss(I_z C_l + I_{xz} C_n)\} \tag{2.4}$$

$$\dot{r} = \{1/(I_x I_z - I^2_{xz})\}\{\bar{q}Ss(I_x C_n + I_{xz} C_l)\} \tag{2.5}$$

$$\dot{\phi} = p \tag{2.6}$$

$$\dot{\theta} = -r\sin\phi \tag{2.7}$$

where $\beta = v/V$

$$\bar{q} = (1/2)\rho(u^2 + v^2 + w^2)$$

$$V = (u^2 + v^2 + w^2)^{1/2}$$

$$C_l = C_{lo} + C_{lp}\left(\frac{ps}{V}\right) + C_{lr}\left(\frac{rs}{V}\right) + C_{l\beta}\beta + C_{l\delta a}\delta a + C_{l\delta r}\delta r$$

$$C_n = C_{no} + C_{np}\left(\frac{ps}{V}\right) + C_{nr}\left(\frac{rs}{V}\right) + C_{n\beta}\beta + C_{n\delta a}\delta a + C_{n\delta r}\delta r$$

$$C_y = C_{yo} + C_{yp}\left(\frac{ps}{V}\right) + C_{yr}\left(\frac{rs}{V}\right) + C_{y\beta}\beta + C_{y\delta a}\delta a + C_{y\delta r}\delta r$$

In this case, the Kiran MK 1A was chosen as the example aircraft and hence the same mass/geometric characteristic as given in Table 2.1 were used in the Eq. (2.3) to (2.7). It may be mentioned that lateral-directional aerodynamic parameters of Kiran aircraft were not readily available. Therefore, to generate simulated flight data, tentative values based on analogous comparison with similar sized aircraft were used. These tentative values as shown in Table 2.3 below will be henceforth called as the true values for the lateral-

directional stability and control derivatives. In this case, since the parameters C_{lo} , C_{no} and C_{yo} were unknown, they were assumed to be zero.

Table 2.3 Aerodynamic characteristic of the Kiran aircraft - Lateral-Directional Motion

Sl. No.	Parameter	Value used (per radian)
1.	C_{lp}	-1.203
2.	C_{lr}	0.189
3.	$C_{l\beta}$	-0.144
4.	$C_{l\delta r}$	0.032
5.	C_{np}	-0.210
6.	C_{nr}	-0.805
7.	$C_{n\beta}$	0.193
8.	$C_{n\delta r}$	-0.165
9.	C_{yp}	0.990
10.	C_{yr}	1.594
11.	$C_{y\beta}$	-0.773
12.	$C_{y\delta r}$	0.302

The control input form used for generating the simulated flight data for lateral-directional motion was the flight δr doublet input as presented in Fig. 2.1b. Having described the procedure for the generation of simulated flight data, the next paragraph gives the details of the procedure followed to generate real flight data by performing different types of maneuvers using Kiran aircraft.

2.4 GENERATION OF REAL FLIGHT DATA

Aircraft and Systems Testing Establishment (ASTE) of IAF is a premier flight test agency in the country. It is responsible for undertaking all flight test activities of Indian Armed Forces. This unit located at Bangalore, is also additionally responsible for training of test pilots and flight test engineers. Hence, it was decided to conduct the flight

trials for the present work at ASTE, IAF. The test aircraft chosen for the flight trials was the IAF trainer aircraft called as 'KIRAN MARK IA'. This aircraft is a twin seater low wing aircraft fitted with a single jet engine.

The standard instrumentation scheme presently available with ASTE, IAF was used for flight data acquisition for this work. The list of parameters acquired are as listed in Table 2.4 below. The instrumentation scheme is a digital data acquisition system based on pulse code modulation (PCM) concept. The resolution and accuracy of the instrumentation scheme is as shown in Table 2.4.

Table 2.4 List of Parameters Acquired by the PCM based DAQ Instrumentation System

Sl. No.	Parameter	Symbol	Unit	Resolution	Sampling Rate
1.	Altitude	Zp	millibar	0.256	16
2.	IAS	Vi	millibar	0.097	16
3.	AOA	α	degree	0.034	16
4.	AOS	β	degree	0.034	16
5.	Elevator Position *	δe	degree	0.019	16
6.	Aileron Position *	δa	degree	0.012	16
7.	Rudder Position *	δr	degree	0.015	16
8.	Pitch Rate	q	degree/sec	0.049	16
9.	Yaw Rate	r	degree/sec	0.049	16
10.	Roll Rate	p	degree/sec	0.365	16
11.	Longitudinal Load Factor	n_x	g	0.0005	16
12.	Lateral Load Factor	n_y	g	0.0005	16
13.	Normal Load Factor	n_z	g	0.0023	16

* Control Surface Positions

A total of five sorties were flown each of approximately one hour duration in calm and fine weather conditions. The details of the sorties are as shown in Table 2.5 .

Table 2.5 Details of the Sorties Flown for Generating Real Flight data

Flight No.	Date Flown	Duration	Purpose
FLT 1	06th July 2000	01:05h	Shake down sortie for the instrumentation scheme.
FLT 2	06th July 2000	01:00h	Angle of attack calibration in flight
FLT 3	07th July 2000	01:10h	To excite the longitudinal response of the aircraft
FLT 4	10th July 2000	00:55h	To excite longitudinal response of the aircraft.
FLT 5	13th July 2000	01:10h	To excite lateral-directional response of the aircraft.

The importance of choosing appropriate inputs (control surface deflections) for exciting specific modes of an aircraft or executing specific maneuvers during flight testing for parameter estimation has been well recognized[9]. The accuracy and reliability of parameter estimates depends heavily on the amount of information available in the aircraft response. It is necessary that the correct mode of aircraft response is excited by giving carefully selected inputs.

Based on Ref. 9, the following test inputs were used to generate the aircraft flight data:-

(a) Pulse input of different amplitudes and time period.

(b) Doublet inputs.

(c) 3-2-1-1 inputs.

(d) Roll maneuvers as described in Ref. 9.

Although, it is well known that the 3-2-1-1 input is the most optimal input,[21,22,23] the other input forms were used so as to initiate a study on sensitivity of parameter estimates to different input forms. However, due to paucity of time, this aspect could

not be studied in detail. Hence in the present work the flight data generated using the 3-2-1-1 elevator input for longitudinal motion and doublet rudder/aileron input for lateral directional motion have been used for FFNN modeling and subsequent parameter estimation by the Delta method. The data sets which could not be analyzed in this thesis will be taken up for study in future.

The test altitude was chosen as Z_p =12,000 feet with a tolerance band of ±200 feet for all the maneuvers. The speeds were chosen so as to cover the cruise range of the aircraft, namely 160, 180, 200 and 220 knots, indicated airspeed (KIAS). All the maneuvers were undertaken for undercarriage retracted and no flap deflection configuration.

For the present work, the data sets obtained, pertaining to different maneuvers or the test points executed, are specified by the indicated airspeed (V_i). Because more than one maneuver or test point were done/performed at the same speed, they are designated additionally by the flight number and the sequence number in which the maneuvers were executed. Accordingly, a simple nomenclature system is formulated to refer to the various data sets analyzed. Each set of data is referred to by the flight number, designated as FLT x where x=3, 4 or 5 followed by a slash and then the corresponding test point number (that is, sequence number of the maneuver) written as TPy where y = 1, 2, 3 etc. Thus FLT 4 /TP 2 refers to the data set obtained in flight number 4, test point (or maneuver) number 2.

The real flight data thus generated was then analyzed. The first step in the analysis was to carry out the data compatibility check which is described in the next paragraph.

2.5 DATA COMPATIBILITY CHECK

Real flight data generally have unknown biases, scale factors and time shifts in the recorded data[9,18]. Bias or zero shift errors take place due to drift in the transducer from its zero position after calibration. This will be a constant value error. The scale error takes place due to an interference effect during the measurement process. This causes a constant scale error to be introduced in the output of the transducer. These errors cause data incompatibility. Data incompatibility could arise by way of the measured incidence angles not being in agreement with those reconstructed from the accelerometer and rate gyro measurements. Therefore, it is essential that the data compatibility check be carried out before using the data for aerodynamic modeling and parameter estimation. In other words, the data compatibility check, which is also called as the flight path reconstruction, is an integral part of aircraft parameter estimation. For conventional methods of aircraft parameter estimation, it is well known that data compatibility checks prior to estimation of derivatives helps to improve the accuracy of the estimates[9]. Using the well defined kinematic model, the data compatibility check provides an accurate estimates of the aircraft states, and estimates of biases, scale factors and time shifts in recorded data[9,18].

To estimate the aircraft states, the unknown scale factors and biases of the state variables for the real flight data of Kiran aircraft, a suitable 'Maximum Likelihood Estimation' program was developed (in Matlab 5.3). In applying the MLE technique, the following model was used for the longitudinal motion[9].

$$\dot{u} = (a_x - \Delta a_x) - (q - \Delta q)w - g\sin(\theta) \tag{2.8}$$

$$\dot{w} = (a_z - \Delta a_z) + (q - \Delta q)u + g\cos(\theta) \tag{2.9}$$

$$\dot{\theta} = (q - \Delta q) \tag{2.10}$$

where Δax , Δaz , Δq are the biases in accelerations along X and Z axis and pitch rate about Y axis, respectively.

The observation equations used were[9]

$$V_m = V_n$$

$$\alpha_m = K_\alpha \tan^{-1}(w_n / u_n) + \Delta\alpha$$

where $\Delta\alpha$ is the bias in angle of attack (AOA) and K_α is the scale factor error in AOA. The following additional equations relating true airspeed at cg to true airspeed measured at the nose boom were used.

$$V_n = \sqrt{(u_n)^2 + (w_n)^2}$$

$$u_n = u + (q - \Delta q)Z_n$$

$$w_n = w + (q - \Delta q)X_n$$

where X_n and Z_n are distances along X and Z axes from cg to pressure port. For the MLE program for the longitudinal case, the following set of unknown parameters was considered adequate[9],

$$\theta^T = [\Delta a_X, \Delta a_Z, \Delta q, \Delta\alpha, K_\alpha]$$

The initial conditions used for the aircraft states were the same as obtained from the measured time history. Further, it must be noted that since the three accelerometer locations were offset from cg, suitable corrections were made to the measured accelerations. The accelerations a_x, a_y and a_z at c.g. are obtained from the accelerations a_{xa}, a_{ya} and a_{za} (measured at a point away from the cg) through the following relations.

$$a_x = a_{xa} + (q^2 + r^2)X_a - (pq - \dot{r})Y_a - (pr + \dot{q})Z_a \tag{2.11}$$

$$a_y = a_{ya} - (pq+\dot{r})X_a + (r^2+q^2)Y_a - (rq-\dot{p})Z_a \quad (2.12)$$

$$a_z = a_{za} - (pr-\dot{q})X_a - (qr+\dot{p})Y_a + (p^2+q^2)Z_a \quad (2.13)$$

where X_a , Y_a and Z_a represent the offset distances of the accelerometers from the c.g. location.

The onboard instrumentation scheme used for Kiran aircraft does not provide measurements of $\dot{p}$, $\dot{q}$ and $\dot{r}$. Therefore, the angular accelerations were obtained by numerical differentiation of the measured angular rates. Since the angular rates measurement were of reasonably good quality, it was expected that their differentiation will provide fairly accurate information about respective angular accelerations.

For Lateral and Directional motion, the simplified model used was as follows[9]

$$\dot{u} = -qw + (r - \Delta r)v \quad (2.14)$$

$$\dot{v} = -(r - \Delta r)u + (p - \Delta p)w + (a_y - \Delta a_y) \quad (2.15)$$

$$\dot{w} = -(p - \Delta p)v + qu \quad (2.16)$$

where Δp, Δr, Δa_y are the biases in roll rate, yaw rate and lateral acceleration respectively. The observation equations used were

$$V_{nm} = \sqrt{(u_n)^2 + (v_n)^2 + (w_n)^2}$$

$$\beta_{nm} = K_\beta \mathrm{Sin}^{-1}\left[\frac{v_n}{\sqrt{(u_n)^2 + (v_n)^2 + (w_n)^2}}\right] + \Delta\beta$$

where u_n , v_n and w_n denote the velocity components along the three axes at the nose-boom, $\Delta\beta$ is the bias in angle of sideslip (AOS) and K_β is the scale factor error in AOS.

For the lateral-directional motion, the following set of unknown parameters was considered adequate[9].

$$\theta^T = [\Delta a_y, \Delta p, \Delta r, \Delta \beta, K_\beta]$$

The MLE program was then run to estimate the respective correction factors for the longitudinal and lateral-directional motion. The cost function (refer Appendix 'B') was minimized by minimizing the error between the computed and measured observation variables. For longitudinal motion, the observation variables were true airspeed and angle of attack. For lateral-directional motion, the observation variables were true airspeed and angle of sideslip.

The results of the data compatibility checks are as shown in Table 2.6a, 2.6b and 2.7 for the longitudinal and lateral-directional cases respectively.

Table 2.6a Results of Data Compatibility Checks for FLT3 (Longitudinal Motion)

Sl. No.	Parameters	Units	FLT3/TP2 (V_i=160 KIAS)	FLT3/TP13 (V_i=180KIAS)
1.	Δa_x	m/s^2	-1.0574 (0.0884)*	-1.1398 (0.1853)
2.	Δa_x	m/s^2	-0.9576 (0.2550)	-0.5661 (0.5574)
3.	Δq	rad	0.0499 (0.0022)	0.0429 (0.0032)
4.	$\Delta \alpha$	rad	0.0293 (0.0016)	0.0230 (0.0052)
5.	K_α		0.7390 (0.0056)	0.6582 (0.0195)

* Cramer Rao Bounds

Table 2.6b Results of Data Compatibility Checks for FLT4 (Longitudinal Motion)

Sl. No.	Parameter	Units	FLT4/TP2 (V_i=160KIAS)	FLT4/TP8 (V_i=180KIAS)	FLT4/TP15 (V_i=220KIAS)
1.	Δa_x	m/s^2	-0.7117 (0.1084)*	-0.7732 (0.0882)	-0.8081 (0.0623)
2.	Δa_x	m/s^2	-1.0578 (0.3961)	-1.0327 (0.5422)	3.3966 (0.6192)
3.	Δq	rad	0.0367 (0.0033)	0.0292 (0.0042)	0.0076 (0.0033)
4.	$\Delta\alpha$	rad	0.0116 (0.0029)	0.0636 (0.0040)	0.0294 (0.0045)
5.	K_α		0.8238 (0.0121)	0.7019 (0.0160)	0.7544 (0.0261)

* Cramer Rao Bounds

Table 2.7 Results of Data Compatibility Checks - (Lateral & Directional Motion)

Parameter	Units	FLT5/TP1 (V_i = 160 KIAS)	FLT5/TP9 (V_i = 180 KIAS)	FLT5/TP17 (V_i = 200 KIAS)	FLT5/TP24 (V_i = 220 KIAS)
Δa_y	m/s^2	-0.4332 (1.1874)*	-4.2584 (1.9292)	-3.2500 (1.1761)	-1.6518 (0.4920)
Δp	rad/sec	-1.1445 (0.1006)	-1.2281 (0.0248)	-0.8129 (0.0823)	-0.6776 (0.0560)
Δr	rad/sec	-0.1196 (0.0101)	-0.0274 (0.0177)	-0.0450 (0.0071)	-0.0174 (0.0061)
$\Delta\beta$	rad	-0.0436 (0.0043)	-0.0569 (0.0022)	-0.0688 (0.0060)	-0.0724 (0.0070)
K_β		0.8521 (0.0655)	0.9296 (0.0252)	0.8445 (0.0820)	0.7840 (0.0735)

* Cramer Rao Bounds

Fig. 2.2a shows the match obtained between the measured and computed angle of attack and true airspeed at the end of the data compatibility check for the longitudinal motion. Similarly the match obtained between the measured and computed angle of sideslip and true airspeed for lateral-directional motion are presented in Fig. 2.2b.

These figures show that a good match is obtained between the computed and measured observation variables. This implied that the correction factors have been estimated with reasonable accuracy. From Table 2.6 and 2.7, it is observed that the scale

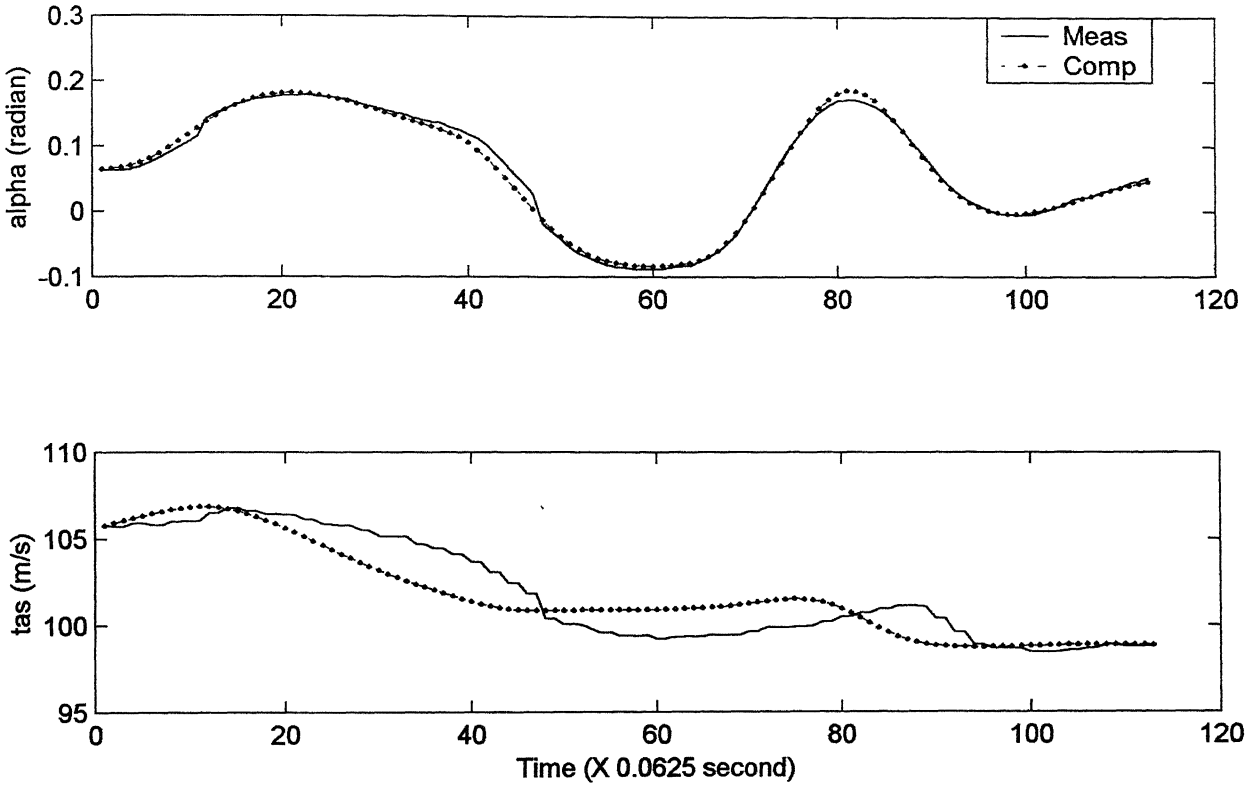

Fig. 2.2a Data Compatibility Check -- Comparision Of Measured And Computed Angle of Attack And True Airspeed

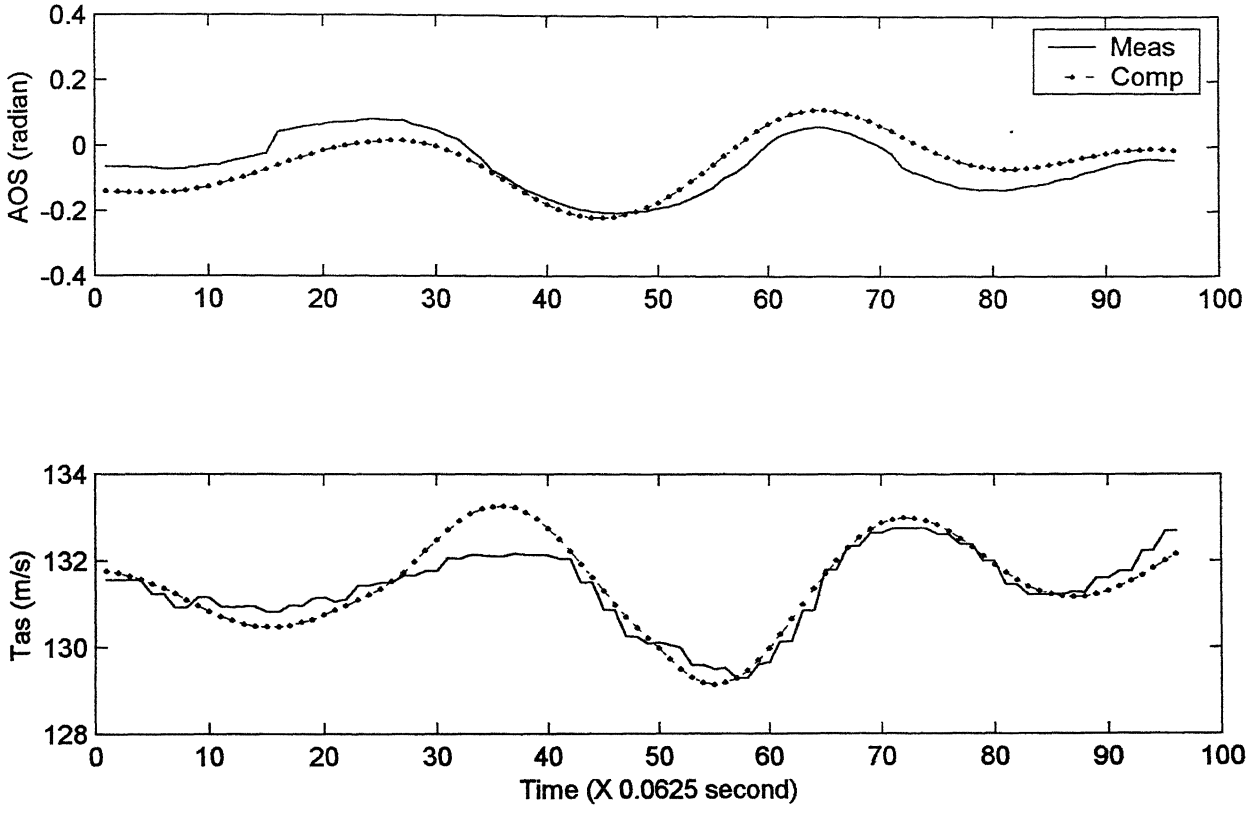

Fig. 2.2b Data Compatibility Check -- Comparision Of Measured And Computed Angle Of Sideslip(AOS) & True Airspeed (Tas)

factor for angle of attack (AOA) is of the order of 0.75 and that for angle of sideslip (AOS) is 0.85. This is also correlated physically by considering the location of AOA/AOS vane. The vane is mounted in a plane just behind the blunt tip of the aircraft nose (the nose tip is blunt in shape because the landing light of the aircraft is fitted in the nose tip). The spindle on which the vane is mounted protrudes approximately 10 cm from the surface of aircraft body. This implied that the vane will be immersed in the near flow field of the aircraft nose. Hence, it is expected that the vane will experience flow interference as well as a certain amount of turbulent flow shed by the blunt nose tip, especially during maneuvers. The angle measured by the vane will be the 'local' angle. Therefore, the values of corrections factor $\Delta\alpha$, $\Delta\beta$, K_α and K_β , seems to be reasonable and acceptable. The correction factors Δq and Δr were observed to be estimated with low values of Cramer Rao bounds and hence were acceptable. However, the values for correction factor Δa_x , Δa_y Δa_z and Δp are on the higher side then would normally be expected. This could have been due to the fact that we have not estimated the initial conditions separately. Therefore, these correction factors were ignored.

Thus, the raw flight data obtained from ASTE, IAF was corrected for the bias errors in angular rates, the scale factor and bias error for AOA and AOS, as well as for the offset of accelerometers from the c.g. of the aircraft. The flight data obtained after applying these corrections is henceforth called as the 'corrected' flight data. Parameter estimation was then carried out on the corrected flight data as well as on the raw data using the Delta method. The details of the Delta method are now explained in the subsequent paragraph.

2.6 DELTA METHOD[19]

The parameters occurring in the equations of motion of an aircraft represent partial derivatives of aerodynamic force and moment coefficients with respect to the corresponding motion or control input variables. The fundamental definition of partial derivatives is that they represent the change in the given function, when one variable is changed by a small amount, while the rest of the variables are held constant. Thus the parameters occurring in the equations of motion can be considered as variation in aerodynamic coefficients due to a small variation in one of the motion or control variable (about its nominal value) while the rest of the variables are held constant at their nominal values. Let us now assume that the FFNN is already trained to map the network input variables to the given output variable. Figure 2.3a and 2.3b show a pictorial representation of the trained FFNN for longitudinal & lateral-directional cases.

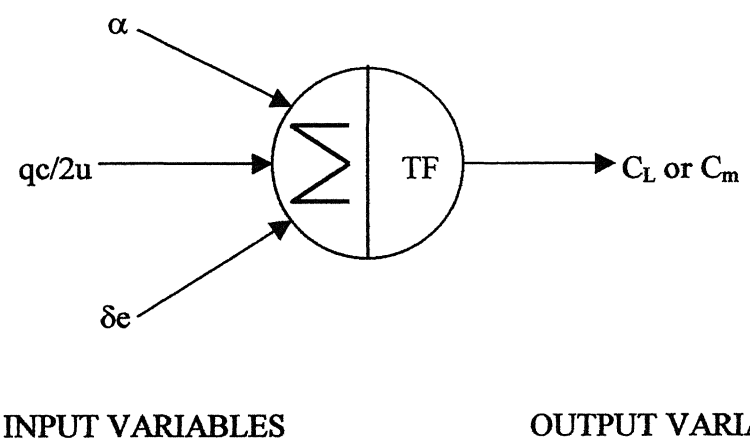

Fig.2.3a Schematic Representation of the Trained FFNN For Longitudinal Motion

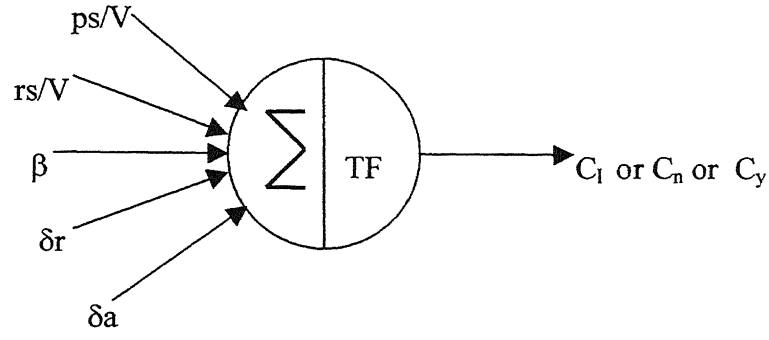

Fig.2.3b Schematic Representation of the Trained FFNN For Lateral–Directional Motion

Now only one of the network inputs is given a small (delta, Δ) perturbation at each time point, while all others are held at their original values. Such a modified input file is then presented to the trained neural network to predict the perturbed value of aerodynamic coefficient at its output node. The difference in the predicted value of the aerodynamic coefficient from the value predicted for the original value of the input is due to the perturbation in the value of that particular network input variable. The difference, so calculated, in the value of the aerodynamic coefficient divided by the perturbation value yields the corresponding aircraft parameter. For example, say, α is perturbed by a small value $\Delta\alpha$ and the difference observed in predicted value of C_m (for longitudinal case) for α and $\alpha+\Delta\alpha$ is ΔC_m. Then $\Delta C_m/\Delta\alpha$ yields the stability derivative $C_{m\alpha}$. Similarly, the perturbation in δe and corresponding ΔC_m observed will yield the control derivative $C_m\delta e$, where $C_m\delta e=\Delta\ C_m/\Delta\delta e$. To avoid bias due one sided differences, motion and control variables are perturbed in both increasing and decreasing direction.

For example, if C_L values for $\alpha+\Delta\alpha$ and $\alpha-\Delta\alpha$ are predicted to be C_L^+ and C_L^- respectively, then

$$C_{L\alpha} = (C_L^+ - C_L^-)/2\Delta\alpha$$

It must be noted that for each of the perturbed value at each time point, there will be a corresponding predicted value of aerodynamic coefficient and hence a different calculated value of the parameter estimate. Ideally speaking, all these values should have been identical so as to yield a single value of the parameter. However, in reality there is variation in the predicted values. The estimated values showed a near normal distribution and hence the mean value is used as the estimate and standard deviation about mean as the measure of accuracy of the estimates.

CHAPTER 3

RESULTS AND DISCUSSIONS

3.1 SIMULATED FLIGHT DATA (LONGITUDINAL MOTION)

The procedure as described in article §2.2 of Chapter 2 was adopted to generate the simulated flight data for longitudinal motion. The set of simulated flight data thus obtained will be referred to as the 'no noise' case, since they contain neither process nor measurement noise. This no noise data set was first used to estimate the longitudinal aerodynamic parameters ($C_{L\alpha}$, C_{Lq}, $C_{L\delta e}$, $C_{m\alpha}$, C_{mq} and $C_{m\delta e}$) by the Delta method.

As required by the Delta method, the network input training file was prepared consisting of α, $\frac{qc}{2u}$ and δe. The network output file consisted of the aerodynamic coefficient C_L or C_m. The FFNN was trained using these input-output file for different architectures of the FFNN. The training function used for training of the FFNN was the "Trainrp" function from the Neural Network Toolbox of Matlab 5.3. The transfer function used for the neurons of the hidden layer of the FFNN was the standard "Log Sigmoidal" function from the Neural Network Toolbox of Matlab 5.3 (refer Eq. (A.1) of Appendix 'A'). The different architectures of the FFNN were obtained by varying the network parameters, such as learning rate, number of neurons in the hidden layer and logistic gain etc[14]. The architecture which gave the minimum 'Mean Square Error (MSE)' was frozen for the prediction phase[14] (refer Eq. (A.2) of Appendix 'A'). The table below

shows the range of values of the network parameters used for training the FFNN to map inputs (α, $\frac{qc}{2u}$, δe) to output (C_L or C_m).

Network Parameter	Range
Logistic gain	0.1 to 0.9
Number of hidden layers	1
Number of iterations	5000
Learning rate	0.1 to 0.9
Number of neurons	4 to 8
Performance criteria	Mean Square Error

The number of iterations were kept fixed at 5000 because it was found that the decrease in MSE beyond 5000 iterations was marginal.

Once the training phase is over, the Delta method was then used to estimate the aerodynamic parameters[15,16,17,18]. The values of the parameters estimated by applying the Delta method on the no noise simulated flight data (longitudinal) is presented in third column of Table 3.1. On comparing these estimates with the true values (used for generating the simulated data) given in column 2 of Table 3.1, it is seen that the estimated values are in good agreement with the true values. Further, the accuracy of the estimates are high as they have very low standard deviations.

A study was also carried out to see the effect of measurement noise on the estimates of longitudinal parameters. Accordingly, simulated pseudo random noise of

varying intensity was added to the motion variables (α, $\frac{qc}{2u}$) and the aerodynamic coefficients (C_L,$C_{m.}$). The noise was simulated by generating successive uncorrelated pseudo random numbers having normal distribution with zero mean and assigned standard deviation, the standard deviation corresponds approximately to designated percentage (in the present work 5%, 10% and 15% were used) of the maximum amplitude of the corresponding variable. The results of the parameter estimation for 5%, 10% and 15% noise cases are presented in columns 4, 5 and 6 of Table 3.1. As seen from the Table 3.1, the Delta method yields good results even in the presence of noise. This implied that the addition of noise had a very marginal effect on the estimated parameters. In fact, except for $C_{L\delta e}$ and C_{mq} , the rest of the parameters have been estimated very well even in presence of 15% noise (which is unusually high level of noise). This only goes to reaffirm the robustness of the Delta method which is able to extract the parameters reasonably well even from noisy data[18]. In real life situations, the flight data will be noisy and the Delta method will be capable of handling it.

In order to check the accuracy of the estimates, the aerodynamic coefficients (C_L,$C_{m.}$) were estimated by feeding the values of the estimates obtained for the 15% noise case into the following equations.

$$C_L = C_{Lo} + C_{L\alpha}\alpha + C_{Lq}\left(\frac{qc}{2u}\right) + C_{L\delta e}\delta e \qquad (3.1)$$

$$C_m = C_{mo} + C_{m\alpha}\alpha + C_{mq}\left(\frac{qc}{2u}\right) + C_{m\delta e}\delta e \qquad (3.2)$$

The values of the parameters C_{Lo} and C_{mo} were taken as zero in the above Eq. (3.1) and (3.2). Fig. 3.1 shows a comparison of the plot of the measured (simulated) and estimated

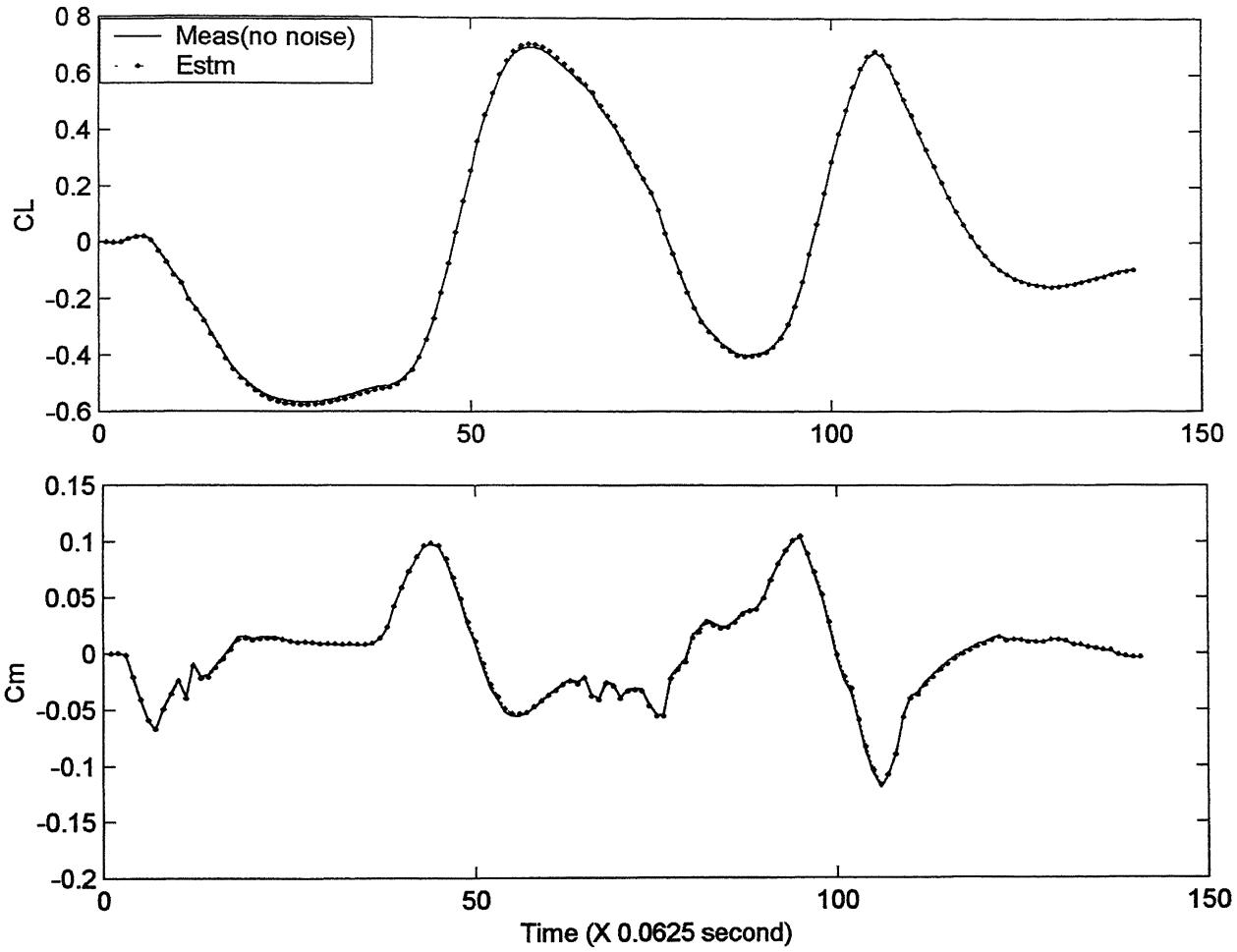

Fig. 3.1 Plot of Measured and Estimated Aerodynamic Coefficients For Simulated Flight Data

aerodynamic coefficients. From the Fig. 3.1, it is seen that the estimated coefficients lie very close to the corresponding measured coefficients. This implied that the estimates obtained from the Delta method are fairly accurate, even when estimated from flight data with unusually high measurement noise (15%).

3.2 REAL FLIGHT DATA (LONGITUDINAL MOTION)

3.2.1 General

The real flight data for the longitudinal motion was generated from two flights, namely, FLT 3 and FLT 4, as discussed in article §2.4 of Chapter 2 (refer Table 2.5). From these two flights a total of eight data sets were obtained at different speeds. These are as follows : three data sets each for V_i = 160 KIAS and V_i = 180 KIAS and two data sets for speed V_i = 220 KIAS. The test input used for all the eight data sets was the 3-2-1-1 δe input. It must be noted that all the eight test inputs were not exactly identical. This is because firstly they were given by different test pilots and secondly four inputs began with positive elevator deflection and four with negative elevator deflection. Using the nomenclature system described in article §2.4 of Chapter 2, these eight real flight data

sets will hereafter be referred to as given below:

Data Set	Nomenclature
1.	FLT3/TP2 (V_i = 160 KIAS)
2.	FLT3/TP13 (V_i = 180 KIAS)
3.	FLT4/TP1 (V_i = 160 KIAS)
4.	FLT4/TP2 (V_i = 160 KIAS)
5.	FLT4/TP7 (V_i = 180 KIAS)
6.	FLT4/TP8 (V_i = 180 KIAS)
7	FLT4/TP14 (V_i = 220 KIAS)
8.	FLT4/TP15 (V_i = 220 KIAS)

It can be seen from the above, that the maneuvers have been repeated for a given speed. This was done to ensure repeatability of data as well as to provide a sufficient database for analysis.

The longitudinal parameters that are estimated in the present work are $C_{L\alpha}$, C_{Lq} , $C_{L\delta e}$, $C_{m\alpha}$, C_{mq} and $C_{m\delta e}$. Of these, it is well known that C_{Lq} and $C_{L\delta e}$ are weak derivatives, in the sense that, even with a large change in C_{Lq} amd $C_{L\delta e}$, there will be little or no appreciable change in C_L. In other words, the aerodynamic coefficient C_L is less sensitive to the longitudinal parameters C_{Lq} and $C_{L\delta e}$. The major contribution to C_L is from $C_{L\alpha}$.

3.2.2 Problem of C_L Obtained From a_z

As was discussed in preceding article §3.1, for training of the FFNN, the first step was to prepare the network input file consisting of α, $\frac{qc}{2u}$ and δe variables. In order to

cater for the thrust effect, instead of α, q and δe, the input variables $\alpha-\alpha^*$, $q-q^*$ and $\delta e-\delta e^*$ have been used, where α^*, q^* and δe^* are the trim values for the given test point. By doing so, the perturbed α, q and δe have been modeled along with the perturbed C_L or C_m.. Accordingly, the output file was prepared with perturbed C_L or C_m. These coefficients were calculated as follows

$$C_L = \frac{2mg}{\rho u^2 S}(a_Z - 1) \tag{3.3}$$

$$C_L = \frac{-2m}{\rho u S}[\dot{\alpha} - q] \tag{3.4}$$

$$C_m = [2\dot{q}I_y]/[\rho u^2 Sc] \tag{3.5}$$

C_L was calculated using a_z as well as $\dot{\alpha}$ from Eq. (3.3) and (3.4) respectively. $\dot{\alpha}$ was obtained by the numerical differentiation of α. Therefore, $\dot{\alpha}$ is bound to contain errors due to numerical differentiation. The values of lift coefficients (C_L) obtained from both the equations were compared and it was found that the C_L calculated from a_z showed very sharp and wild peaks. This was found to be so for all the test points analysed. In order to observe the relationship between C_L and α, the lift coefficient (C_L) obtained for simulated data was plotted against α. For real flight data, both the lift coefficients (C_L from a_z and $\dot{\alpha}$) were plotted against α. These three plots are presented in Fig. 3.2. As seen from the Fig.3.2, the plot of C_L versus α for simulated data revealed that all the points fall neatly into a very narrow and linear band having a positive slope. However, the plot of C_L (from a_z) versus α, for real flight data, showed a large spread of the data points. In contrast, the plot of C_L (from $\dot{\alpha}$) versus α showed that although the points were spread in

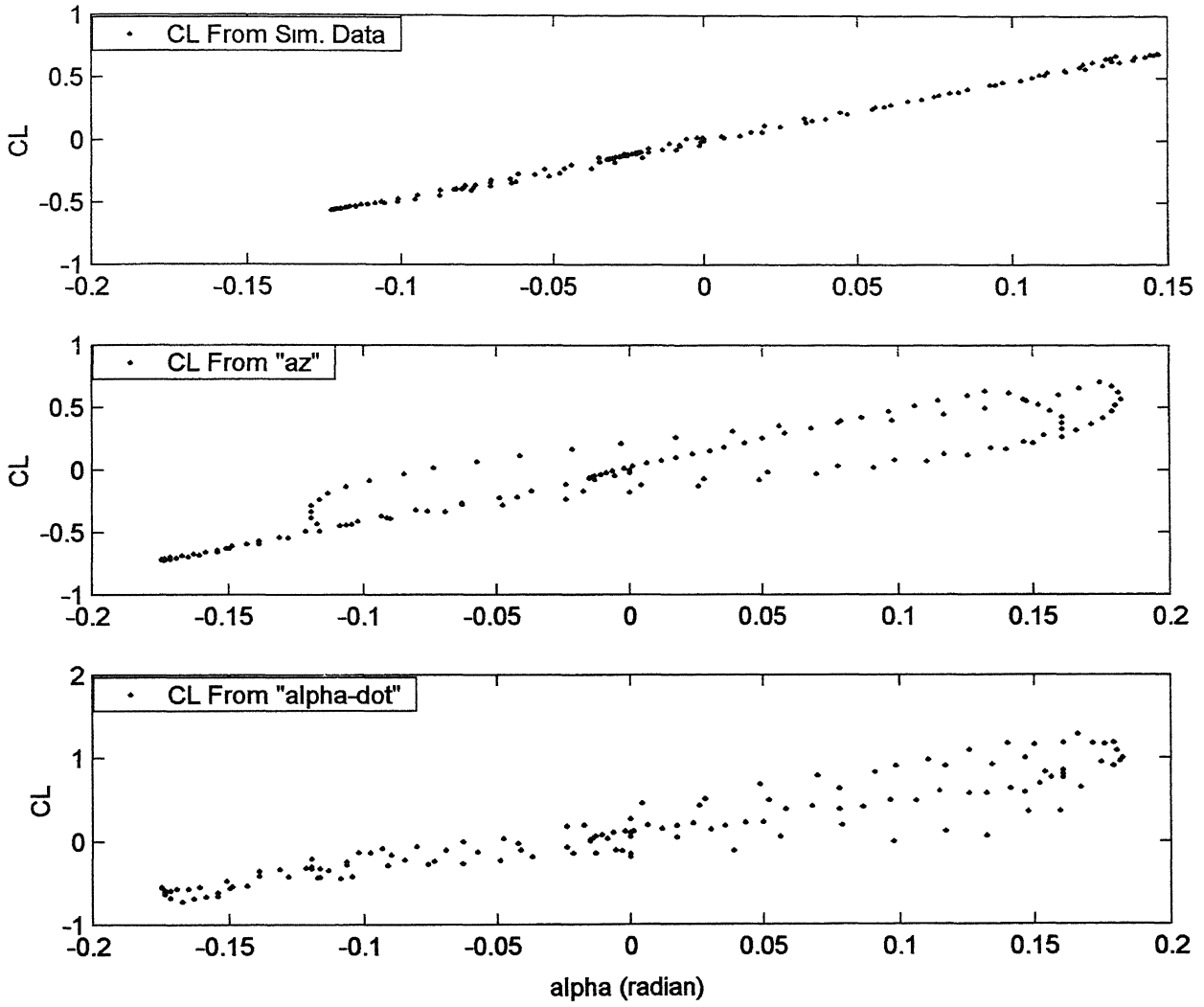

Fig. 3.2 Plot Of CL Versus Alpha

a relatively broad band, yet clearly there was a linear pattern with positive slope, almost similar to that seen for simulated flight data. At this stage, it was conjectured that probably there was some problem in a_z recording. This was subsequently proved to be true after examining the values of the aerodynamic parameters estimated from C_L (calculated from a_z) using the Delta and MLE methods. The values of the estimates were found to be widely varying with very high standard deviations. Hence, it was decided not to use C_L calculated from a_z for estimation process. All the estimates for longitudinal parameters have been obtained using C_L calculated from $\dot{\alpha}$ in the present work.

3.2.3 Procedure Used For Estimating Parameters From Real Flight Data

In the present work for the longitudinal motion, apart from estimation by the Delta method, the parameters were also estimated using MLE algorithm. This was done to provide a basis for comparison for the Delta method estimates with the MLE estimates. The MLE method requires a priori fix of the aerodynamic model. It is well known that the MLE method is sensitive to the initial guess values used. In absence of realistic guess values (based on analytical method or wind tunnel tests), initially arbitrary guess values were used as starting values. However, frequently it was observed that the MLE method with these guess values was not able to estimate large number of parameters to the desired accuracy. In order to run the MLE programs, the estimated values obtained from the Delta method of FFNN were used as the initial guess values for the MLE algorithm. It was observed that MLE estimates now were of desired accuracy in terms of sign and magnitude.

From Ref. 20, it was reported that FFNN are capable of extracting parameters from raw flight data containing bias and scale factor errors. In the present work, the parameters were estimated from raw flight data using the Delta and MLE method.

It is well known that in order to improve the accuracy of the estimates[9], data compatibility checks must be done on the raw flight data. Accordingly, data compatibility checks were applied (refer Chapter 2, article §2.5) to the raw data and 'corrected' flight data was obtained. The parameters were then estimated from the corrected flight data using both the Delta and MLE methods.

A systematic procedure, as given below, was followed to estimate the aerodynamic parameters from real flight data (longitudinal) for both the raw and corrected flight data using the Delta and MLE method.

1. Aerodynamic parameters ($C_{L\alpha}$, C_{Lq} , $C_{L\delta e}$, $C_{m\alpha}$, C_{mq} and $C_{m\delta e}$) are estimated by the Delta method using raw flight data.
2. Using the above estimates as initial guess values, the MLE program is executed to estimate aerodynamic parameters ($C_{L\alpha}$, C_{Lq} , $C_{L\delta e}$, $C_{m\alpha}$, C_{mq} and $C_{m\delta e}$) from raw flight data.
3. Next, the raw data is preprocessed using the correction factors given in Table 2.6 and 2.7 in Chapter 2. In other words, data compatibility checks are done on the raw flight data. This flight data is referred to as 'corrected' flight data.
4. Steps 1 and 2 are repeated for the corrected flight data. This is done to estimate the aerodynamic parameters using corrected data.

The typical time history plots obtained for raw and corrected flight data following the above procedure are presented in Fig. 3.3 and 3.4.

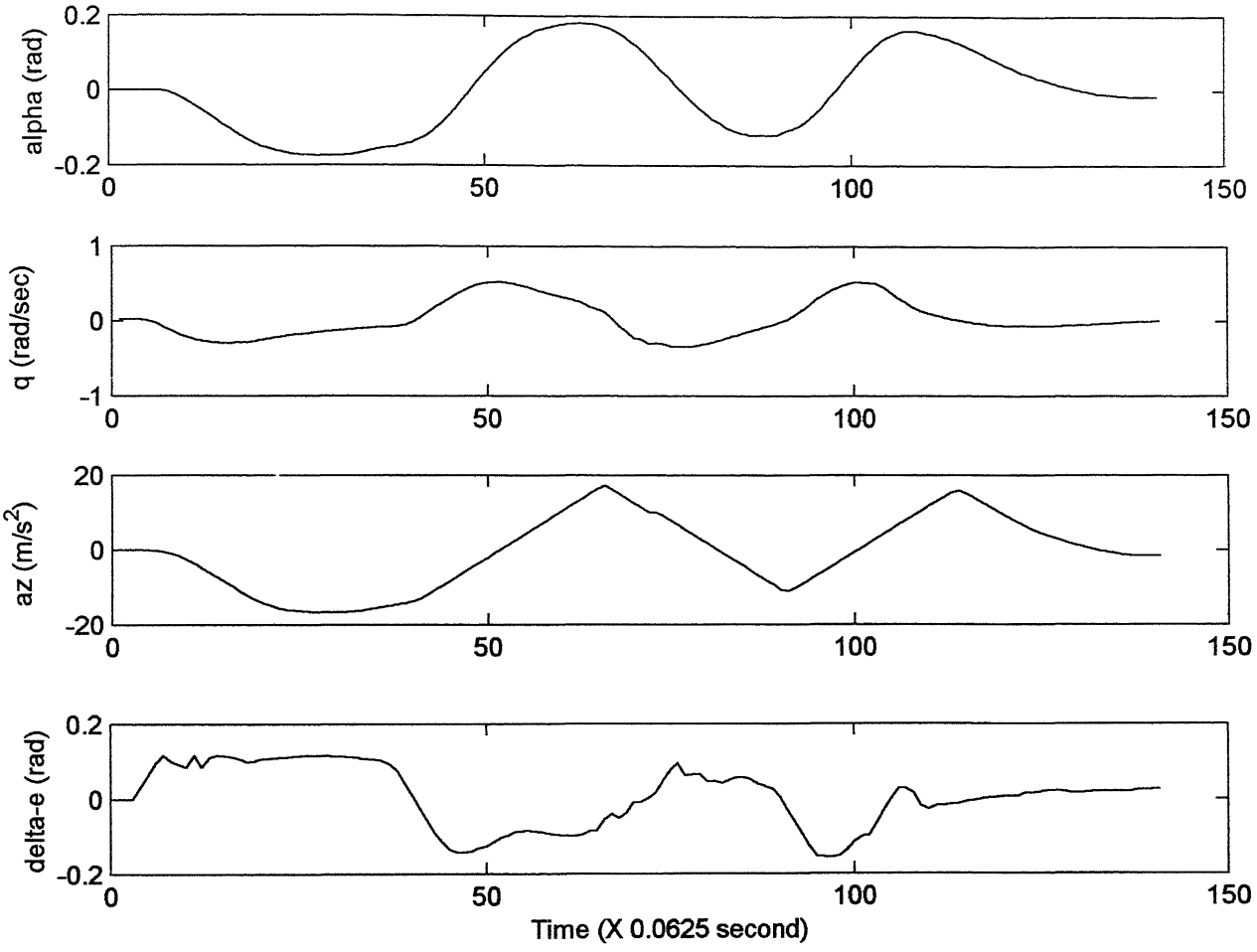

Fig. 3.3 Plots Of Time History For Test Point FLT3/TP2,Vi=160 KIAS For Raw Data

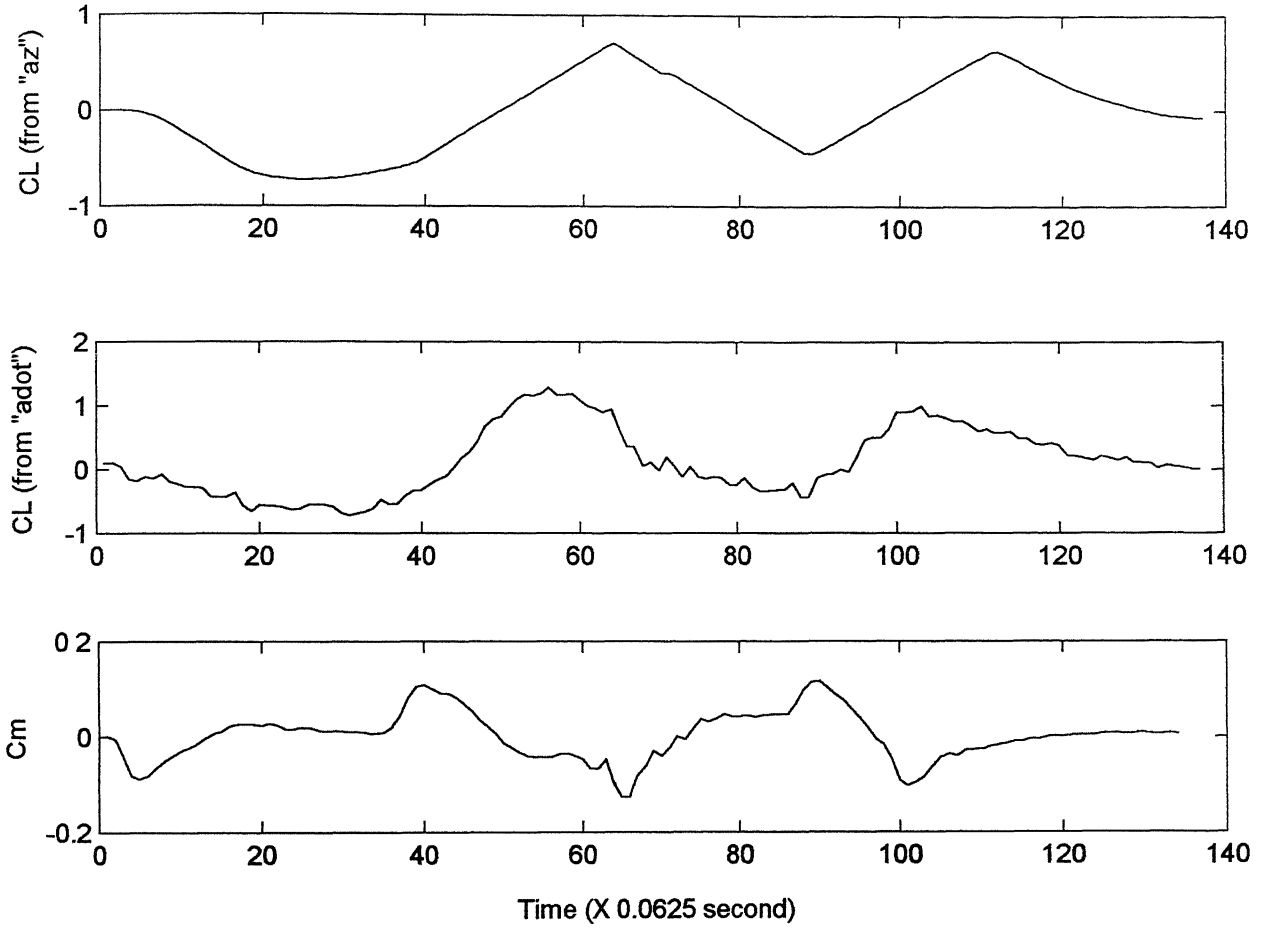

Fig. 3.3 Concluded

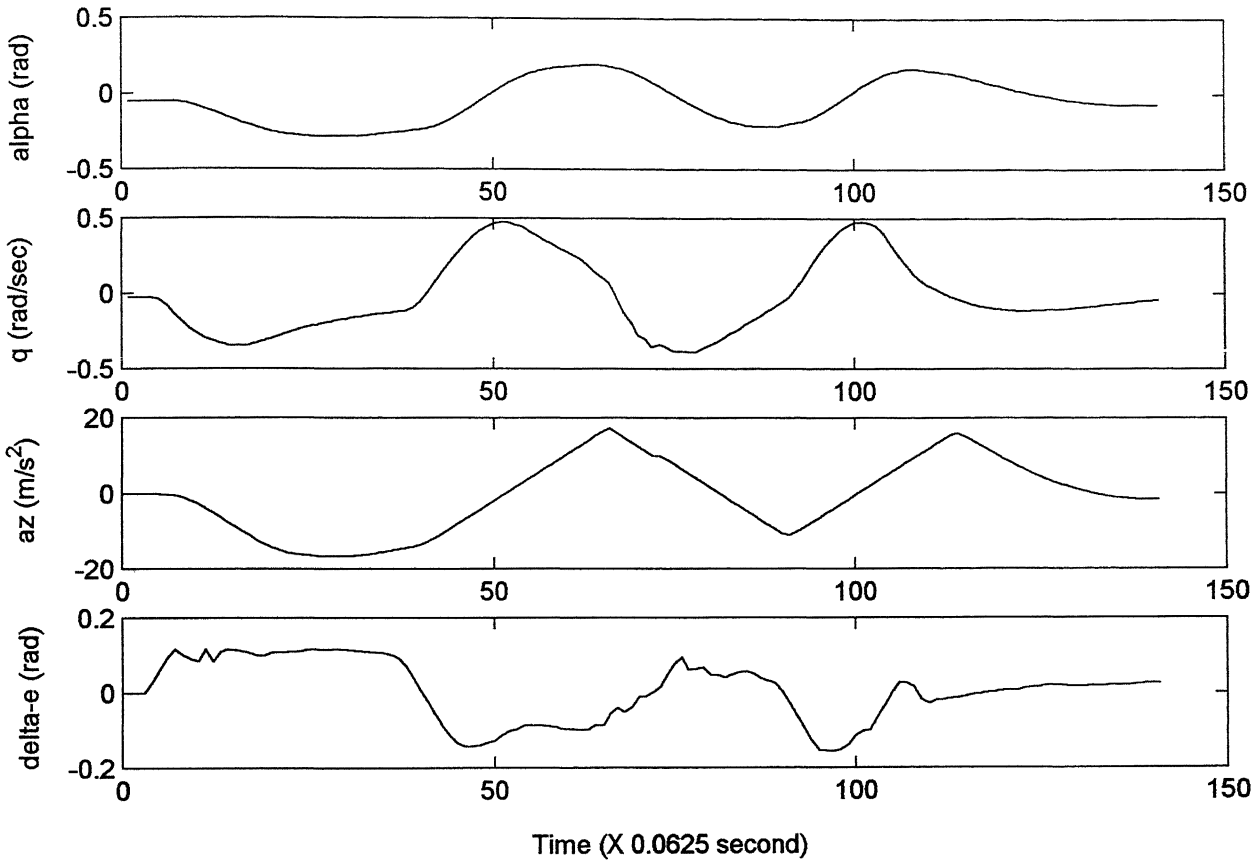

Fig. 3.4 Plots Of Time History For Test Point FLT3/TP2,Vi=160 KIAS For Corrected Data

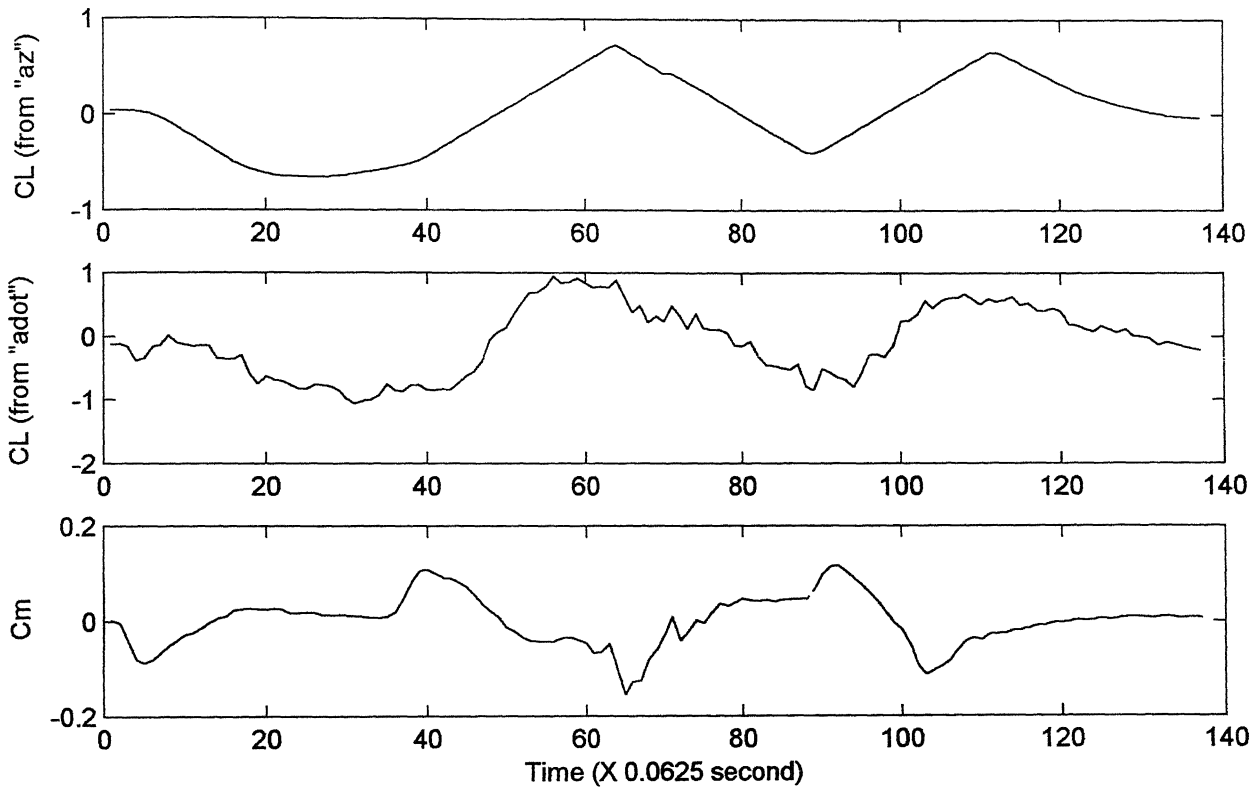

Fig. 3.4 Concluded

3.2.4 Parameter Estimates From Raw Flight Data

As explained above, the first step was to estimate the parameters from raw flight data using the Delta method. Accordingly, the aerodynamic modeling using different architectures of FFNN was carried out with network input training file having variables α-α^*, q-q^* and δe-δe^* and output file having aerodynamic coefficients C_L (obtained from $\dot{\alpha}$) or C_m. The architecture that gave the minimum MSE was frozen for the prediction phase. Fig. 3.5a and 3.5b show the plot of actual and predicted (after training) aerodynamic coefficients (C_L ,C_m.) obtained from the raw data. From the Fig. 3.5a and 3.5b, it is seen that good training of the FFNN has taken place. In other words, the FFNN is able to map the input-output relationship accurately. This trained FFNN represented a reasonably good aerodynamic model for the aircraft under study.

The Delta method was then used to estimate the parameters from raw flight data. The estimates for the longitudinal motion obtained from the Delta method of FFNN for the raw flight data are presented in Table 3.2a and 3.2b for flights FLT3 and FLT4 respectively.

As mentioned in step 2 above, for comparison purpose, the parameters were also estimated by the MLE method from the raw flight data, using the Delta method estimates as initial guess values. The results of the MLE method are presented in Table 3.3a and 3.3b for flights FLT3 and FLT4 respectively.

From a study of results of the Delta method for raw flight data (Table 3.2a and 3.2b), it is observed that all the strong derivatives ($C_{L\alpha}$, $C_{m\alpha}$, C_{mq} and $C_{m\delta e}$) have been estimated with reasonably good accuracy. Further, the estimates from the Delta method (Table 3.2a and 3.2b) for all the test points at different speeds show a fairly consistent

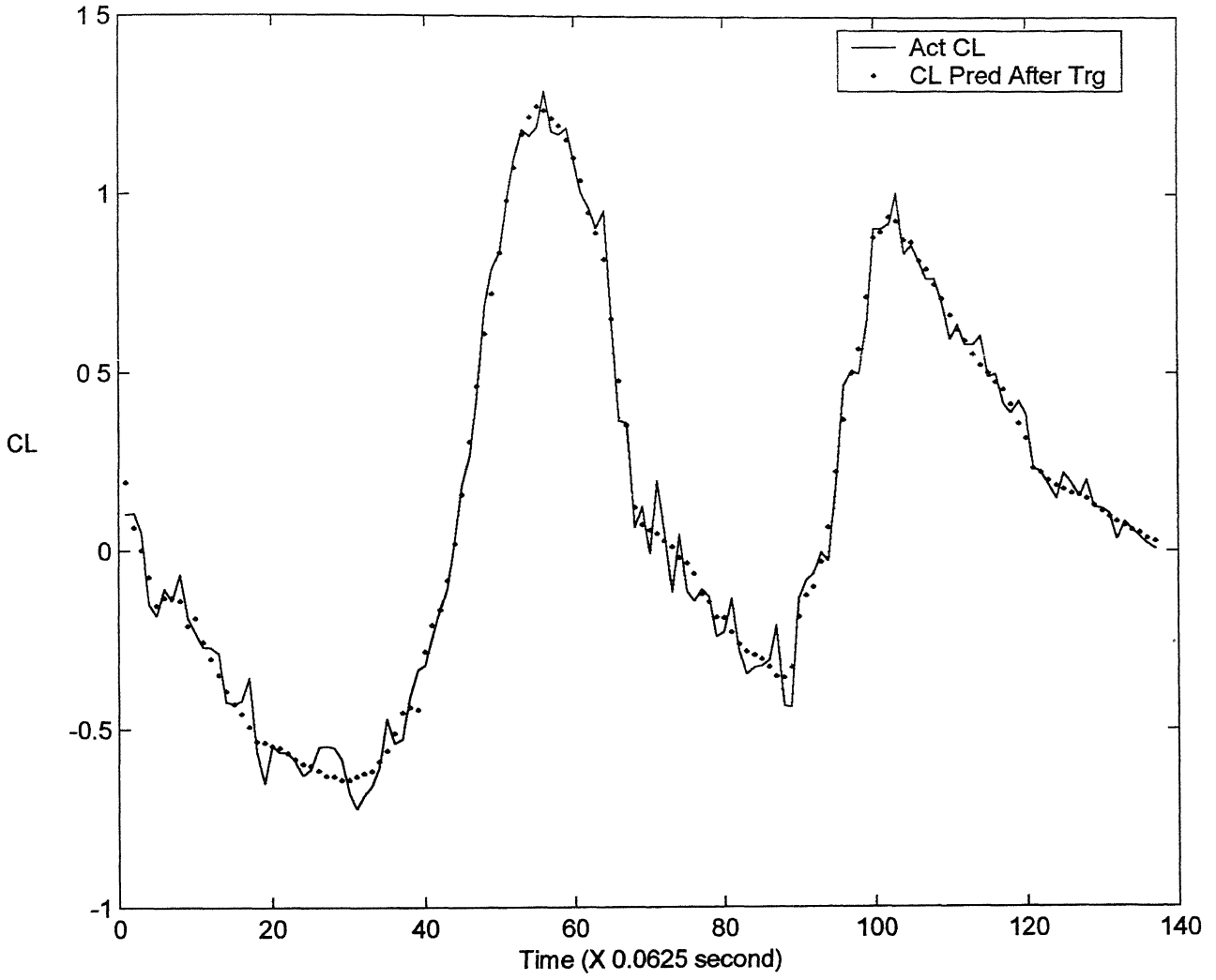

Fig. 3.5a Plot Of Actual And Predicted (After Training) CL For Test Point FLT3/TP2,Vi=160 KIAS For Raw Data

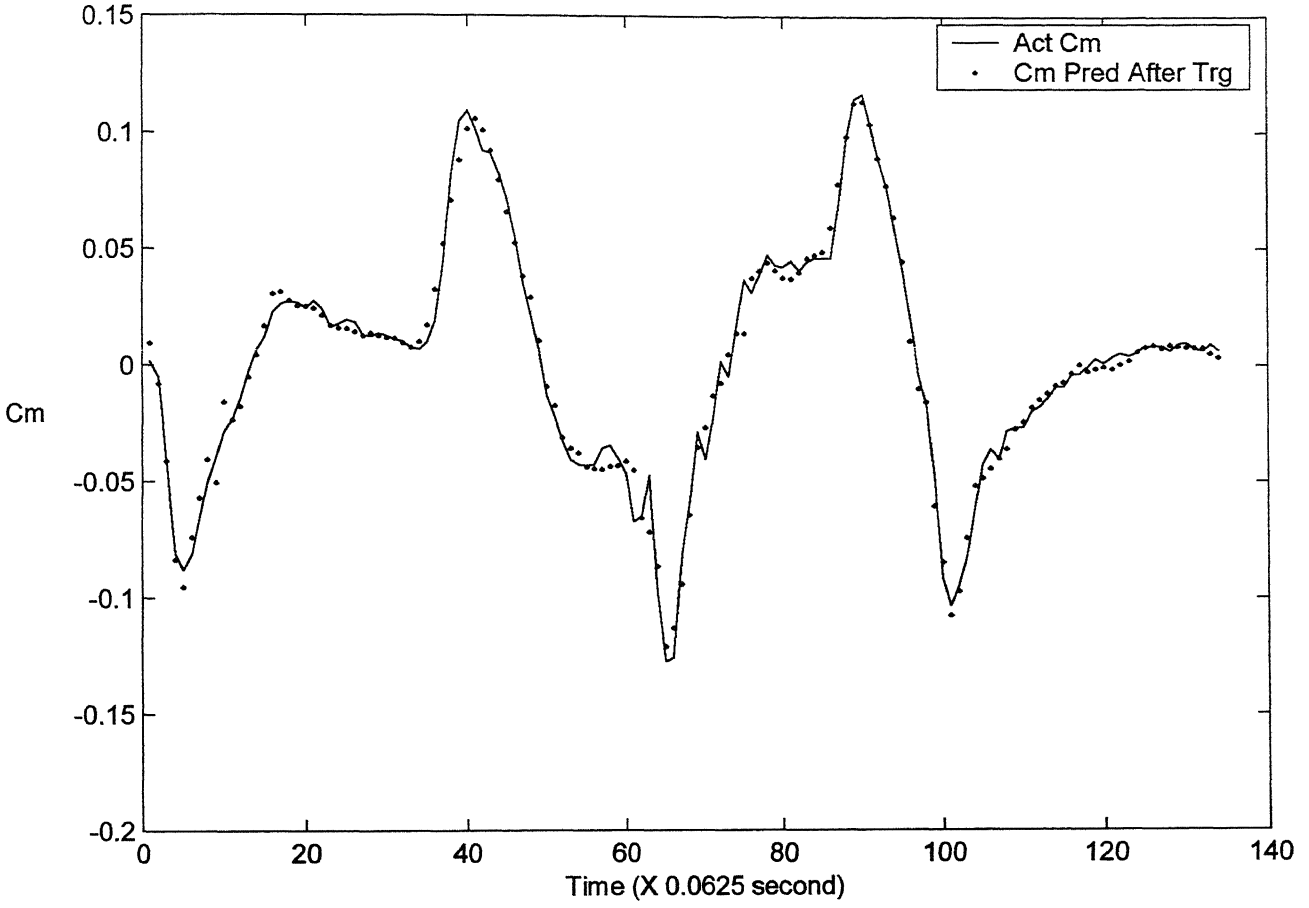

Fig. 3.5b Plot Of Actual And Predicted (After Training) Cm For Test Point FLT3/TP2,Vi=160 KIAS For Raw Data

trend and increase the level of confidence in the results. From the first row of Table 3.2a and 3.2b, it is also seen that the standard deviation obtained for $C_{L\alpha}$ is slightly on the higher side for all the test points, ranging from 0.2674 for FLT4/TP14 to 0.5841 for FLT4/TP1. Although the standard deviation for $C_{L\alpha}$ are consistently on the higher side, it must be remembered that this parameter has been estimated from C_L obtained from $\dot{\alpha}$, with all its inherent errors due to numerical differentiation of α. Seen against this background, it can said that the value of $C_{L\alpha}$ estimated using the Delta method are reasonably good, despite the slightly higher standard deviation. This reaffirms, as reported in Ref. 18, that the Delta method can be advantageously applied to estimate parameters from raw flight data, which may possibly contain scale factors and bias errors. This is a distinct advantage of the FFNNs. In fact, for future application one can quickly set up the FFNN and run it to have a quick look at the values of the parameters, if so be desired. Then subsequently, with little additional fine tuning of the network, reasonably good estimates can be obtained without the requirement of the preprocessing of the flight data.

As seen from the Table 3.3a and 3.3b, the MLE estimates obtained for the strong derivatives are in close agreement with those obtained from the Delta method. It must be stressed that to initiate MLE algorithm, parameters estimated by the Delta method were used as initial guess values for the derivatives. However, as observed from the Tables 3.2 and 3.3, the weak derivatives C_{Lq} and $C_{L\delta e}$ have not been estimated very weil by either the Delta or the MLE method.

After estimating the parameters from the raw data, the next step was to check the accuracy of these estimates. This can be done by finding out the estimated total

aerodynamic coefficients (C_L, C_m) using the parameters estimated above and comparing it with the actual (measured) coefficients (obtained from Eq. (3.4) and (3.5)). The estimated aerodynamic coefficients were calculated by feeding the parameters estimated above into the Eq. (3.1) and (3.2). However as seen from the Eq. (3.1) and (3.2), the parameters C_{Lo} and C_{mo} are not known, as they have not been estimated separately.

In order to compute C_{Lo} and C_{mo} from the raw flight data, the following procedure was adopted[18]. Firstly, using the estimates from the Delta method, the estimated C_L and C_m are calculated from the Eq. (3.1) and (3.2) by ignoring the terms, C_{Lo} and C_{mo} . These estimated total aerodynamic coefficients (C_L, C_m) do not carry any information about parameters C_{Lo} and C_{mo}. However, the actual (measured) total aerodynamic coefficients of the aircraft carries the complete information, including C_{Lo} and C_{mo} (refer Eq. (3.4) and (3.5) given earlier). The above estimated coefficients were subtracted from the respective measured coefficients to obtain the values of C_{Lo} and C_{mo}[18]. However, since there are a number of time steps, the parameters C_{Lo} and C_{mo} have a value for each time step. The mean of this distribution of C_{Lo} and C_{mo} is taken to arrive at a single value. The results obtained for the different test points are shown in Table 3.4 .

Figures 3.6, 3.7 and 3.8 show the comparative plots of the actual and estimated total aerodynamic coefficients (obtained from raw flight data) for three typical test points, after adding the parameters C_{Lo} and C_{mo}. These figures show that a fairly good match is obtained. This implied that the parameters have been estimated reasonabiy well at each test point for different speeds.

In order to further compare the values of the estimates obtained from the Delta and MLE methods from raw data, it was decided to compare the estimated and measured

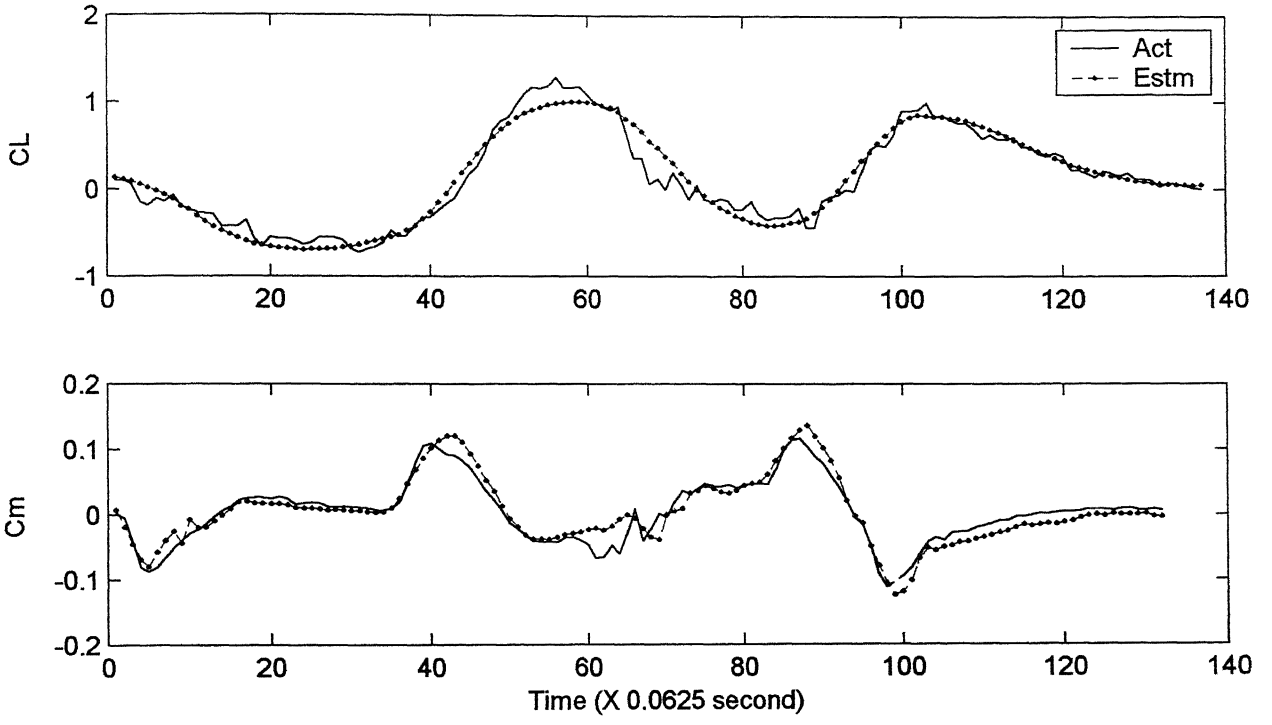

Fig. 3.6 Comparision of Actual And Estimated Total Aerodynamic Coefficients For FLT3/TP2, Vi=160 KIAS For Raw Data

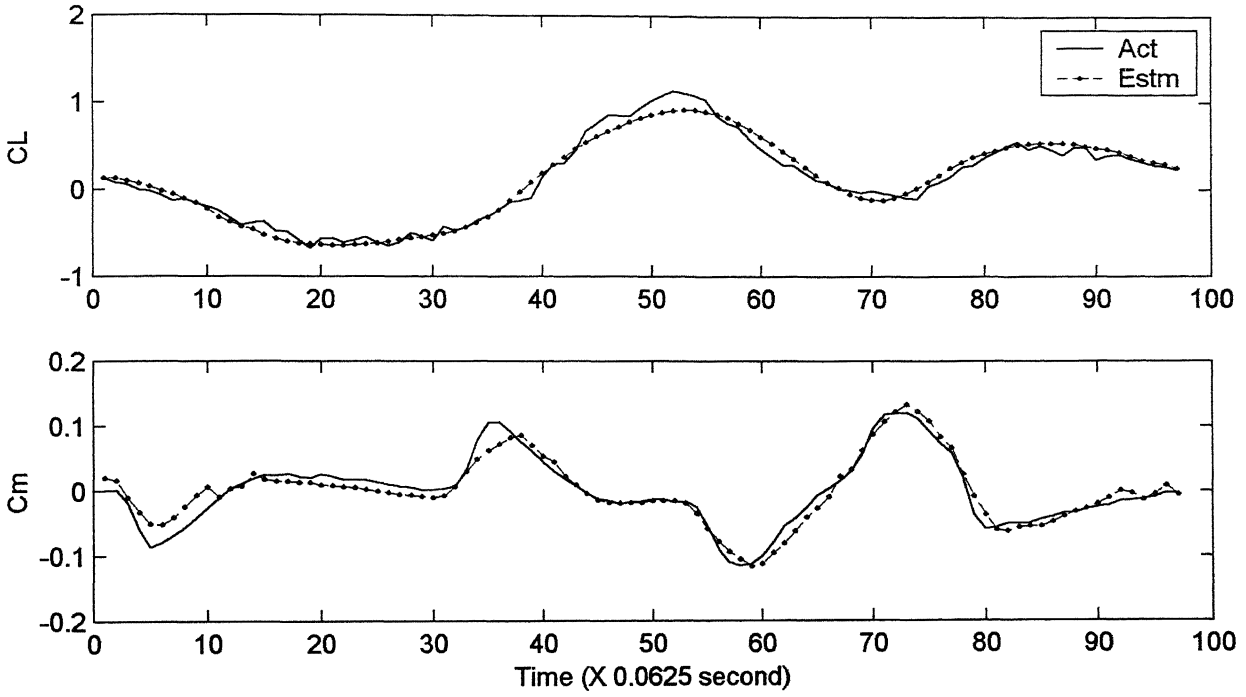

Fig. 3.7 Comparision of Actual And Estimated Total Aerodynamic Coefficients For FLT3/TP13,Vi=180 KIAS For Raw Data

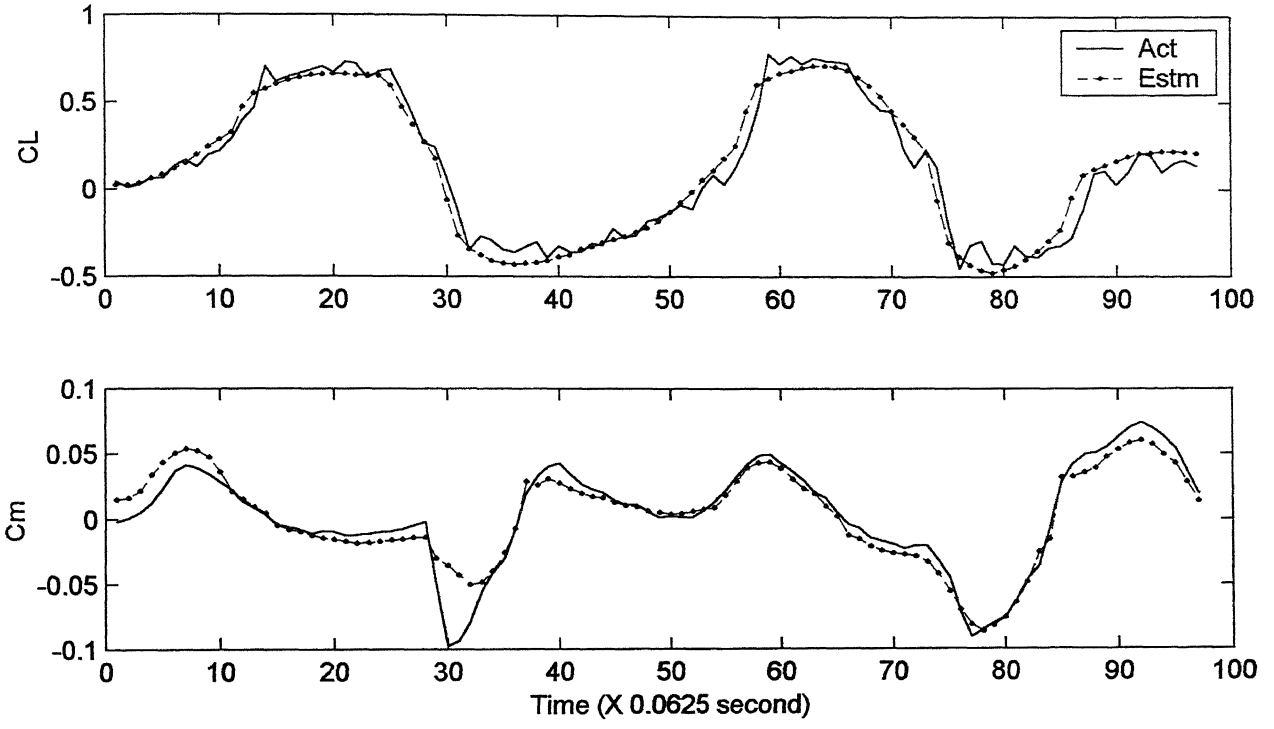

Fig. 3.8 Comparision of Actual And Estimated Total Aerodynamic Coefficients For FLT4/TP14,Vi=220 KIAS For Raw Data

responses. Accordingly, the set of parameters estimated using the Delta and MLE methods (from the raw flight data) were used to solve the longitudinal equations of motion (refer Eq. (2.1) and (2.2) of Chapter 2) . As stated earlier, these equations were solved using the fourth order Runga-Kutta method to get the longitudinal response of the aircraft in terms of α and q for each test point.

The estimated responses were plotted along with the actual response of the aircraft. These plots are presented in Fig. 3.9, 3.10 and 3.11 corresponding to test points FLT3/TP2, FLT3/TP13 and FLT4/TP14 respectively. These plots reveal that a better match is obtained for FLT3/TP2 and FLT3/TP13 when using parameters estimated from the Delta method. This implied that the estimates from the Delta method are fairly accurate and that these values could be used to construct the mathematical model to generate the flight responses of the aircraft. However, in case of test point FLT4/TP14 (V_i=220 KIAS) it is observed (Fig. 3.11) that the estimated response shows a slight time period shift as compared to the actual response. One of the possible reasons could be the incorrect estimate of C_{Lo}, and C_{mo} obtained for this test point (refer column 4 of Table 3.4).

After completion of analysis of the raw flight data, the corrected flight data was taken up for parameter estimation (Step 3 of procedure explained at the beginning of this paragraph). It would be of interest to see how the results improve after applying the data compatibility checks to the raw flight data.

3.2.5 Parameter Estimates From Corrected Flight Data

The same procedure as described earlier for the raw flight data, was utilized here for the corrected flight data in order to obtain the parameter estimates from the Delta and

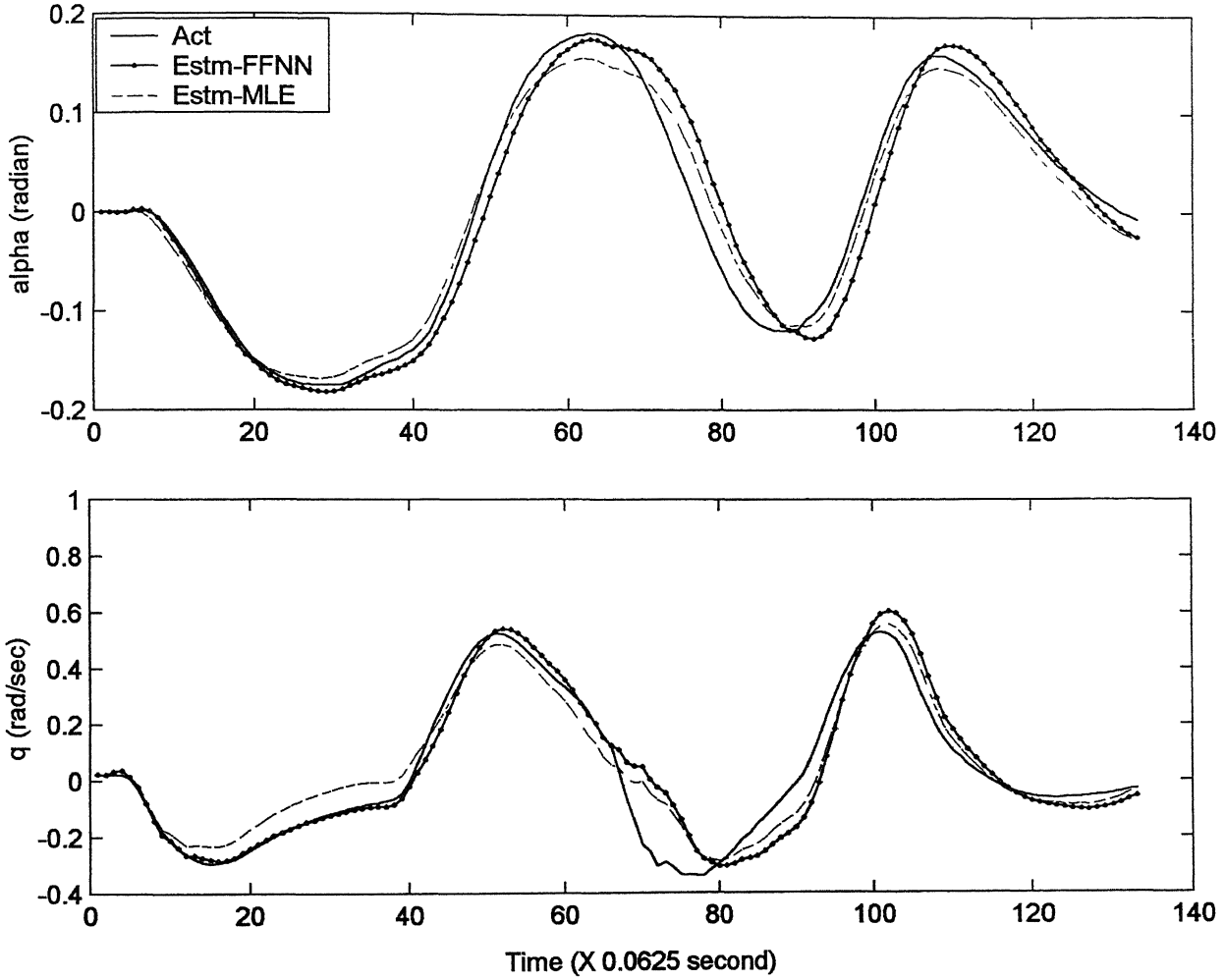

Fig. 3.9 Comparision of Actual And Estimated Response For FLT3/TP2,Vi=160 KIAS For Raw Data

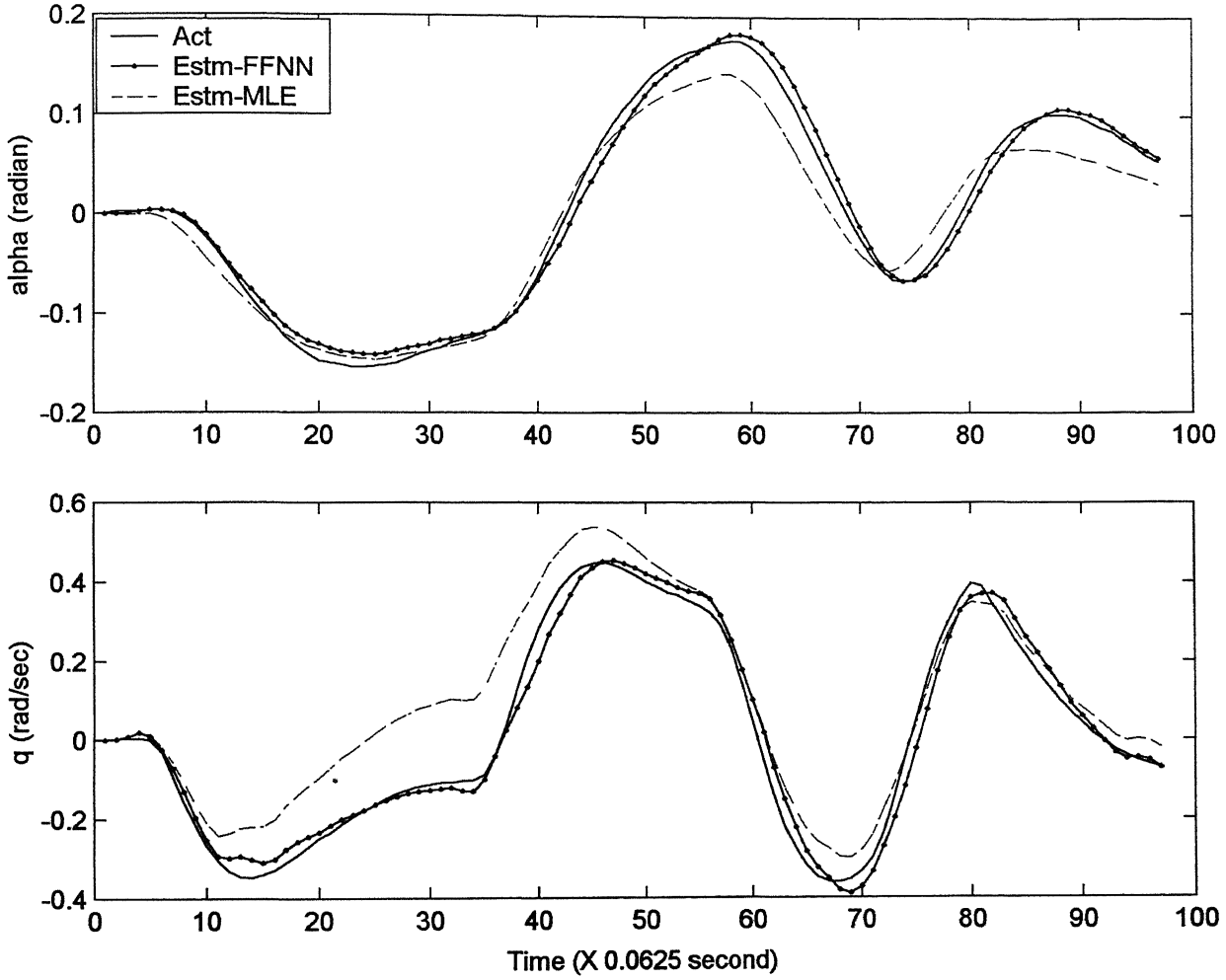

Fig. 3.10 Comparision of Actual And Estimated Response For FLT3/TP13,Vi=180 KIAS For Raw Data

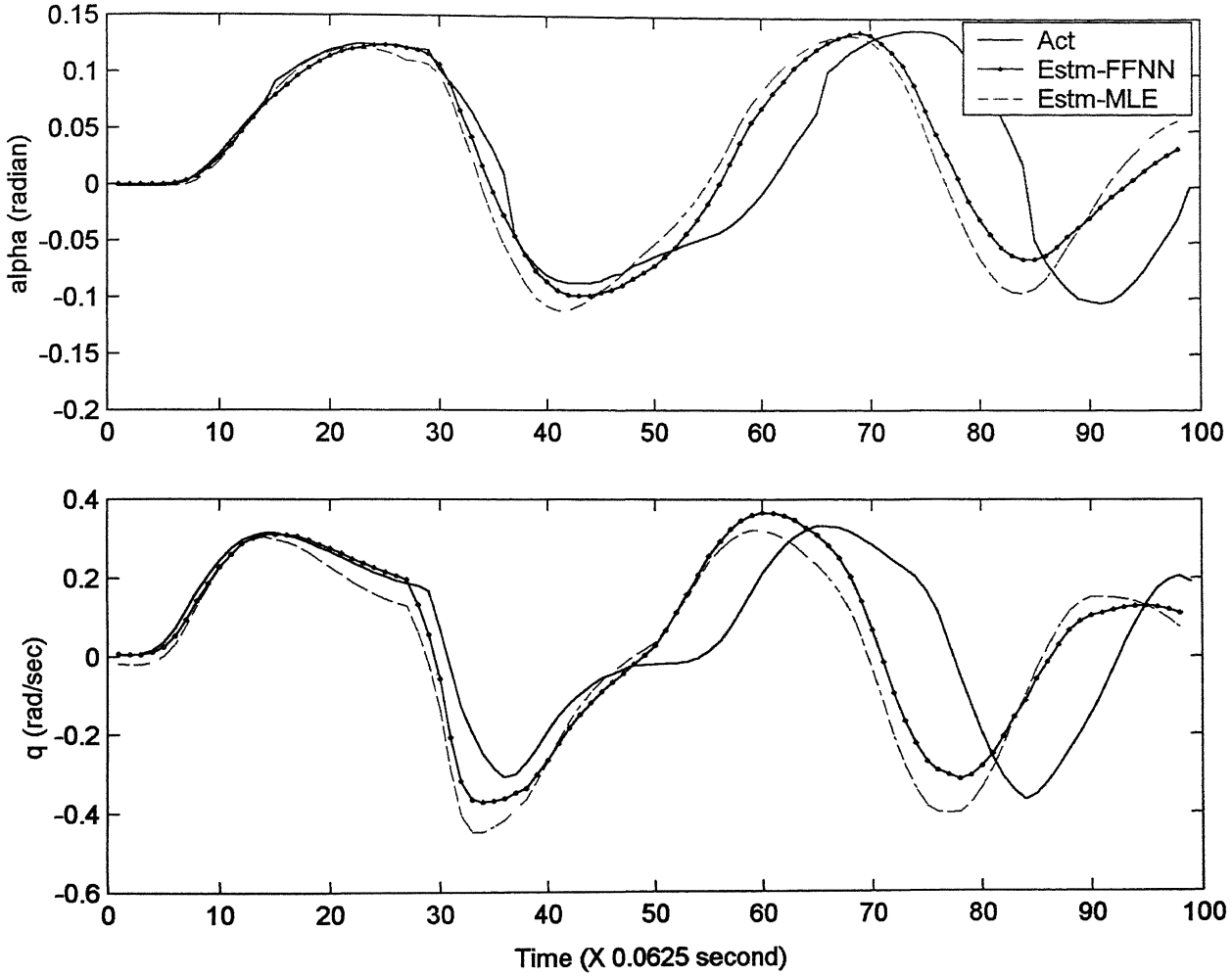

Fig. 3.11 Comparision of Actual And Estimated Response For FLT4/TP14,Vi=220 KIAS For Raw Data

MLE method. Firstly, the aerodynamic modeling using the FFNN was carried out for the corrected flight data. Figures 3.12a and 3.12b show the plot of actual and predicted (after training) aerodynamic coefficients (C_L and C_m) obtained from the corrected flight data. From Fig. 3.12, it is seen that the FFNN has been well trained. The Delta method was then applied to estimate the parameters. The results of the Delta method for corrected flight data are presented in Table 3.5a and 3.5b for flights FLT3 and FLT4 respectively.

The results of the MLE method for corrected flight data are presented in Table 3.6a and 3.6b for flights FLT3 and FLT4 respectively. From Table 3.5a and 3.5b, it is seen that the strong derivatives have been estimated reasonably well by the Delta method. The estimates for $C_{L\alpha}$, $C_{m\alpha}$, C_{mq} and $C_{m\delta e}$ (Table 3.5a and 3.5b) from the Delta method are fairly constant for all the test points at different speeds and show little variation. However, a few values do not fit into the pattern, for example $C_{m\alpha}$ has been obtained as -0.2463 for the data set of FLT4/TP8 (refer Table 3.5b), which is quite low. Further, it is observed that, with increase in speed, the value of $C_{m\delta e}$ decreases slightly, for example, $C_{m\delta e}$ = -0.7397 at V_i = 160 KIAS and $C_{m\delta e}$ = -0.5526 at V_i = 220 KIAS (refer last row of Table 3.5b). Strictly speaking, for the range of Mach number covered by different test points (from 0.3 M to 0.38 M) , the estimates should have been constant. The variation in the values of the estimates could be due to the fact that all the elevator inputs given during the maneuvers were not the ideal 3-2-1-1 δe input.

On comparing the results of the Delta method for corrected flight data (refer Table 3.5a and 3.5b), with those for raw flight data (refer Table 3.2a and 3.2b), a few peculiarities were observed. The estimates of $C_{L\alpha}$, C_{mq} and $C_{m\delta e}$, from the Delta method

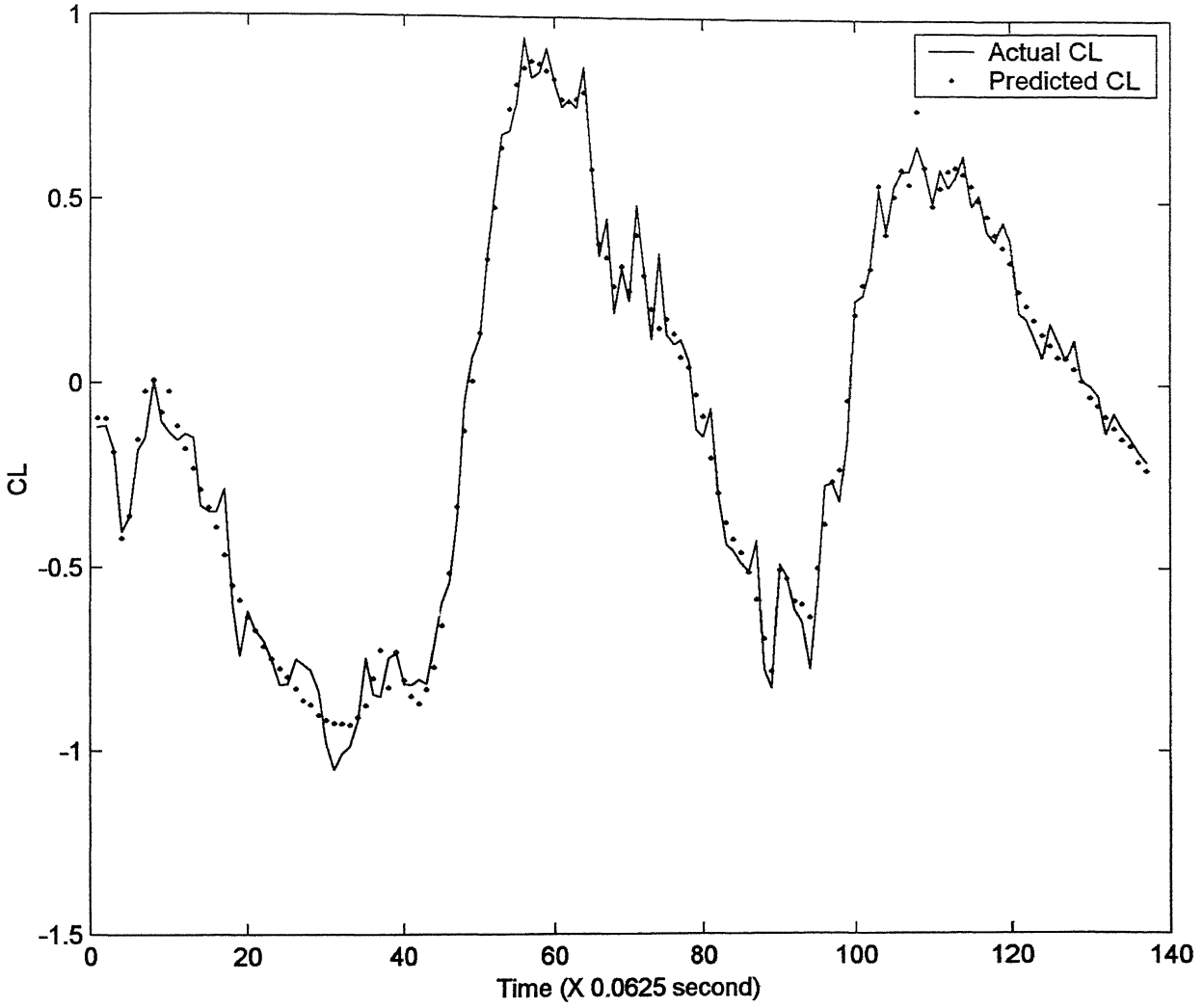

Fig. 3.12a Plot Of Actual And Predicted (After Training) CL For Test Point FLT3/TP2,Vi=160 KIAS For Corrected Data

match fairly well between the corrected and raw flight data. However, the estimate for $C_{m\alpha}$ appears to be suppressed for the corrected flight data (refer Table 3.5a and 3.5b) and consistently lower values of $C_{m\alpha}$ are obtained here.

As seen from the Table 3.6a and 3.6b, the MLE estimates from the corrected flight data are also fairly consistent and reliable. A comparison of the estimates from the Delta method (Table 3.5a and 3.5b) and the MLE method (Table 3.6a and 3.6b) shows that the estimates from both the methods are in close agreement. The Delta method can therefore be successfully employed for parameter estimation from the corrected flight data.

The accuracy of the parameters estimated from the corrected flight data by the Delta method was checked in a similar fashion as was done for the raw flight data. The estimates for the parameters C_{Lo} and C_{mo} obtained for the corrected flight data are presented in Table 3.7.

The estimated aerodynamic coefficients (C_L , C_m) were then found out, using the estimates for corrected flight data obtained by the Delta method. Figures 3.13, 3.14 and 3.15 show the plots of the actual and estimated aerodynamic coefficients (C_L and C_m) for corrected flight data for three typical test points. These plots show that a reasonable match is obtained between the measured and estimated aerodynamic coefficients.

The accuracy of the estimates from the corrected flight data using the Delta and MLE methods were also checked by comparing the measured and estimated responses. The method used to find out the estimated responses was similar to that followed for the raw flight data. The estimated responses for the corrected flight data were then plotted along with the measured response of the aircraft as shown in Fig. 3.16, 3.17 and 3.18.

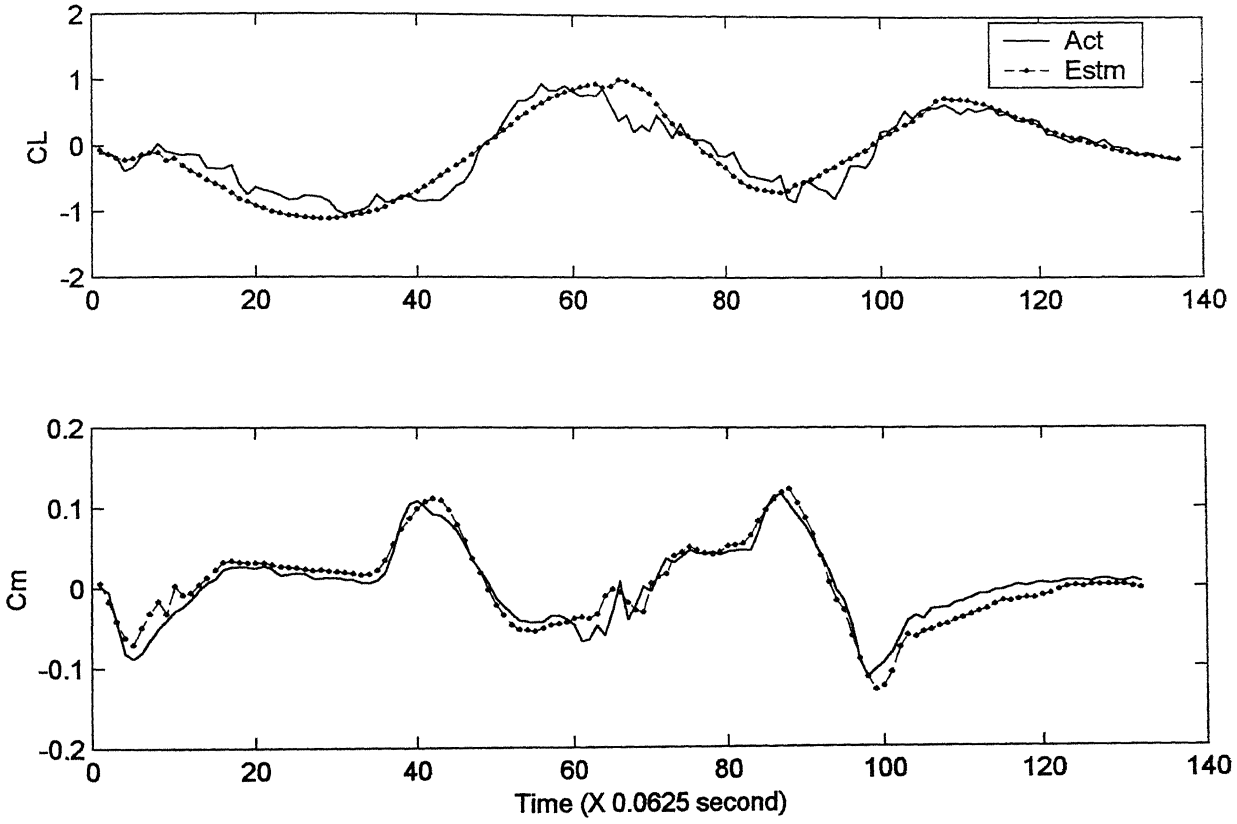

Fig. 3.13 Comparision of Actual And Estimated Total Aerodynamic Coefficients For FLT3/TP2,Vi=160 KIAS For Corrected Data

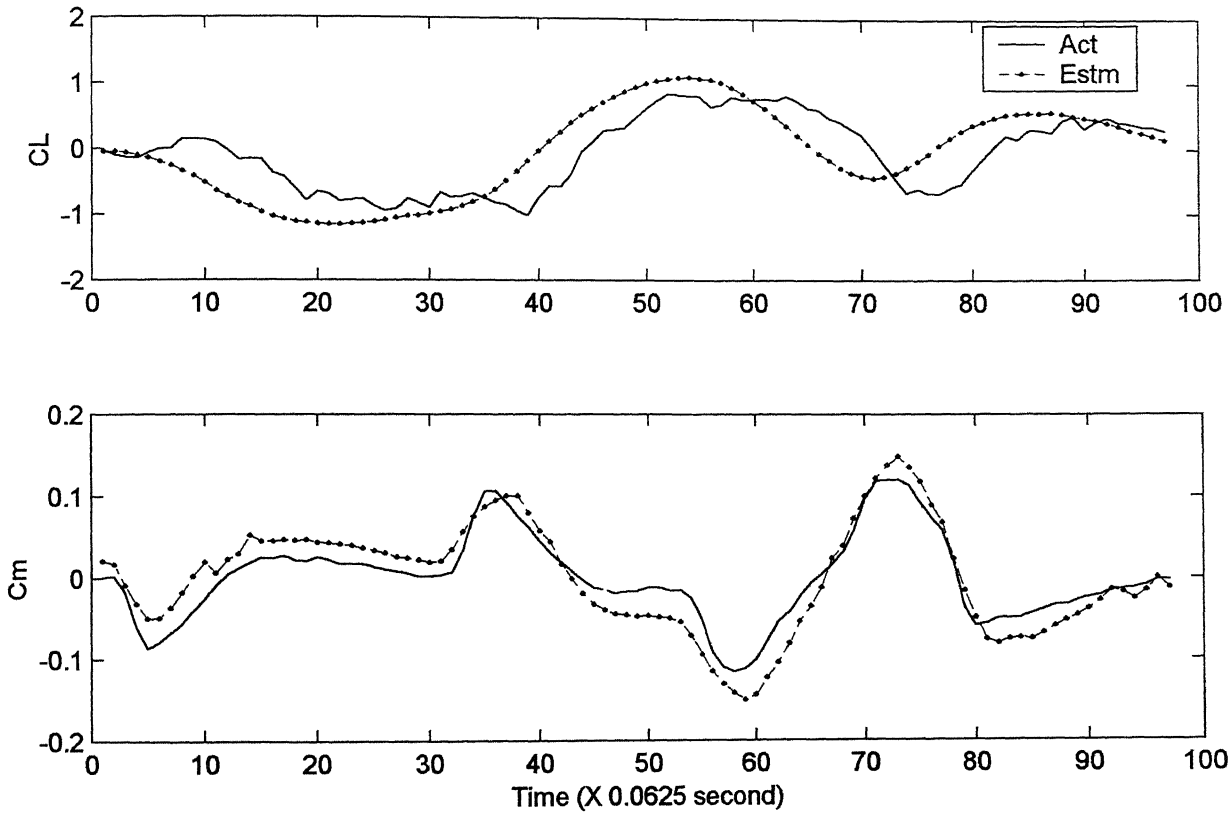

Fig. 3.14 Comparision of Actual And Estimated Total Aerodynamic Coefficients For FLT3/TP13,Vi=180 KIAS For Corrected Data

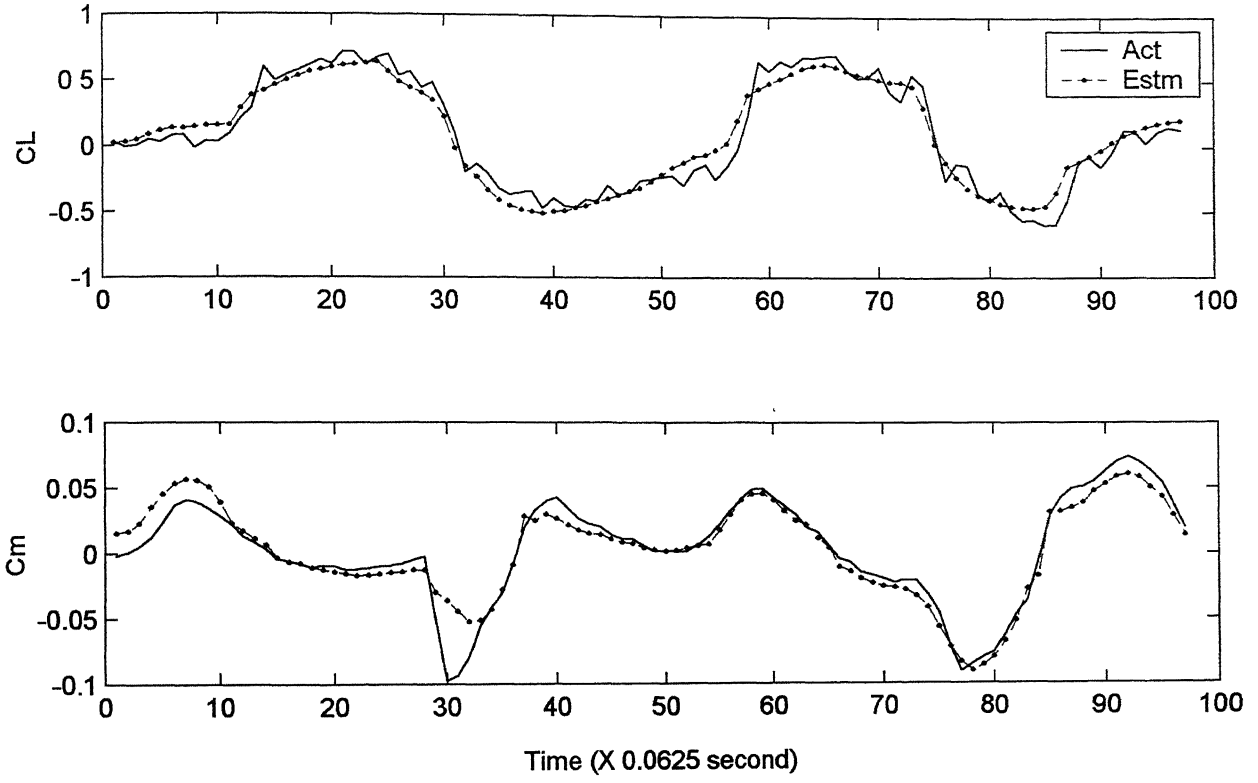

Fig. 3.15 Comparision of Actual And Estimated Total Aerodynamic Coefficients For FLT4/TP14,Vi=220 KIAS For Corrected Data

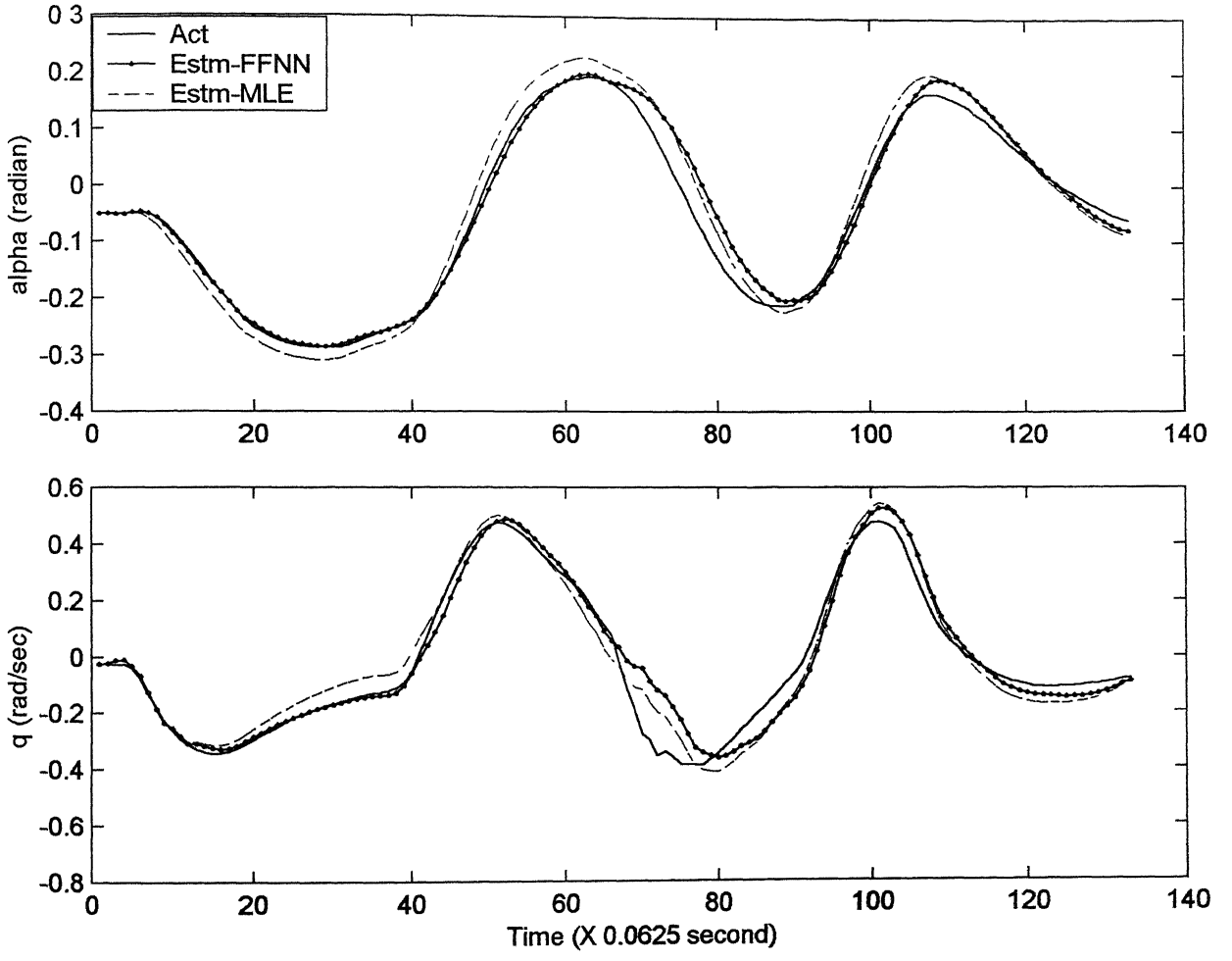

Fig. 3.16 Comparision of Actual And Estimated Response For FLT3/TP2,Vi=160 KIAS For Corrected Data

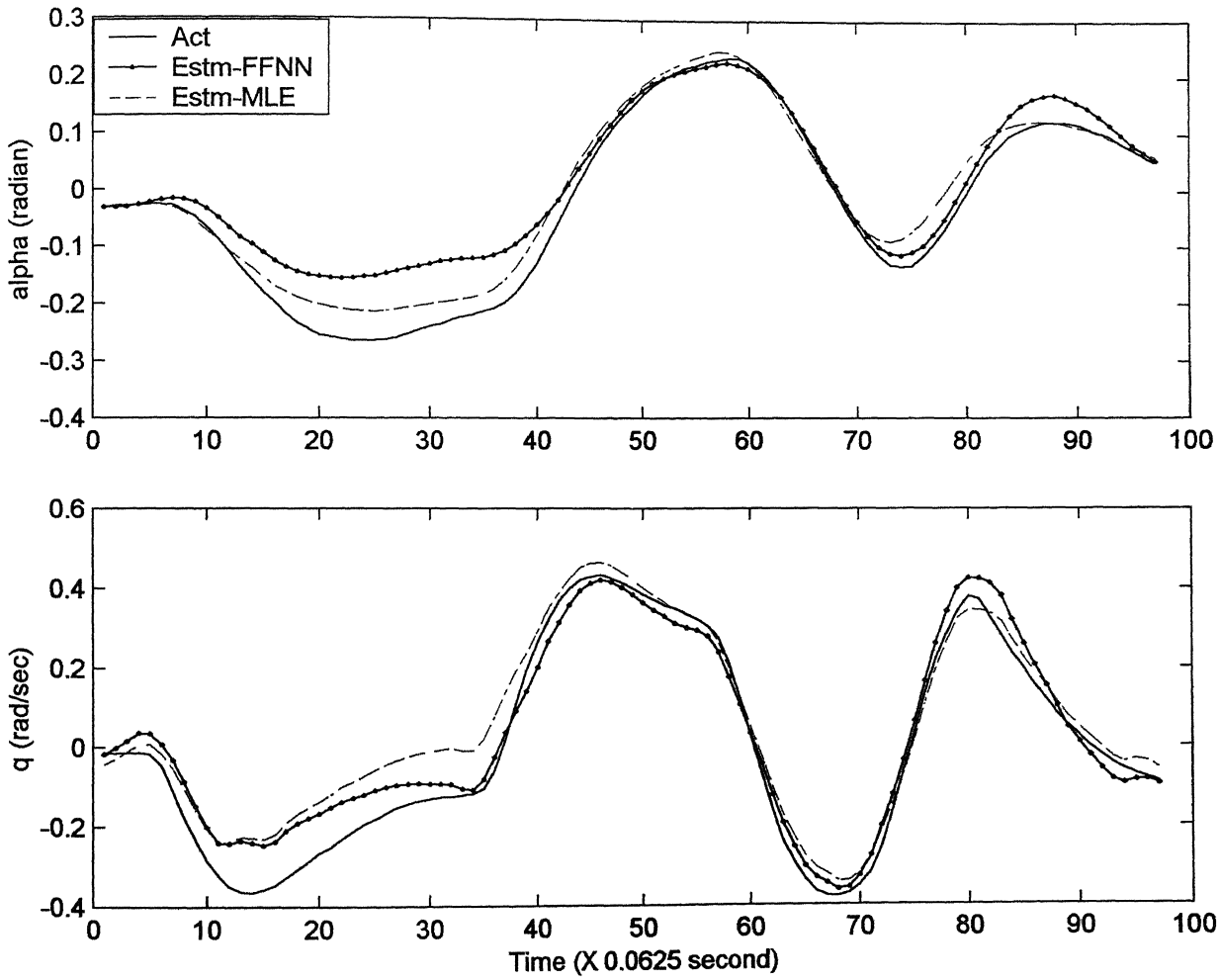

Fig. 3.17 Comparision of Actual And Estimated Response For FLT3/TP13,Vi=180 KIAS For Corrected Data

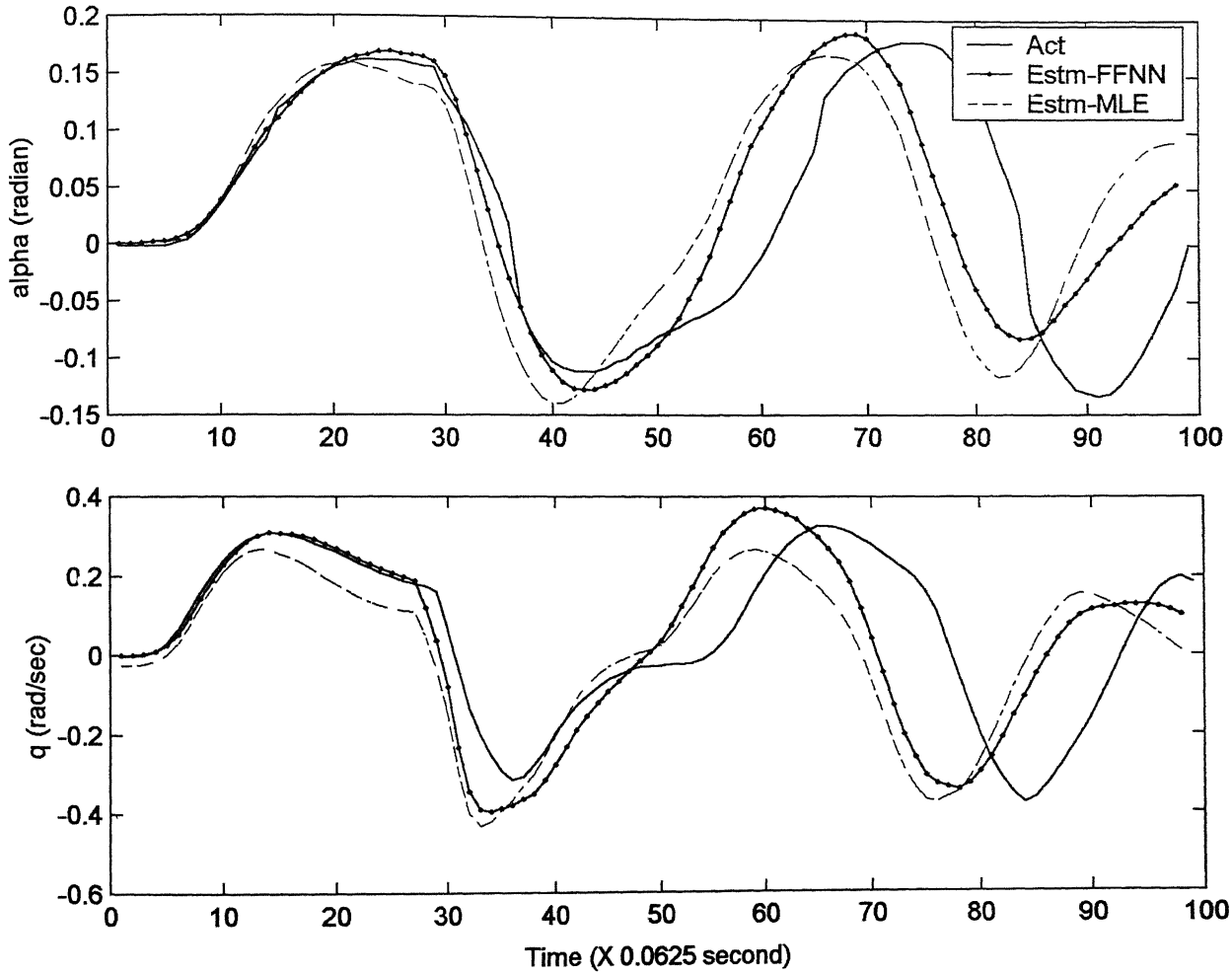

Fig. 3.18 Comparision of Actual And Estimated Response For FLT4/TP14, Vi=220 KIAS For Corrected Data

From these figures, it is observed that, in general, for the corrected flight data, the match between the estimated and measured response are not as good as that for raw flight data (Fig. 3.9, 3.10 and 3.11). However, in case of the corrected flight data, the estimated response using the estimates obtained from the Delta method lies very close to the measured response. Further, at peaks it is observed that there are small differences in absolute values of α and q (Fig. 3.16, 3,17 and 3.18). Also, the time period for the estimated response shows a slight increase (implying a decrease in short period frequency) as compared to the measured response.

On completion of the parameter estimation process, the distribution of the parameters estimated by the Delta method from the raw flight data was plotted and is as shown in Fig. 3.19. As seen from Fig. 3.19, the estimates obtained from the raw flight data using the Delta method are fairly accurate and reliable. This is further corroborated by the fact that, when these Delta method estimates are used as initial guess values in MLE method, the MLE method also gives fairly accurate and consistent results. However, the estimates obtained from the corrected flight data using the Delta method can be improved further by carrying out a rigorous data compatibility check (using the complete six degree of freedom equations of motions[9]). In the present work, this could not be done because the pitch angle (θ) transducer was unserviceable. Hence a reliable recording of pitch angle (θ) was not available. Therefore, a simplified set of longitudinal equations of motions (refer Eq. (2.8), (2.9) and (2.10) given in article §2.5 of Chapter 2) were used for data compatibility checks. Further, it was assumed that the initial conditions for the data compatibility checks were as recorded during the beginning of the maneuver. Probably, the estimation of the initial conditions separately may have helped

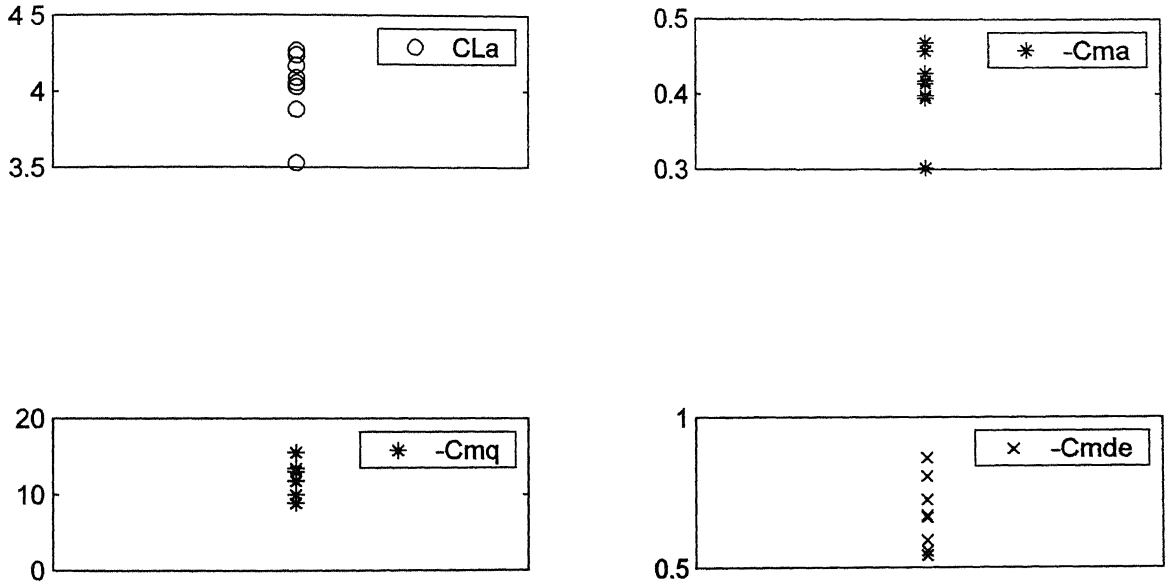

Fig. 3.19 Plot Showing The Distribution Of The Parameters Estimated Using The Delta Method From The Raw Flight Data

in improving the accuracy of the correction factors. And lastly, one of the observable variables used was true airspeed, which in turn was calculated from the dynamic pressure recorded. The transducer used being a pressure transducer is bound to have lags/time delays in its recording. In spite of these discrepancies, it is felt that the match obtained between the estimated response obtained from the Delta method and measured response for the corrected flight data is reasonably good.

3.3 REAL FLIGHT DATA (LATERAL-DIRECTIONAL MOTION)

3.3.1 General

The real flight data for the lateral-directional motion was generated from the last flight of the test program, i.e. from FLT5, as discussed in article §2.4 of Chapter 2. Based on Ref. 9 and 19, it was decided to excite the lateral-directional response of the aircraft by giving separate δa and δr inputs in different test points. This meant that for the first test point when δa input is being given, δr is held constant at its trim position and vice versa for the second test point. The dutch roll in Kiran aircraft is easily excited by giving full δr doublet input alone. Hence for δr inputs, it was decided that only the doublet form of input will be used. However, for aileron (δa) inputs, the following input form were tried out; 3-2-1-1 input of time period of 7 seconds, δa doublet and roll maneuvers[9]. Further, the flight data for lateral-directional motion was generated at four different speed, namely, V_i = 160, 180, 200 and 220 KIAS.

From aerodynamics, it is well known that the rolling moment coefficient (C_l), yawing moment coefficient (C_n) and side force coefficient (C_y) are a function of F(p, r, β, δa, δr). Hence in this case, the number of parameters to be estimated (in order to

determine the function 'F'), becomes large and any parameter estimation process becomes an involved exercise. In the present work, we have attempted to estimate the following parameters : C_{lp} , C_{lr} , $C_{l\beta}$, $C_{l\delta a}$, $C_{l\delta r}$, C_{np} , C_{nr} , $C_{n\beta}$, $C_{n\delta a}$, $C_{n\delta r}$, C_{yp} , C_{yr} , $C_{y\beta}$, $C_{y\delta a}$, $C_{y\delta r}$.

3.3.2 Problem Faced During Parameter Estimation Using MLE Method

The success in estimating the longitudinal parameters using the Delta method embolden us to work directly with the real flight data for this case. Accordingly, no work was done on simulated data for lateral-directional case. Further, like in the longitudinal case, after completion of estimation from the Delta method, it was also attempted to estimate the lateral-directional parameters from the real flight data using the MLE method. Here, again, the Delta method estimates were used as the initial guess values to initiate the MLE program. But, despite rigorous efforts, we could not succeed with the MLE method within the short span of time available to us. The reason for this was very simple. In the MLE algorithm, all the 15 parameters were being estimated simultaneously. Hence, it was found that the MLE method had become very sensitive to the initial guess values used. It was observed that for any given set of initial guess values used, the MLE method correctly estimated only a few parameters. A subsequent run, with a minor change in some of guess values, resulted in few other parameters being estimated correctly. Thus convergence of the MLE method was found to be a direct function of the initial guess values. After considerable discussions, it was suspected that maybe the MLE routine written in house was incorrect. To prove that this was not so, a set of simulated data was generated for the lateral-directional motion using the Delta method estimates (as true values of the aerodynamic parameters) and δr doublet input as

given in actual flight. The Eq. (2.3) to (2.7) as given in Chapter 2 were used for generating the simulated data. Now, the same MLE routine was run using the Delta method estimates as initial guess values for the parameters. The results of this small exercise is placed in Table 3.8. It must be noted that the Delta method estimates used as initial values in the MLE routine were suitably altered by a small random number (refer column 3 of Table 3.8). It was found that the MLE routine quickly converged in the sixth iteration itself and gave us all the correct estimates with minimum cost function being found as 2.1456×10^{-14}. At this stage, it was even more keenly appreciated how an alternate method, which does not require initial guess values to start the estimation process, would be extremely helpful and useful for such similar situations in industry. No further attempts were made with the MLE method for real flight data and we proceed to discuss the Delta method results.

3.3.3 Results of Parameter Estimates From Flight Data Generated by Individual δa and δr Inputs

The Delta method was used to estimate parameters from the raw flight data as well as from the corrected flight data as was done for the longitudinal case. Each test point was analyzed separately. Accordingly, for the δr doublet input test point, the network training files containing $\frac{pb}{2u}$, $\frac{rb}{2u}$, β and δr as input variables and C_l, C_n or C_y as the output variable were prepared. Similarly, for the δa input test point, the network input file contained $\frac{pb}{2u}$, $\frac{rb}{2u}$, β, and δa with output file having C_l, C_n or C_y. The actual (measured) aerodynamic coefficients C_l and C_n were calculated using Eq. (2.4) and (2.5)

as listed in Chapter 2. The actual aerodynamic force coefficient C_y was calculated from the lateral acceleration a_y as follows:

$$a_y = \frac{\bar{q}S}{mg} C_y + (pq + \dot{r})X_a - (r^2 + p^2)Y_a + (rq - \dot{p})Z_a \qquad (3.6)$$

Using such input-output files, the aerodynamic modeling using different architectures of FFNN was carried out. As explained earlier for the longitudinal case, the architecture of FFNN which gave the minimum training MSE was frozen for the prediction phase. The Delta method was then applied to estimate the parameters.

It was observed that, since the maneuvers were executed by giving separate δr, δa inputs, the estimates of the corresponding cross derivatives (C_{lr} , $C_{l\delta r}$, C_{np} and $C_{n\delta a}$) obtained by the Delta method (for raw flight data) were showing lot of scatter and inconsistency. Also the standard deviation obtained in the above cases were very high. It was conjectured that this was due to the fact, that for Kiran aircraft, the individual control inputs (δa and δr input separately) are probably not sufficient to the excite the complete lateral-directional motion of the aircraft.

3.3.4 Revised Approach For Parameter Estimation

From the above discussions, it is clear that the approach used so far for the estimation process for lateral-directional motion needed to be revised. Several researchers had recommended that although the δa and δr input should not be given simultaneously, but giving the 2 inputs delayed from each other by a small time interval gave satisfactory results. However, the data available with us was for each input δa and δr being given separately. After considerable debate, we decided to try out another approach, wherein we used the fact that for the Delta method, we can always concatenate

data from different time segments. It must be noted that this is not possible for the MLE method. In other words, the Delta method is independent of the time at which the data was generated. In this new approach; we concatenated the data from the two different δa and δr input test inputs for the same speed. It is important to remember here that the aerodynamic coefficients C_l , C_n and C_y must be individually calculated for each test point using all the relevant conditions for the given test points, such as weight, dynamic pressure etc. The steps involved using this new approach for parameter estimation by the Delta method were as follows:

1). For each of the test points for δa and δr inputs (which were given separately) for the same speeds, the separate files containing input variables $\frac{pb}{2u}, \frac{rb}{2u}$, β, and δr and δa with corresponding output variable C_l , C_n and C_y were prepared.

2) Now the two files were merged by putting the δa input file at the end of the δr input file, to form a combined training file. Such a combined file would carry the complete lateral-directional response of the aircraft being excited by δr and δa inputs.

The next issue to be resolved was, as to which of the δa inputs should be used to concatenate the data. The real flight data was generated for three different types of δa input. A brief study revealed here that the δa doublet input gave better estimates for rolling moment derivatives, when this test point was analyzed separately.

Accordingly, it was decided that for the raw and corrected flight data, the aircraft response obtained for separate δr doublet input and δa doublet input would be combined for each speeds. Thus four combined training files were prepared, one each for $V_i = 160$,

180, 200 and 220 KIAS. Accordingly, these four combined data sets have been designated as follows:

Data Set	Nomenclature
1.	FLT5/TP1_5 (V_i = 160 KIAS)
2.	FLT5/TP9_14 (V_i = 180 KIAS)
3.	FLT5/TP17_22 (V_i = 200 KIAS)
4.	FLT5/TP24_28 (V_i = 220 KIAS)

Figures 3.20 and 3.21 shows the typical time history plots of one such combined file for data set of FLT5/TP1_5 for raw and corrected flight data respectively.

3.3.5 Parameter Estimates From Raw Flight Data Using Revised Approach

Using the combined input-output training files, the aerodynamic modeling using different architectures of the FFNN for lateral-directional motion was carried out. The architecture of FFNN, which gave the minimum MSE, was frozen for the prediction phase. Figures 3.22a, 3.22b and 3.22c shows the plot of actual and predicted (after training) aerodynamic coefficients for a typical combined test point for raw flight data . A close match is obtained implying that the FFNN was now well trained. The Delta method is then used to estimate the parameters from the raw flight data.

The results of the estimates from the Delta method for raw flight data using these four combined input files are presented in Table 3.9. From Table 3.9, it is seen that all the strong derivatives have been estimated very well with low value of standard deviation. The estimates are also observed to be fairly constant for all the test points at different speed. As seen from the first row of Table 3.9, the estimate of the roll damping derivative, C_{lp} , has been obtained nearly constant as -1.1 but with slight higher standard

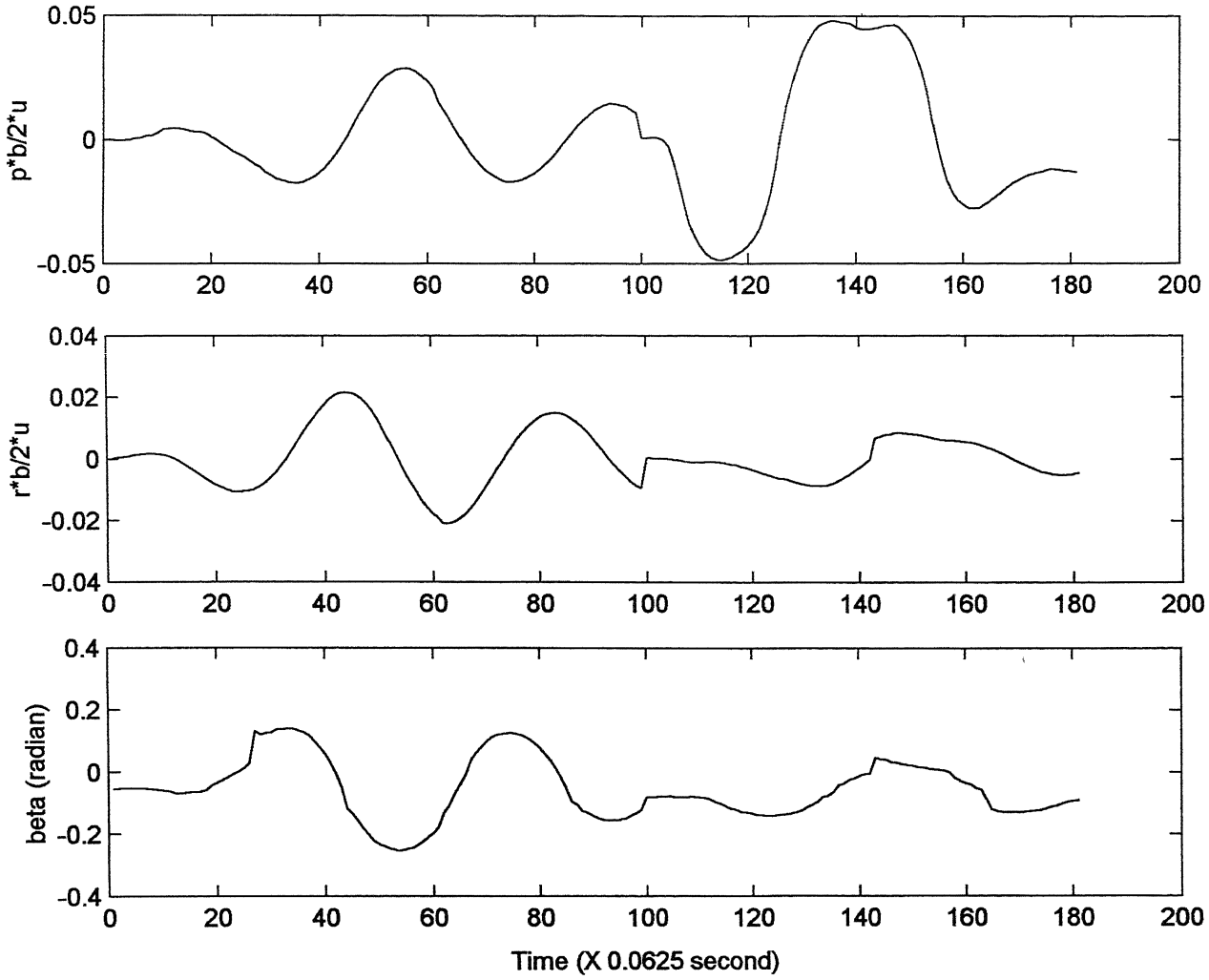

Fig. 3.20 Plot Of Time History For Combined Test Point FLT5/TP1-5, Vi=160 KIAS For Raw Data

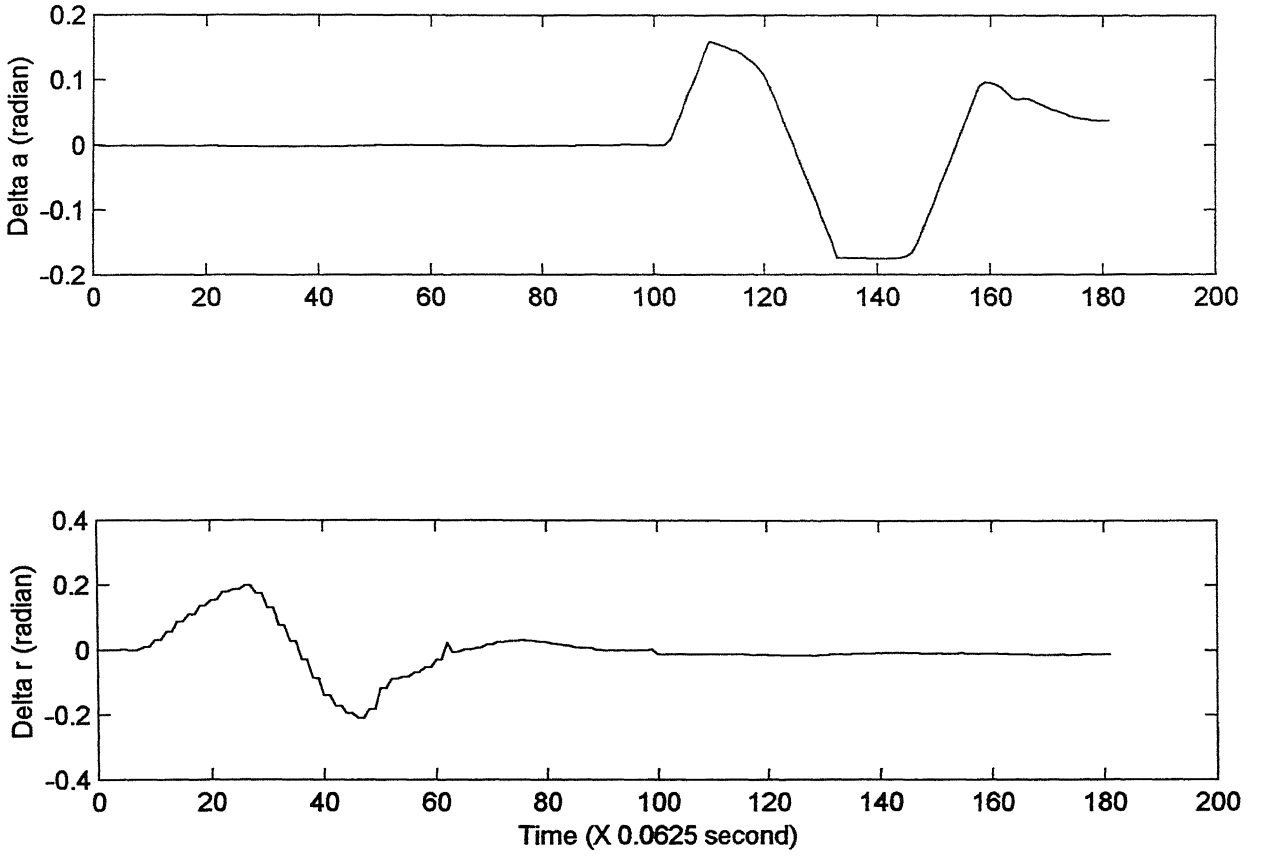

Fig. 3.20 Continued

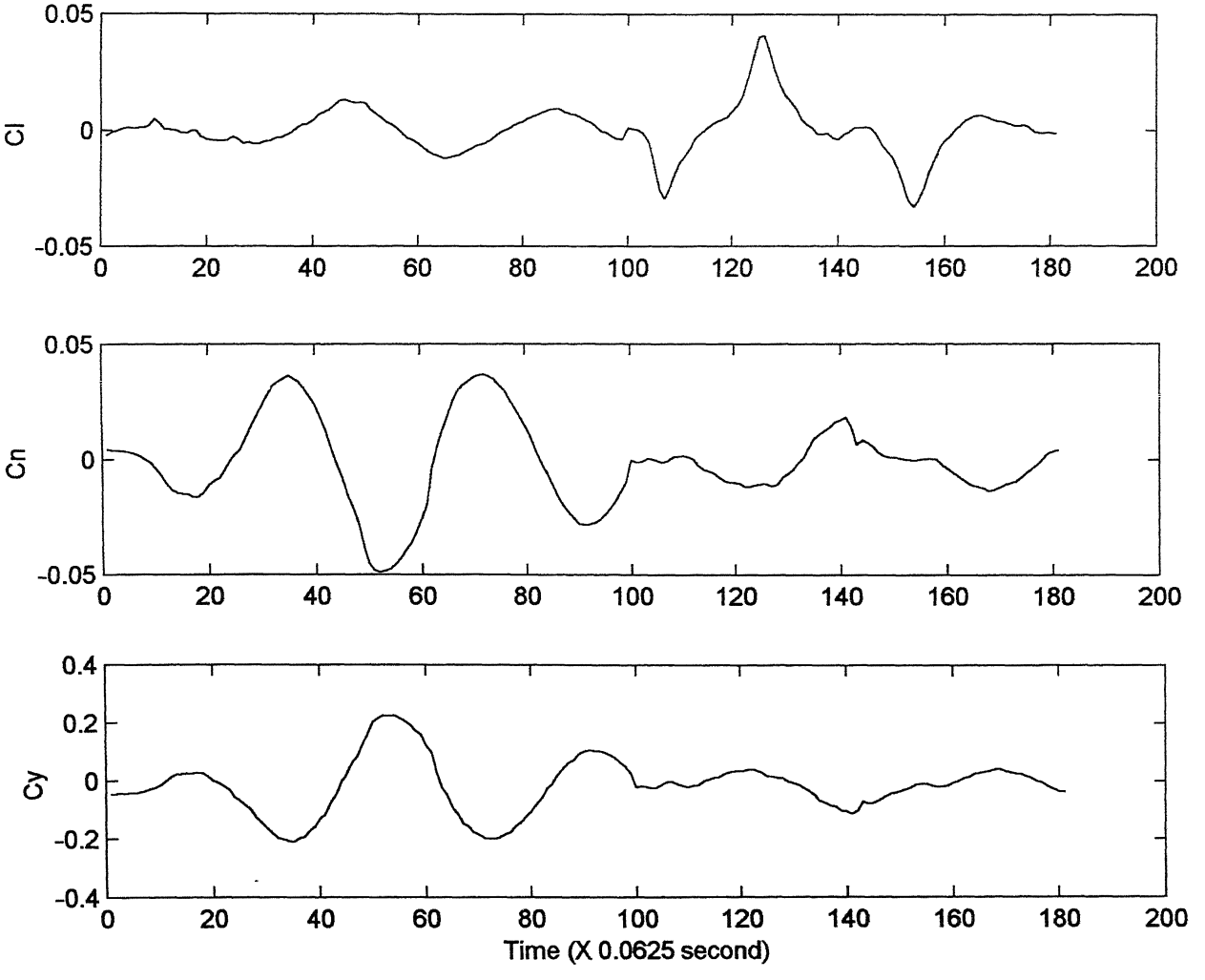

Fig. 3.20 Concluded

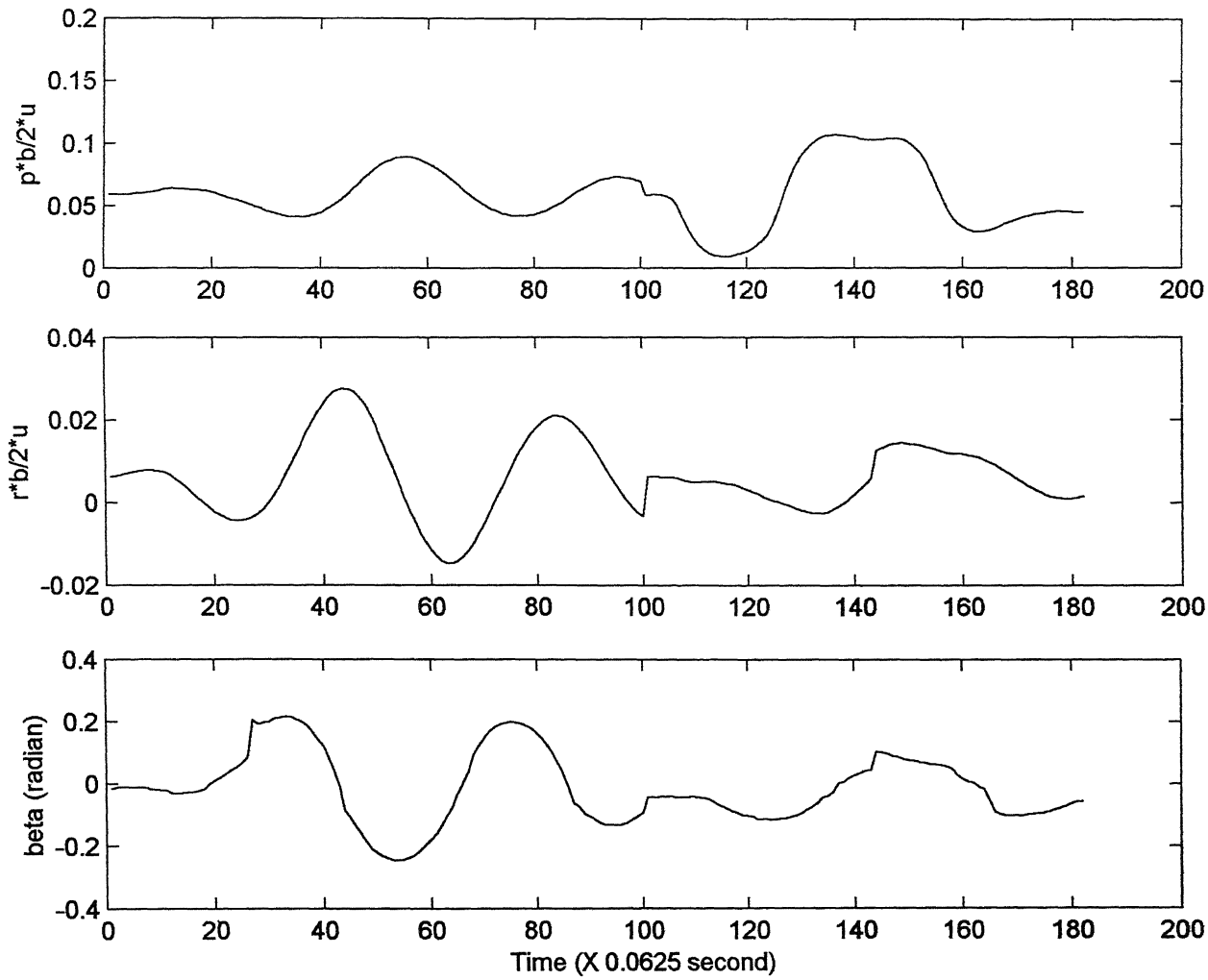

Fig. 3.21 Plot Of Time History For Combined Test Point FLT5/TP1-5,Vi=160 KIAS For Corrected Data

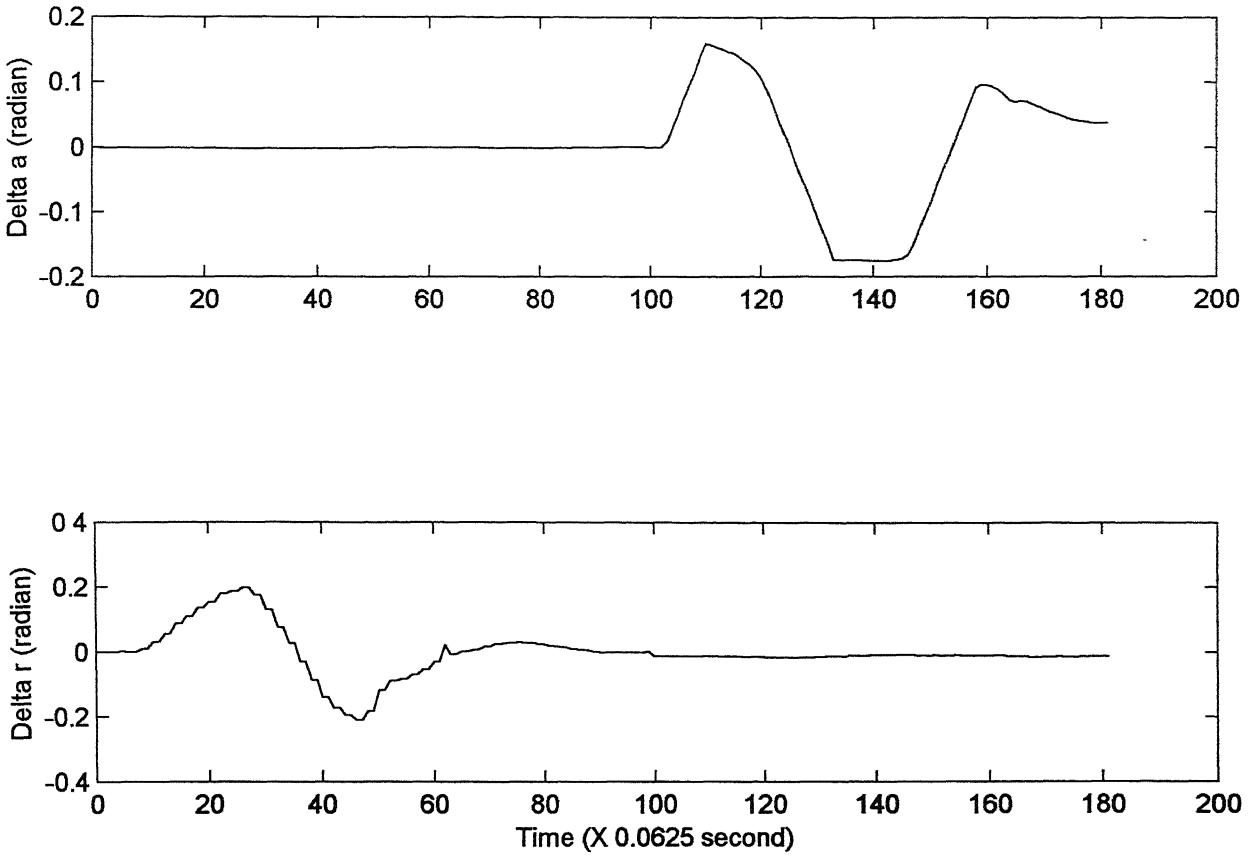

Fig. 3.21 Continued

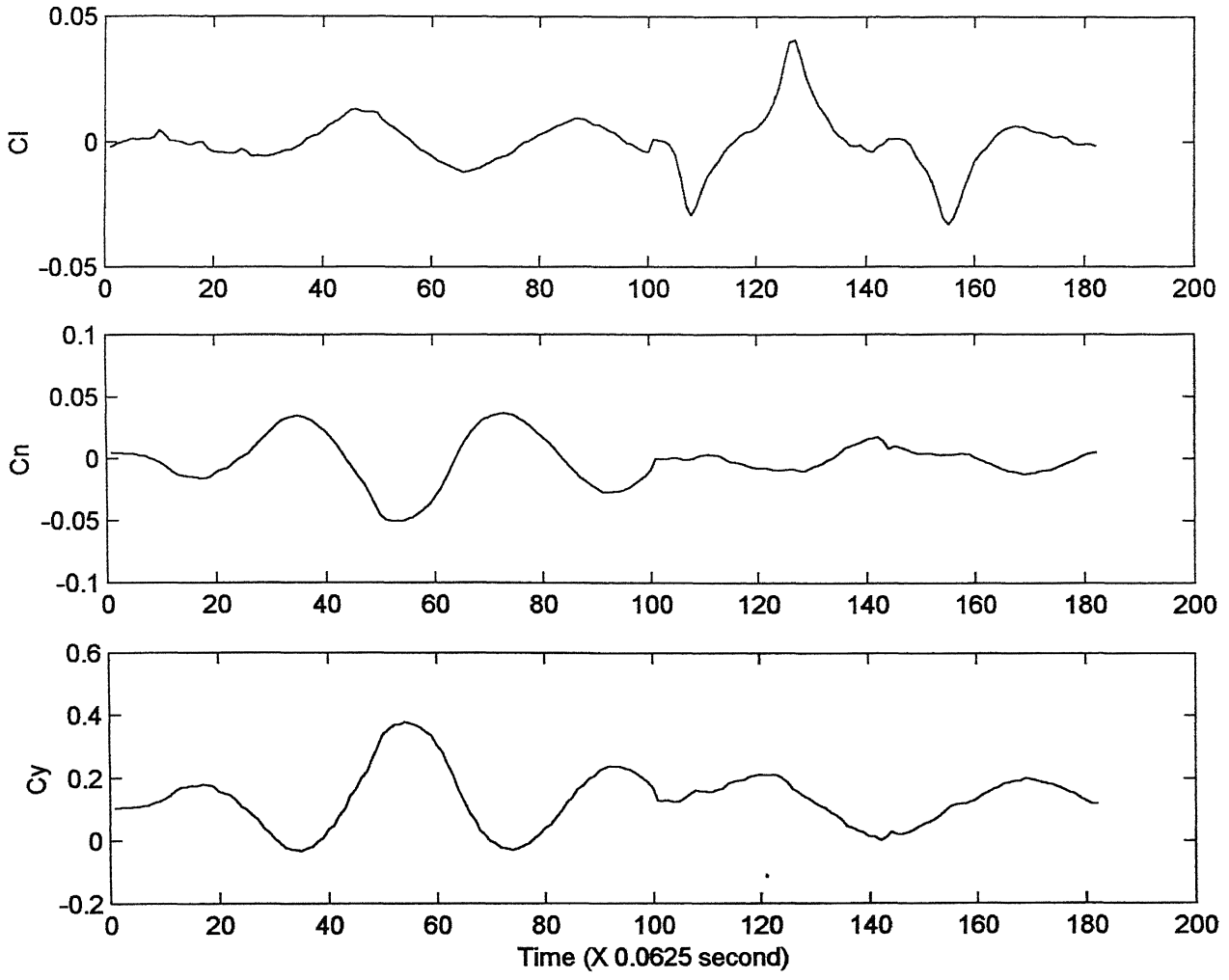

Fig. 3.21 Concluded

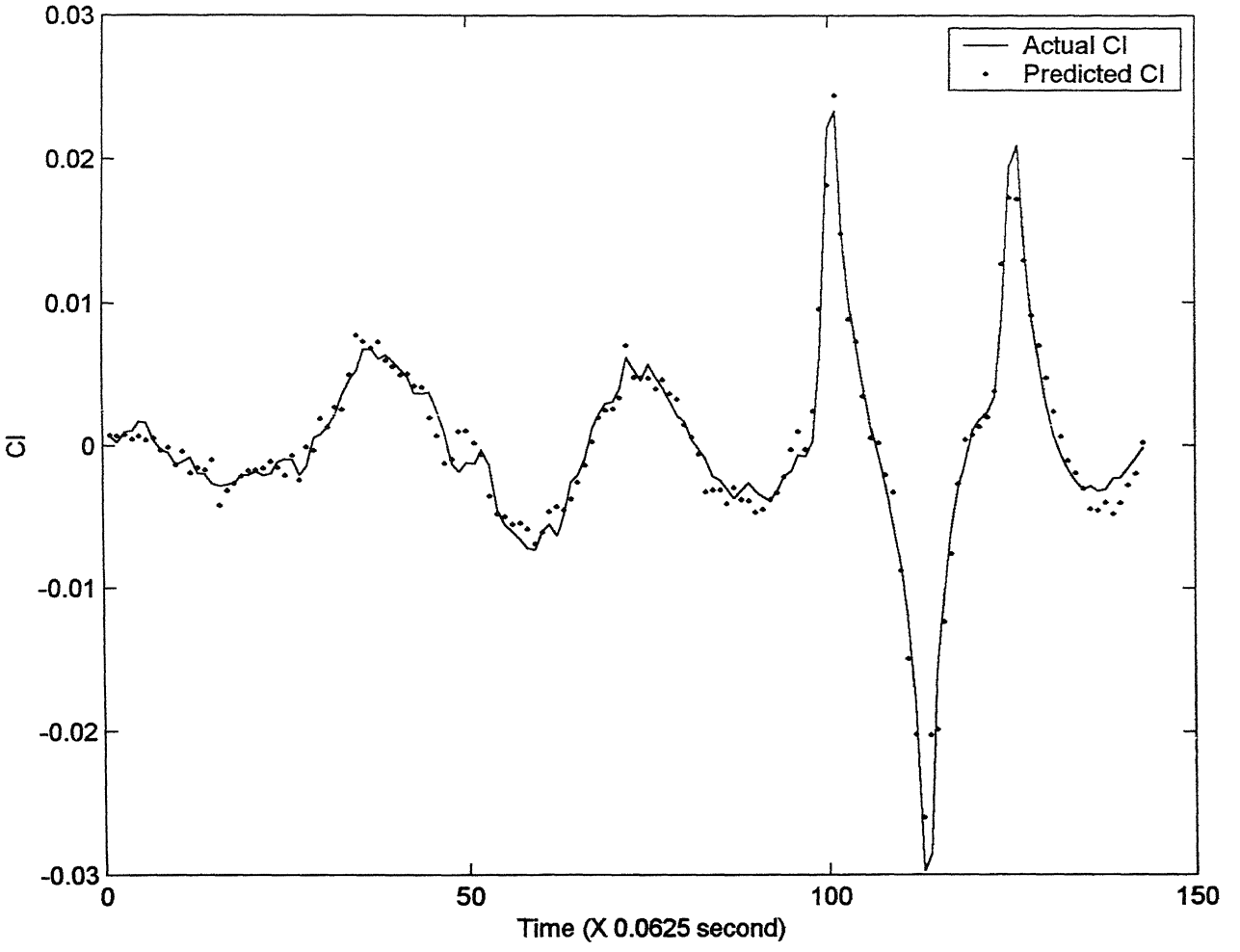

Fig. 3.22a Plot Of Actual And Predicted (After Training) Cl For Combined Test Point FLT5/TP17-22,Vi=200 KIAS For Raw Data

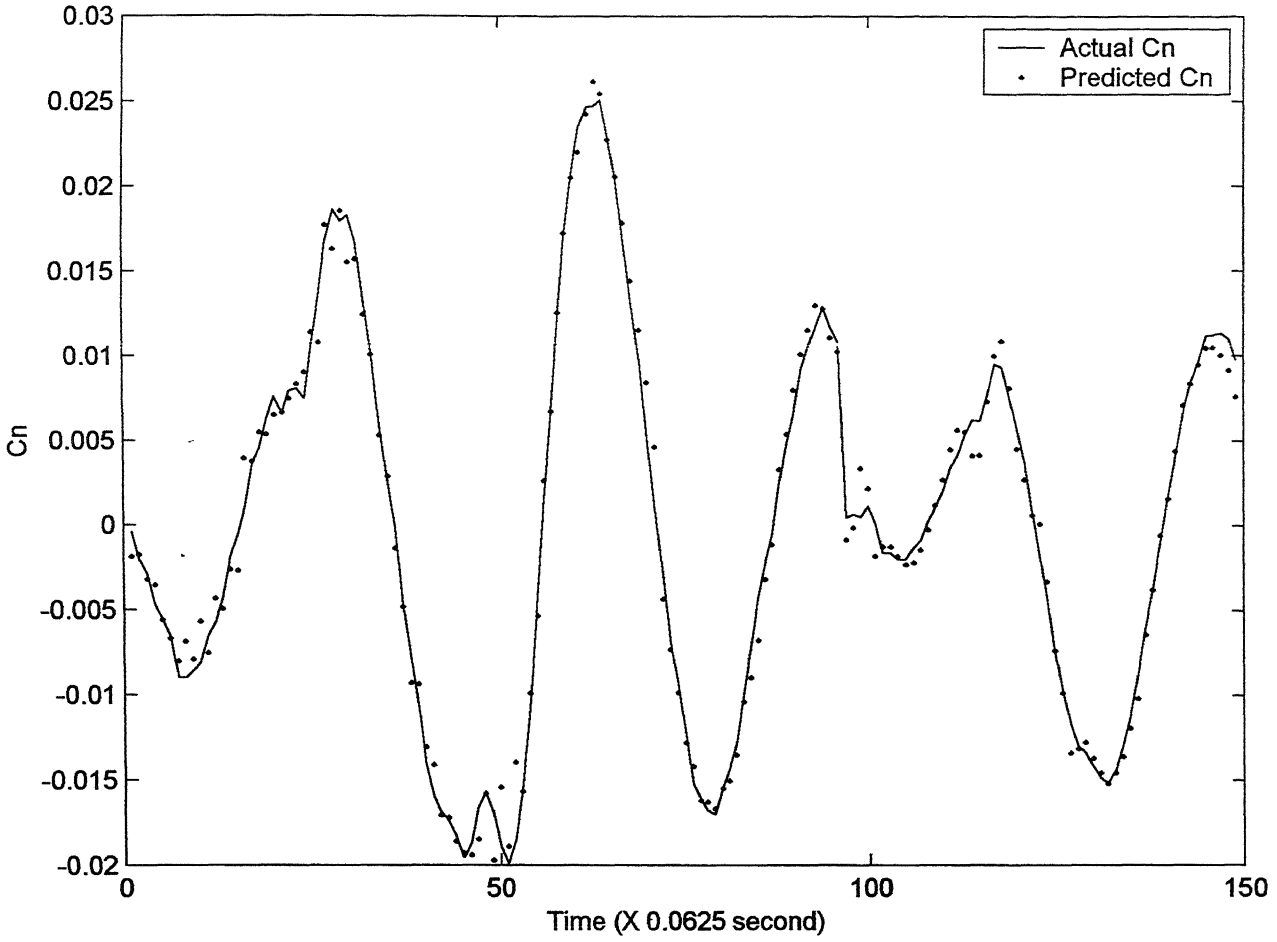

Fig. 3.22b Plot Of Actual And Predicted (After Training) Cn For Combined Test Point FLT5/TP17-22,Vi=200 KIAS For Raw Data

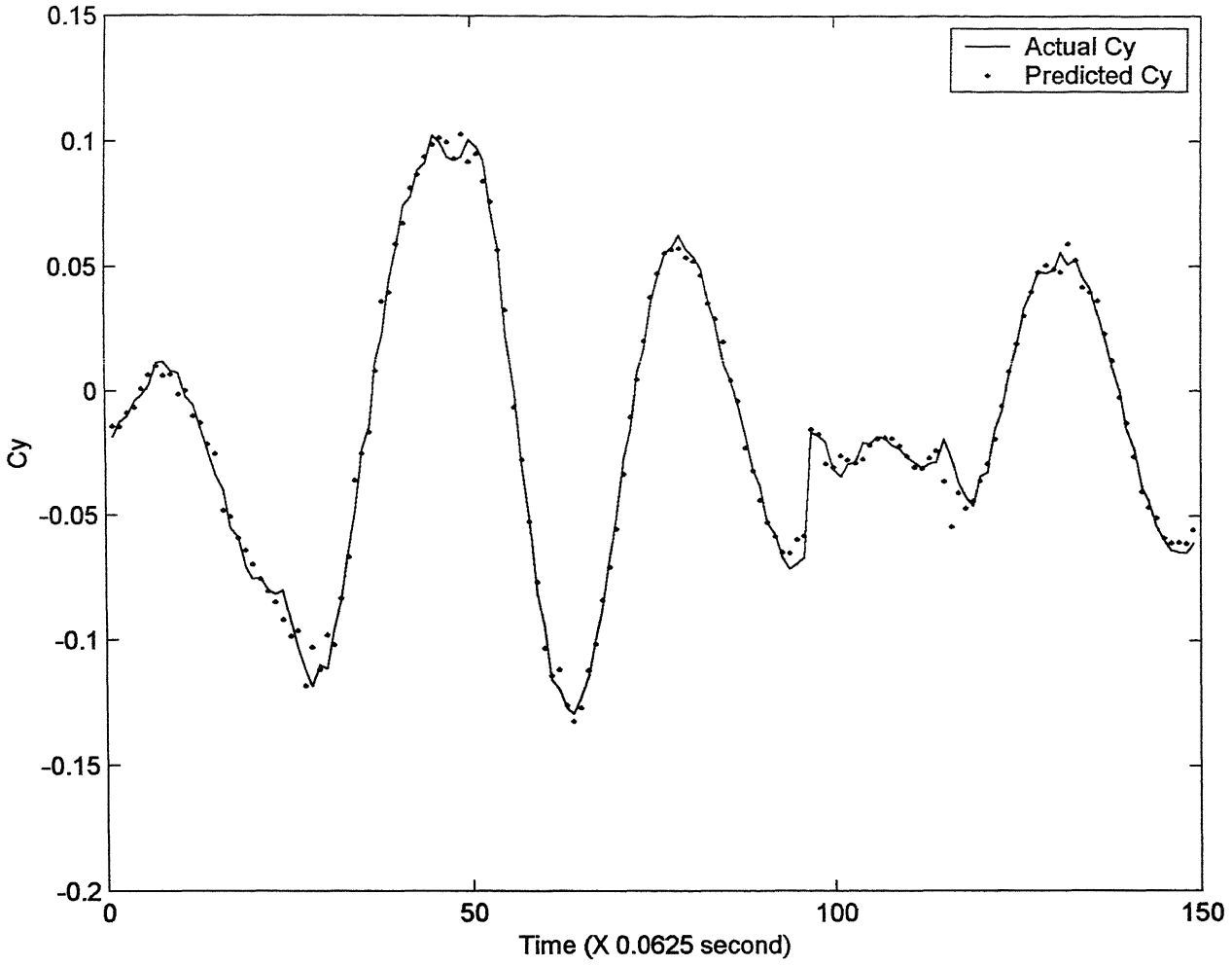

Fig. 3.22c Plot Of Actual And Predicted (After Training) Cy For Combined Test Point FLT5/TP17-22,Vi=200 KIAS For Raw Data

deviation, especially for test point FLT5/TP9_14 (V_i = 180 KIAS) where the standard deviation for C_{lp} is 0.28. However, from the other three test points, the standard deviation is seen to be of the order of 0.18. This is considered acceptable, as it implied that the value of C_{lp} lies between -1.298 to -0.902.

Similarly, the strong control derivatives $C_{l\delta a}$ and $C_{n\delta r}$ have been obtained as -0.35 and -0.12 with standard deviation of the order of 0.08 and 0.04 respectively (refer rows 4 and 10 of Table 3.9). The dutch roll damping derivatives C_{nr} shows a slight scatter in its values for different speeds, from -0.92 at V_i = 160 KIAS to -0.55 at V_i = 220 KIAS, but has been estimated in each case with a low standard deviation (refer row 7 of Table 3.9). The remaining strong derivatives $C_{l\beta}$, $C_{n\beta}$ and $C_{y\beta}$ have been estimated consistently as -0.12, 0.22, -0.9 for all the test points with low standard deviation (refer rows 3, 8 and 13 of Table 3.9).

The cross coupling derivative C_{lr} estimated shows a slight variation, especially for the test point, FLT5/TP9-14 (V_i = 180 KIAS) with a correspondingly higher standard deviation (refer row 2 of Table 3.9). But the estimates for C_{lr} from the other three test points show good consistency with low standard deviation and lead us to place more confidence in these values.

In fact, even the weak derivatives such as $C_{l\delta r}$, C_{np} and $C_{n\delta a}$ have been estimated with remarkable consistency for different test points (refer rows 5, 6 and 9 of Table 3.9). Also, the derivative $C_{y\delta r}$, except for test point FLT5/TP9_14, (V_i = 180 KIAS) has been estimated reasonably well (refer last row of Table 3.9). However the weak derivatives of sideforce coefficients, C_{yp} , C_{yr} and $C_{y\delta a}$ are found to be varying and inconsistent for each

of the test point analyzed and they have not been estimated very well (refer rows 11, 12 and 14 of Table 3.9).

Overall it can be said that, except for these few weak derivatives, the results of the Delta method, as presented in Table 3.9, show good consistency among the estimates for different speeds.

To check the accuracy of the estimates, the estimated total aerodynamic coefficients (C_l , C_n and C_y) were compared with the actual (measured) coefficients (calculated earlier from Eq. (2.4), (2.5) and (3.6)). The estimated aerodynamic coefficients were obtained by feeding the above estimates into the following equations.

$$C_l = C_{lp}\left(\frac{ps}{V}\right) + C_{lr}\left(\frac{rs}{V}\right) + C_{l\beta}\beta + C_{l\delta a}\delta a + C_{l\delta r}\delta r \qquad (3.7)$$

$$C_n = C_{np}\left(\frac{ps}{V}\right) + C_{nr}\left(\frac{rs}{V}\right) + C_{n\beta}\beta + C_{n\delta a}\delta a + C_{n\delta r}\delta r \qquad (3.8)$$

$$C_y = C_{yp}\left(\frac{ps}{V}\right) + C_{yr}\left(\frac{rs}{V}\right) + C_{y\beta}\beta + C_{y\delta a}\delta a + C_{y\delta r}\delta r \qquad (3.9)$$

These estimated total aerodynamic coefficients do not carry any information about the parameters C_{lo} , C_{no} and C_{yo} , since these parameters were not estimated separately. The same procedure as given in previous article §3.2, was used to estimate C_{lo} , C_{no} , C_{yo}. The estimates for the parameters C_{lo} , C_{no} and C_{yo} obtained for raw flight data is presented in Table 3.10.

Figures 3.23, 3.24, 3.25 and 3.26 show the comparative plots of the actual (measured) and estimated C_l , C_n and C_y for the raw flight data for all the four combined test points. From these figures, we see that a fairly good match is obtained for C_n and C_y for all the test points. However from Fig. 3.23, 3.24 and 3.25 (for V_i = 160, 180 and 200 KIAS combined test points) for C_l , a small peculiarity is observed. It is seen that

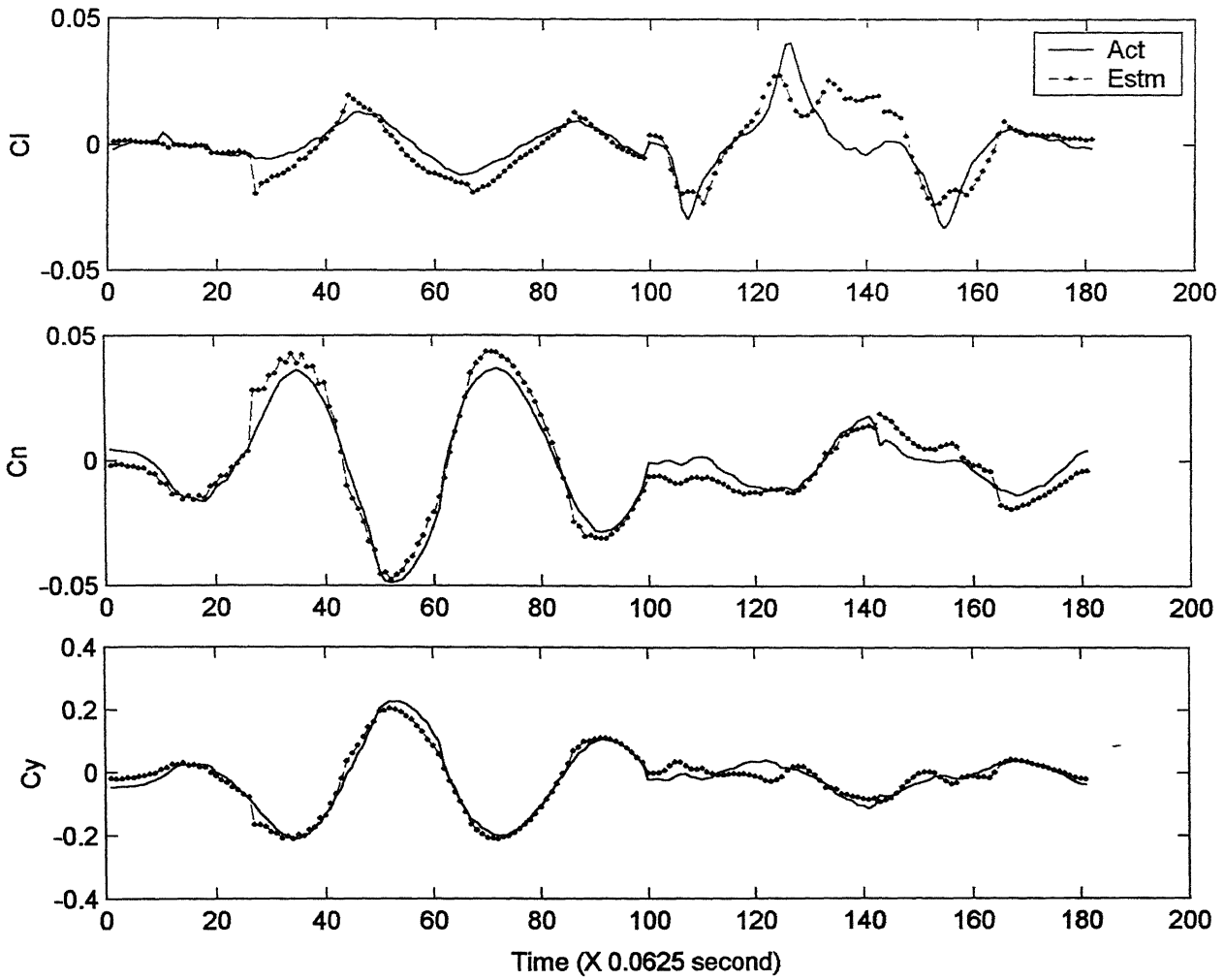

Fig. 3.23 Comparision of Actual And Estimated Total Aerodynamic Coefficients For FLT5/TP1-5,Vi=160 KIAS For Raw Data

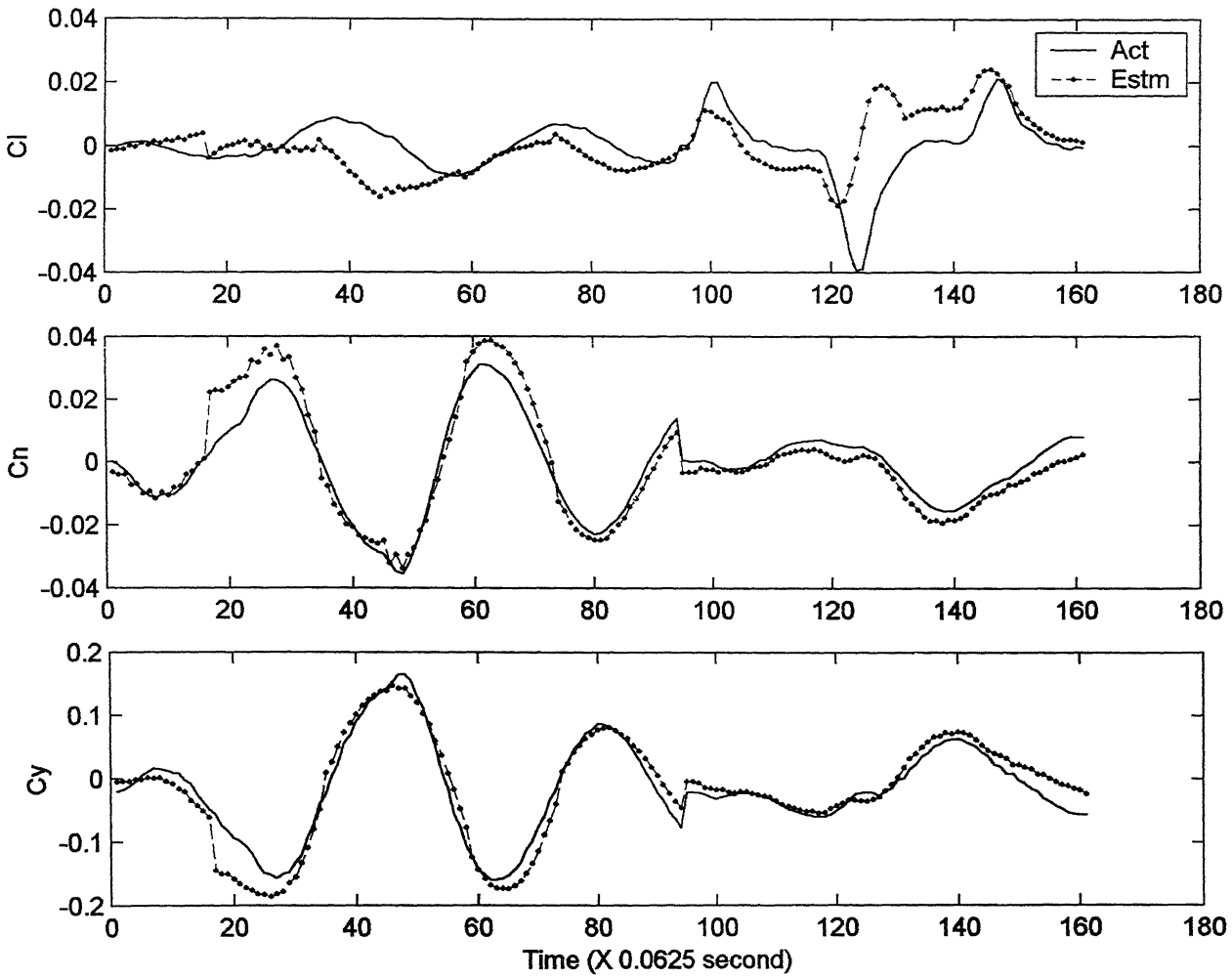

Fig. 3.24 Comparision of Actual And Estimated Total Aerodynamic Coefficients For FLT5/TP9-14,Vi=180 KIAS For Raw Data

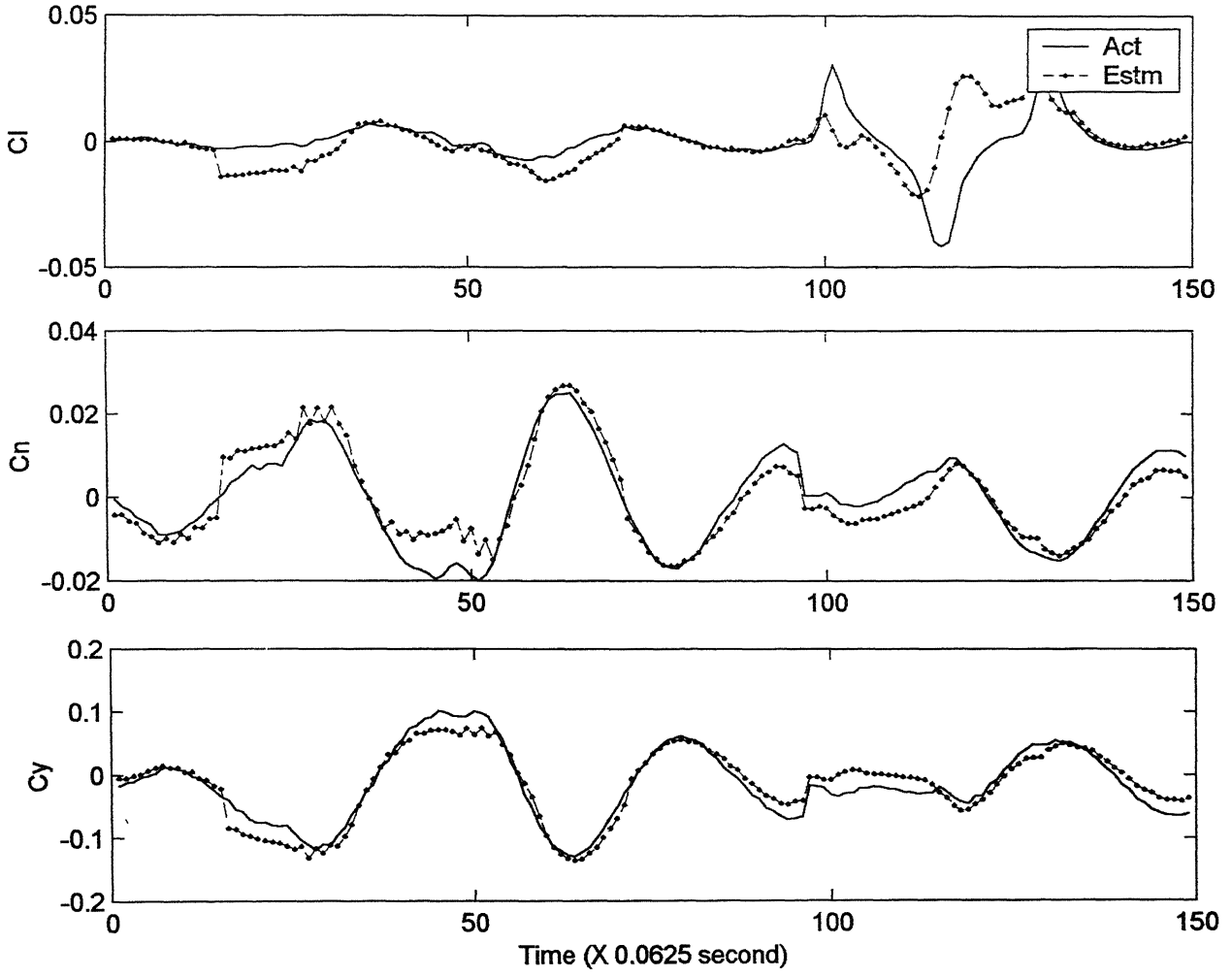

Fig. 3.25 Comparision of Actual And Estimated Total Aerodynamic Coefficients For FLT5/TP17-22,Vi=200 KIAS For Raw Data

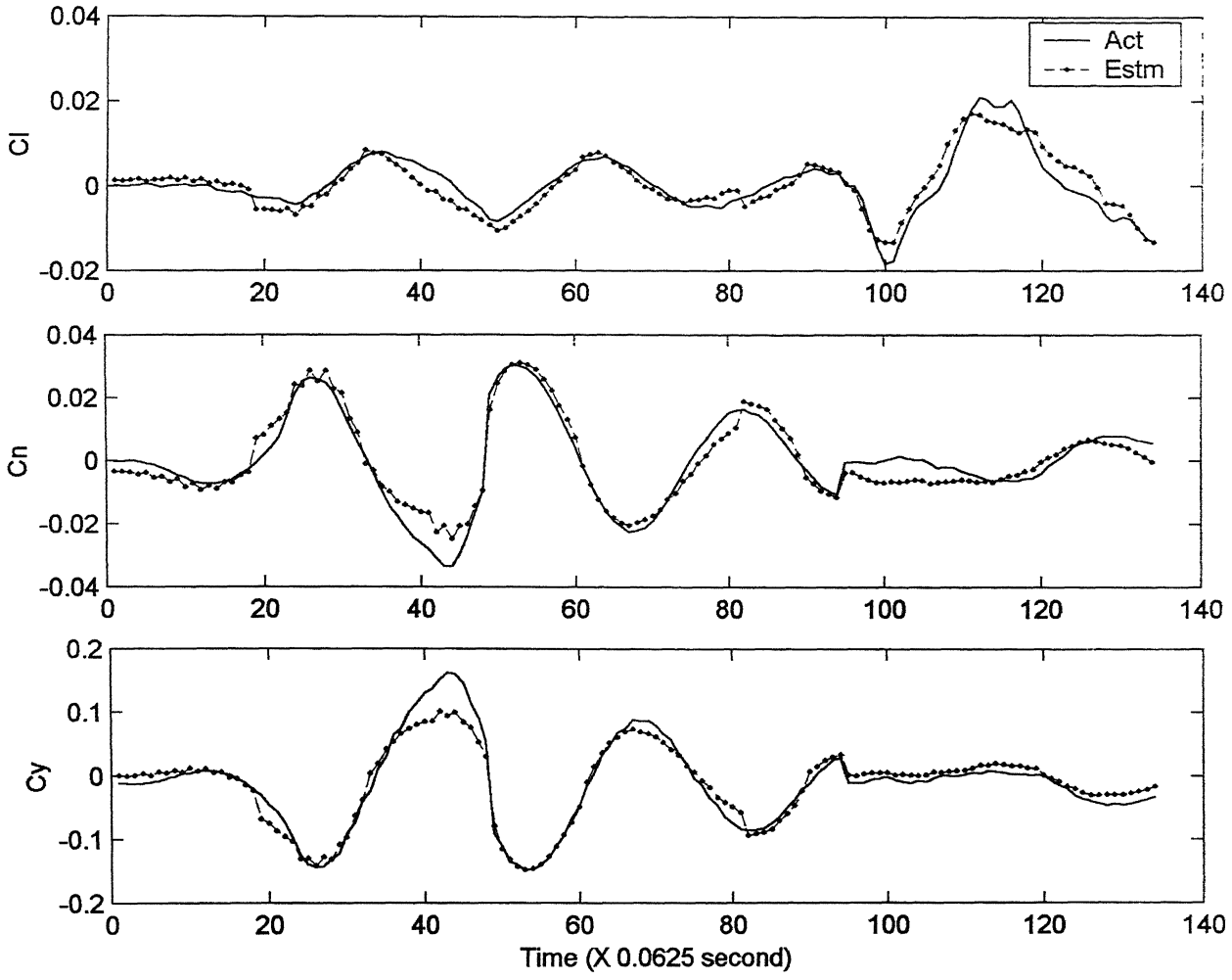

Fig. 3.26 Comparision of Actual And Estimated Total Aerodynamic Coefficients For FLT5/TP24-28,Vi=220 KIAS For Raw Data

although a good match is obtained between the measured and estimated C_l over a large portion the figure, however, in a small time segment of the figure, the match is rather poor. This time segment corresponds to the beginning of the δa doublet input. It can only be conjectured that this may have been due to the fact that δa and δr inputs were given separately in different test points (at same speed). In future, for lateral-directional motion, the δr input should be given first and following 1-2 second delay, the δa input should be given in the same test points.

From the reasonably good match obtained between the actual and estimated aerodynamic coefficients for all the other test points (refer Fig. 3.23, 3.24, 3.25 and 3.26), it can be inferred that the set of parameters estimated by the Delta method from the raw flight data are fairly reliable and accurate.

3.3.6 Parameter Estimates From Corrected Flight Data Using Revised Approach

After completion of parameter estimation process using the raw flight data, the corrected flight data obtained after the data compatibility checks was taken up for analysis. During the data compatibility checks on the raw flight data, the correction factors given in Table 2.7 of Chapter 2 were used. The same procedure as was used for the raw flight data, was utilized here for parameter estimation by the Delta method. In this case also, the combined training files for the four speeds, V_i = 160, 180, 200 and 220 KIAS were prepared. The actual aerodynamic coefficient C_l, C_n and C_y were calculated using Eq. (2.4), (2.5) and (3.6). Next, the aerodynamic modeling using the FFNN was carried out for the corrected flight data. Figures 3.27a, 3.27b and 3.27c shows the plot of actual and predicted (after training) aerodynamic coefficients obtained for a typical

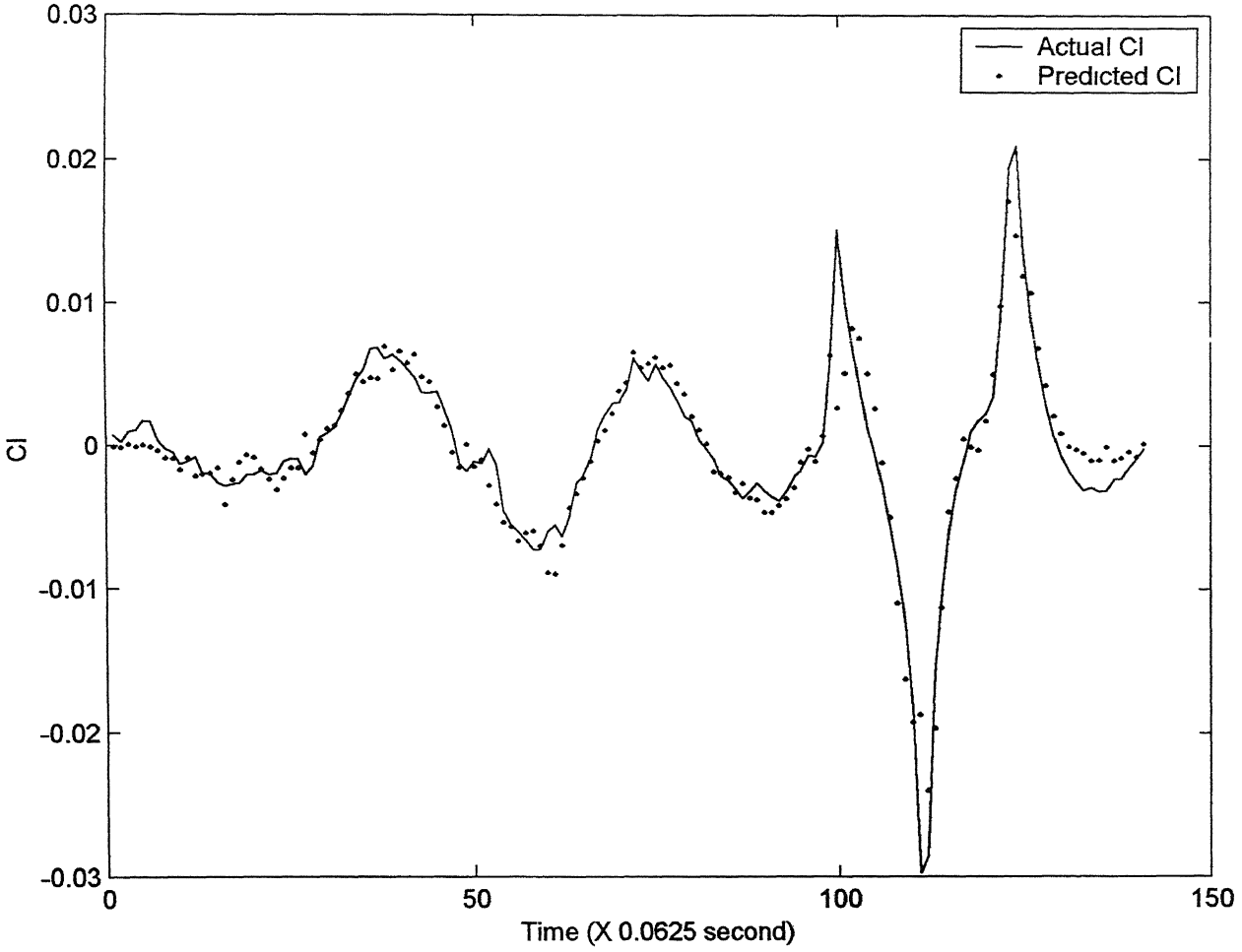

Fig. 3.27a Plot Of Actual And Predicted (After Training) Cl For Combined Test Point FLT5/TP17-22,Vi=200 KIAS For Corrected Data

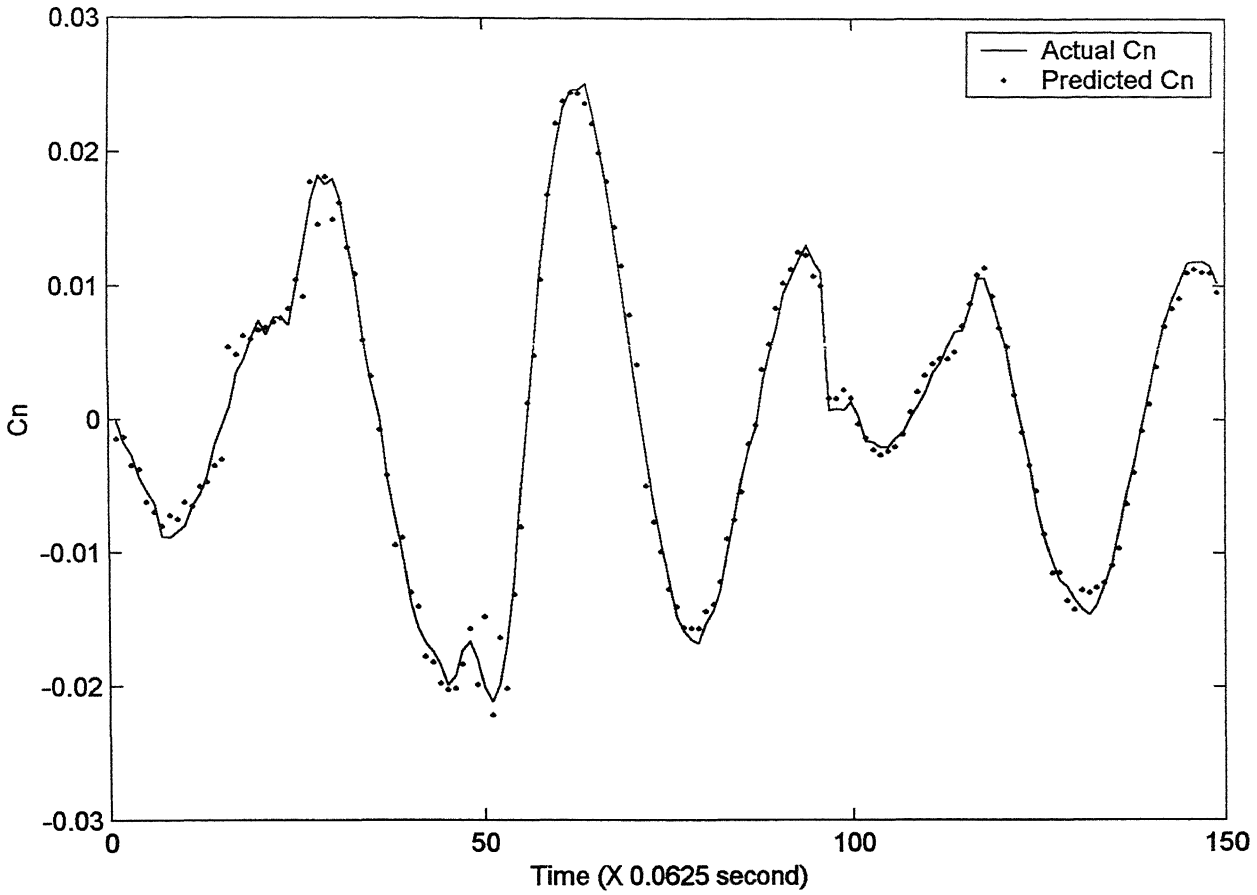

Fig. 3.27b Plot Of Actual And Predicted (After Training) Cn For Combined Test Point FLT5/TP17-22,Vi=200 KIAS For Corrected Data

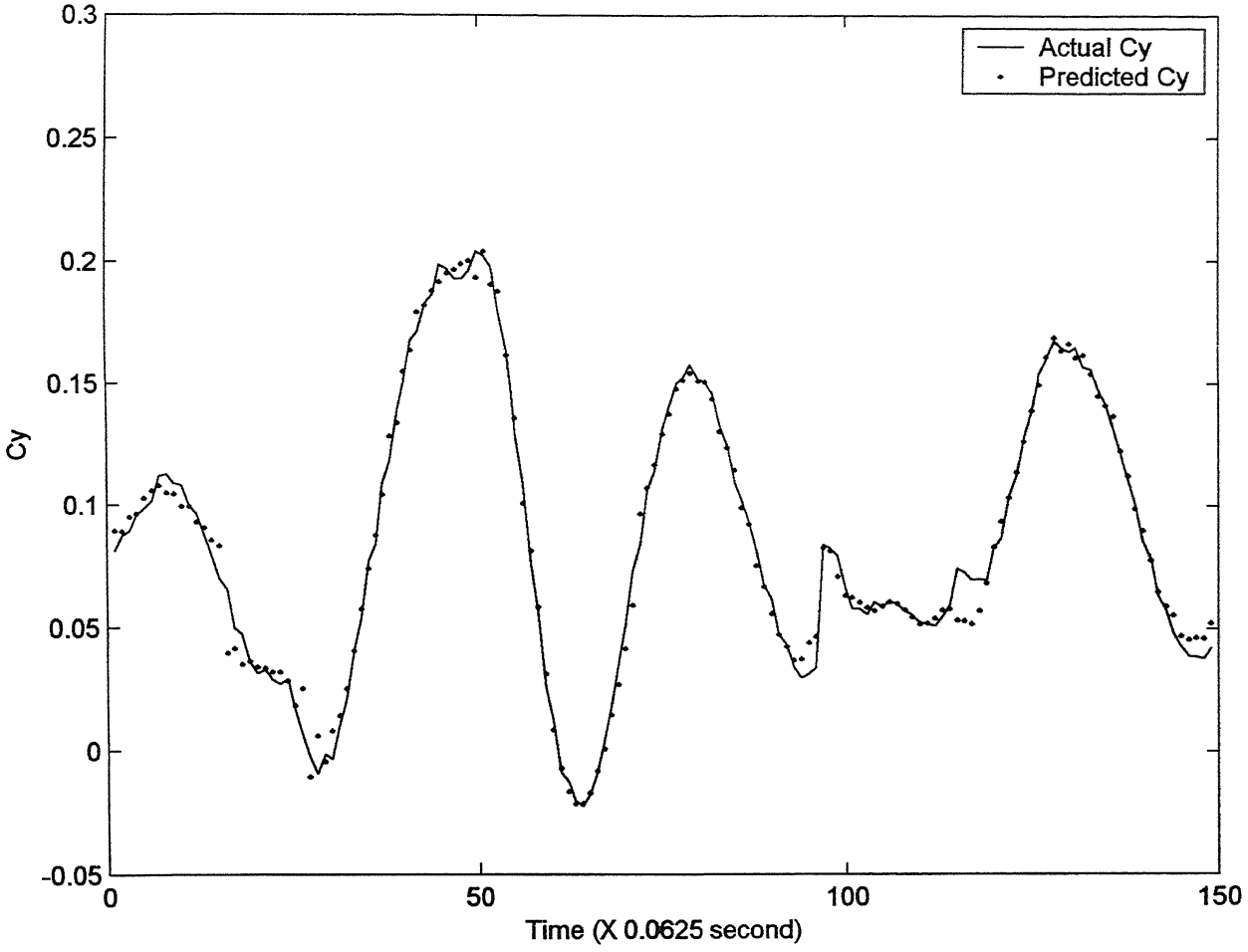

Fig. 3.27c Plot Of Actual And Predicted (After Training) Cy For Combined Test Point FLT5/TP17-22,Vi=200 KIAS For Corrected Data

combined test point. From Fig. 3.27a, 3.27b and 3.27c, it is seen that good training of the FFNN has taken place. The Delta method was then used to estimate the parameters from this trained FFNN.

The results of the estimation process using the Delta method for the corrected flight data is presented in Table 3.11. A study of these results shows that the strong derivatives, C_{lp} , $C_{l\beta}$ and $C_{l\delta a}$ have been estimated reasonably well (refer rows 1, 3 and 4 of Table 3.11). For the control derivative $C_{n\delta r}$, except for test point FLT5/TP24_28, (V_i = 220 KIAS), a good match is obtained for the remaining three test points (refer row 10 of Table 3.11). In addition, the cross derivatives, $C_{l\delta r}$ and $C_{n\delta a}$ are estimated consistently with reasonable accuracy as indicated by the low standard deviation (refer row 5 and 9 of Table 3.11). In this case too, it is found that the estimate for C_{lr} for test point FLT5/TP9-14, (V_i = 180 KIAS) is quite low with a high standard deviation (refer row 2 of Table 3.11). But the estimate of C_{lr} for remaining three data sets matches very well, with low standard deviation being obtained in each case.

The estimates for $C_{l\beta}$, $C_{n\beta}$ and $C_{y\beta}$ derivatives shows good match for all the test points analyzed for the corrected flight data. However, from Table 3.11, it is seen that for corrected flight data, the weak derivatives C_{yp} , C_{yr} and $C_{y\delta a}$ have not been successfully estimated.

On comparing the results, for the raw flight data (Table 3.9) with the corrected flight data (Table 3.11), it is observed that the estimates for derivative, C_{lp} , $C_{l\beta}$, $C_{l\delta a}$, $C_{l\delta r}$, C_{np}, C_{nr}, $C_{n\beta}$, $C_{n\delta a}$ and $C_{n\delta r}$ are fairly consistent. However, for $C_{y\beta}$ it is seen that slightly lower values are obtained for the corrected flight data. Thus, the Delta method is

capable of extracting parameters from the raw as well as from the corrected flight data for lateral-directional motion.

In order to check the accuracy of the estimates obtained from the corrected flight data, the estimated and actual (measured) aerodynamic coefficient,- C_l , C_n and C_y were compared. The parameters C_{lo} , C_{no} and C_{yo} for the corrected flight data were estimated as was done for raw flight data. The results of the estimates for the parameters C_{lo} , C_{no} and C_{yo} are presented in Table 3.12.

Figures 3.28, 3.29, 3.30 and 3.31 show the plots of the actual (measured) and estimated lateral-directional aerodynamic coefficients for the corrected flight data for all the combined test points. These figures reveal that although a good match is obtained for C_n and C_y , in this case too, the same peculiarity for C_l is observed, as was seen for the raw flight data. In view of the good match obtained (refer Fig. 3.28, 3.29, 3.30 and 3.31), it can be stated that the parameter estimated using the Delta method are fairly accurate.

After completion of the parameter estimation process for the lateral directional case, the distribution of the parameter estimated using the Delta method from raw flight data was plotted and is as shown in Fig. 3.32. From the figure, it is seen that all the strong derivatives have been estimated with a very small scatter.

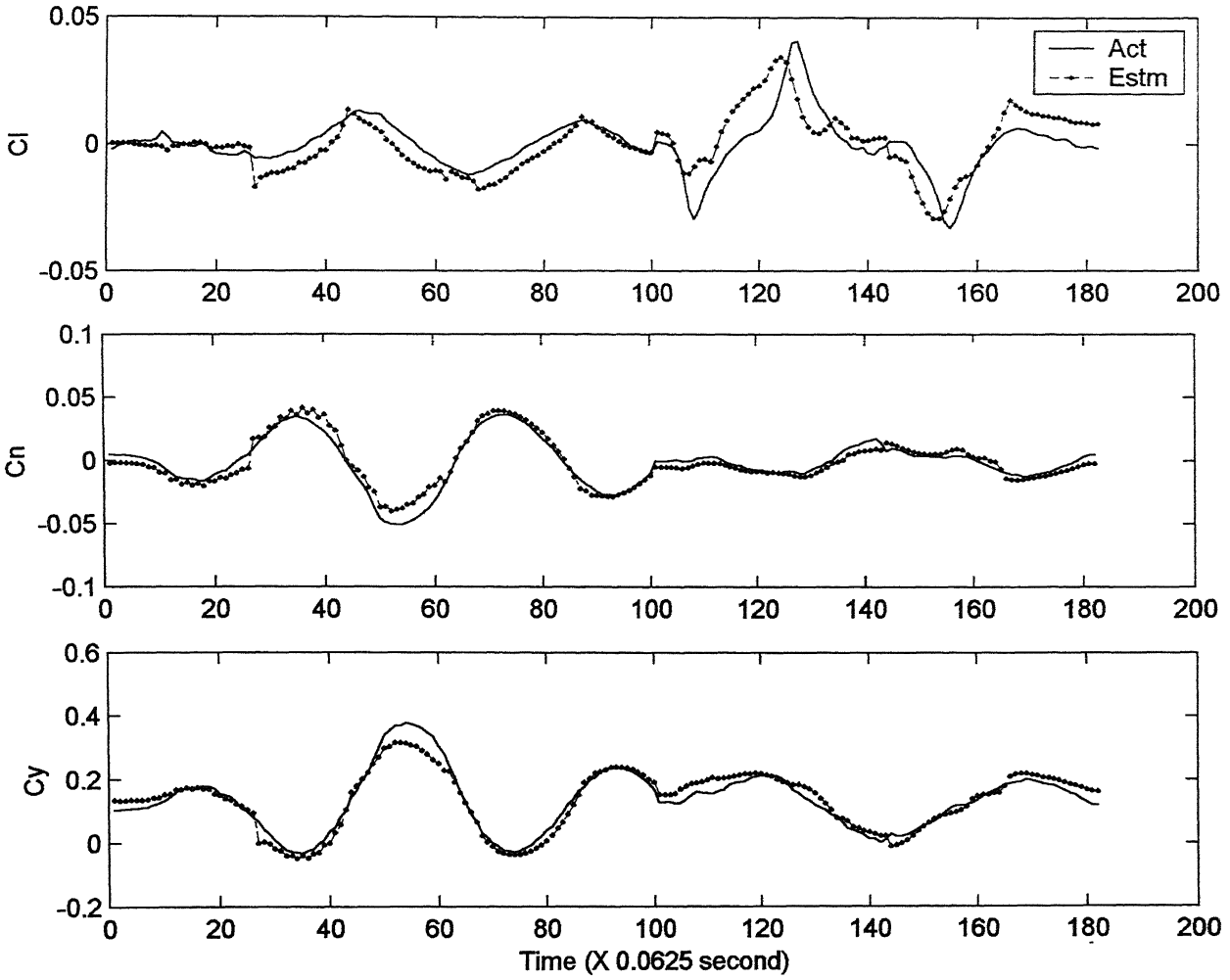

Fig. 3.28 Comparision of Actual And Estimated Total Aerodynamic Coefficients For FLT5/TP1-5,Vi=160 KIAS For Corrected Data

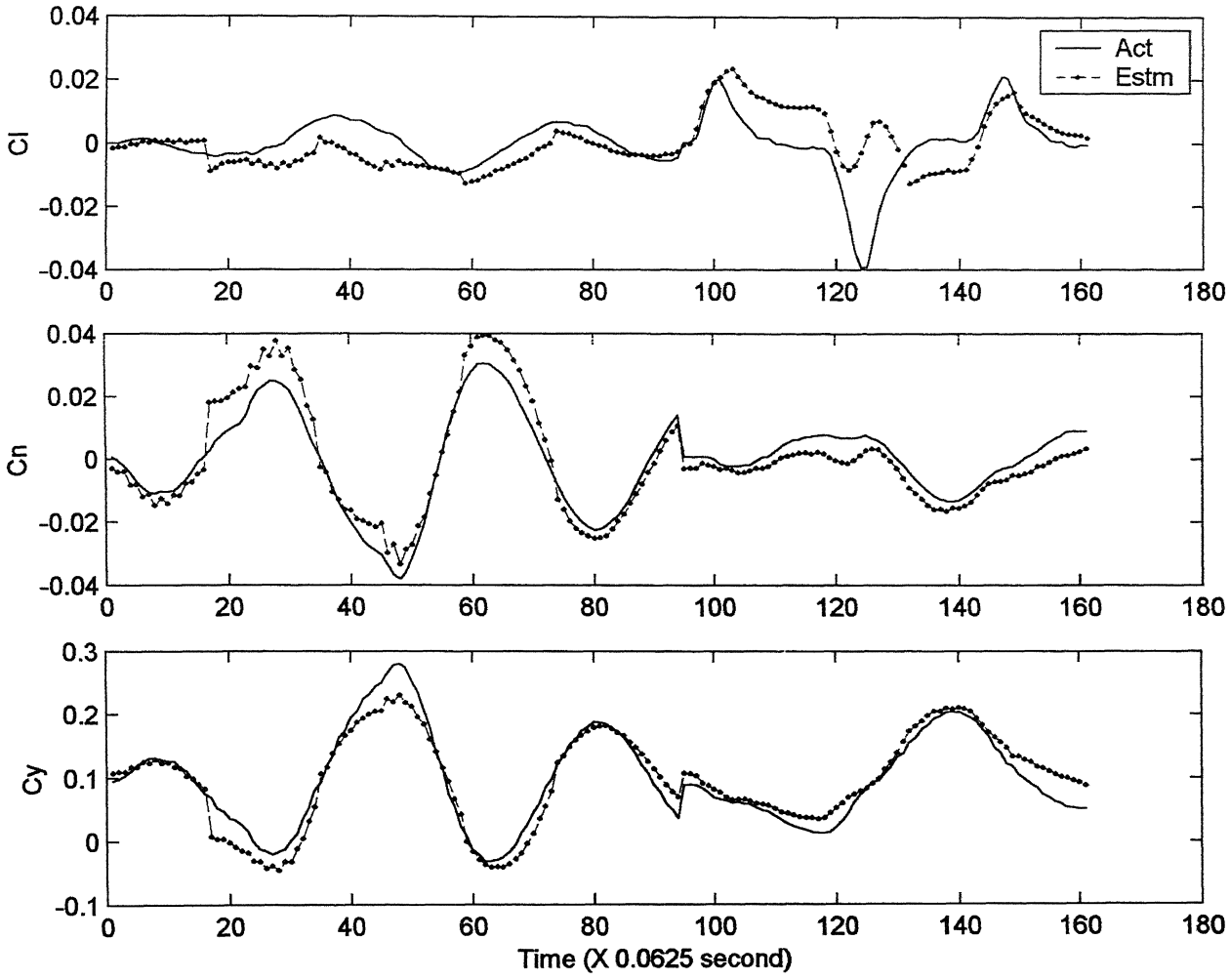

Fig. 3.29 Comparision of Actual And Estimated Total Aerodynamic Coefficients For FLT5/TP9-14,Vi=180 KIAS For Corrected Data

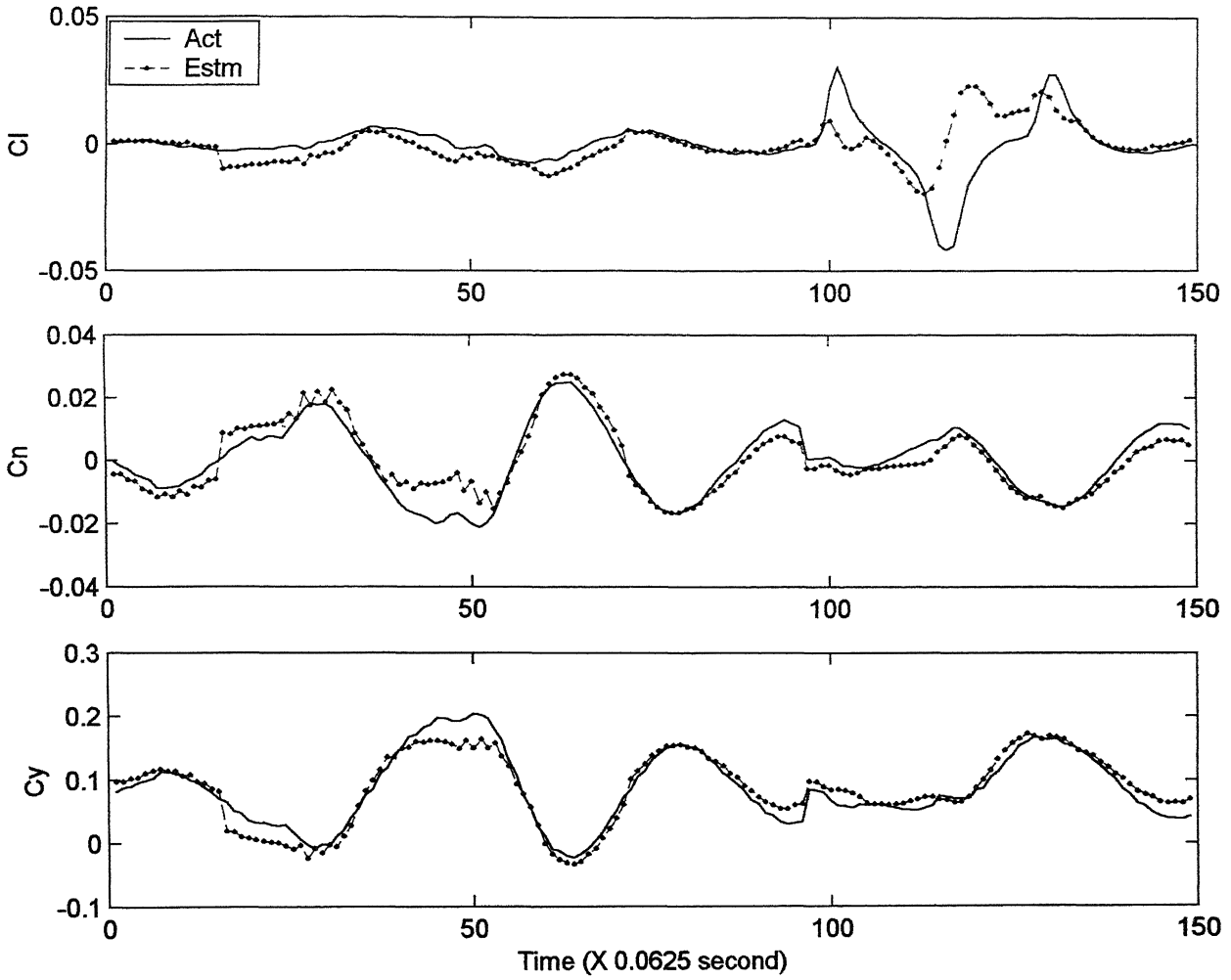

Fig. 3.30 Comparision of Actual And Estimated Total Aerodynamic Coefficients For FLT5/TP17-22,Vi=200 KIAS For Corrected Data

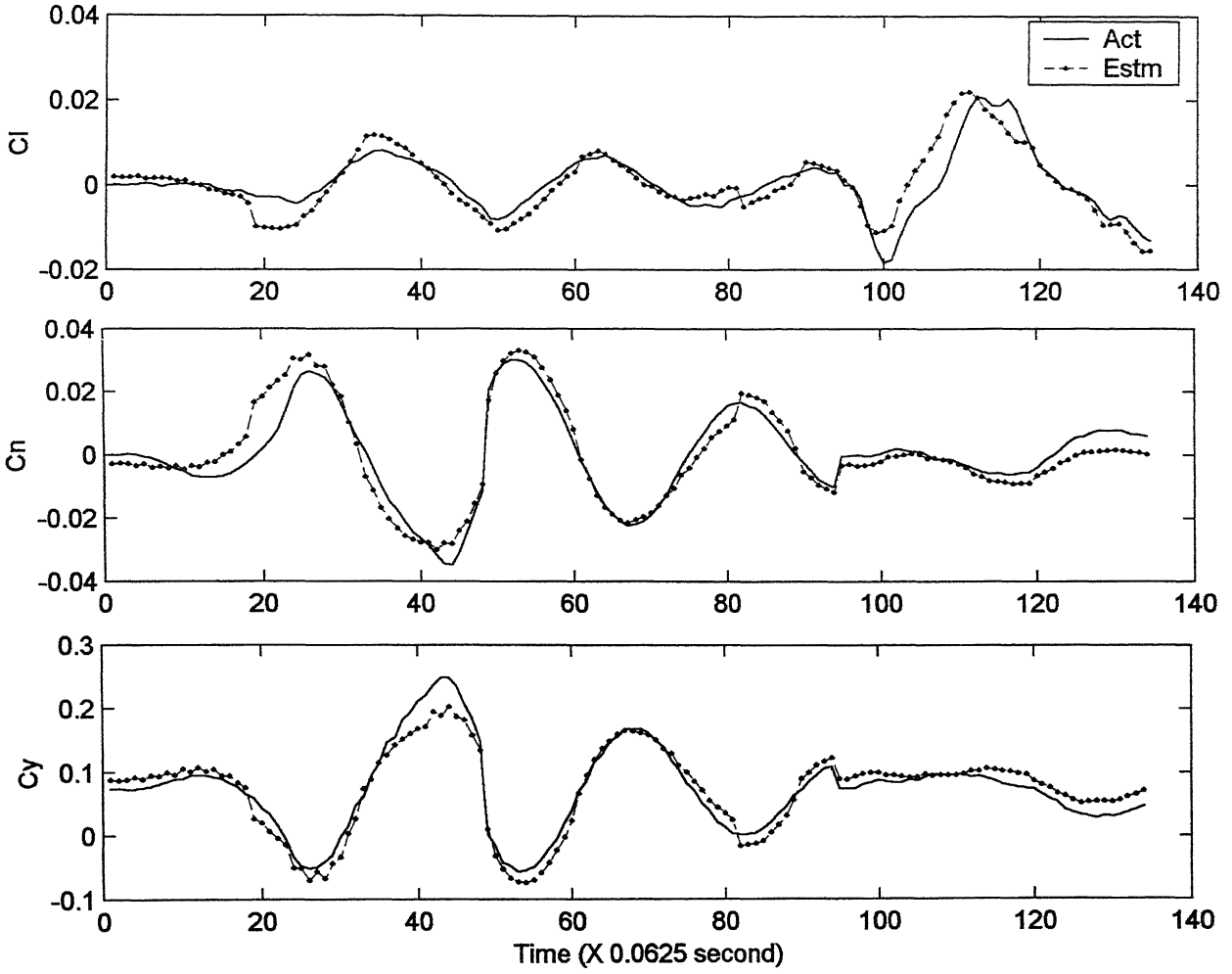

Fig. 3.31 Comparision of Actual And Estimated Total Aerodynamic Coefficients For FLT5/TP24-28,Vi=220 KIAS For Corrected Data

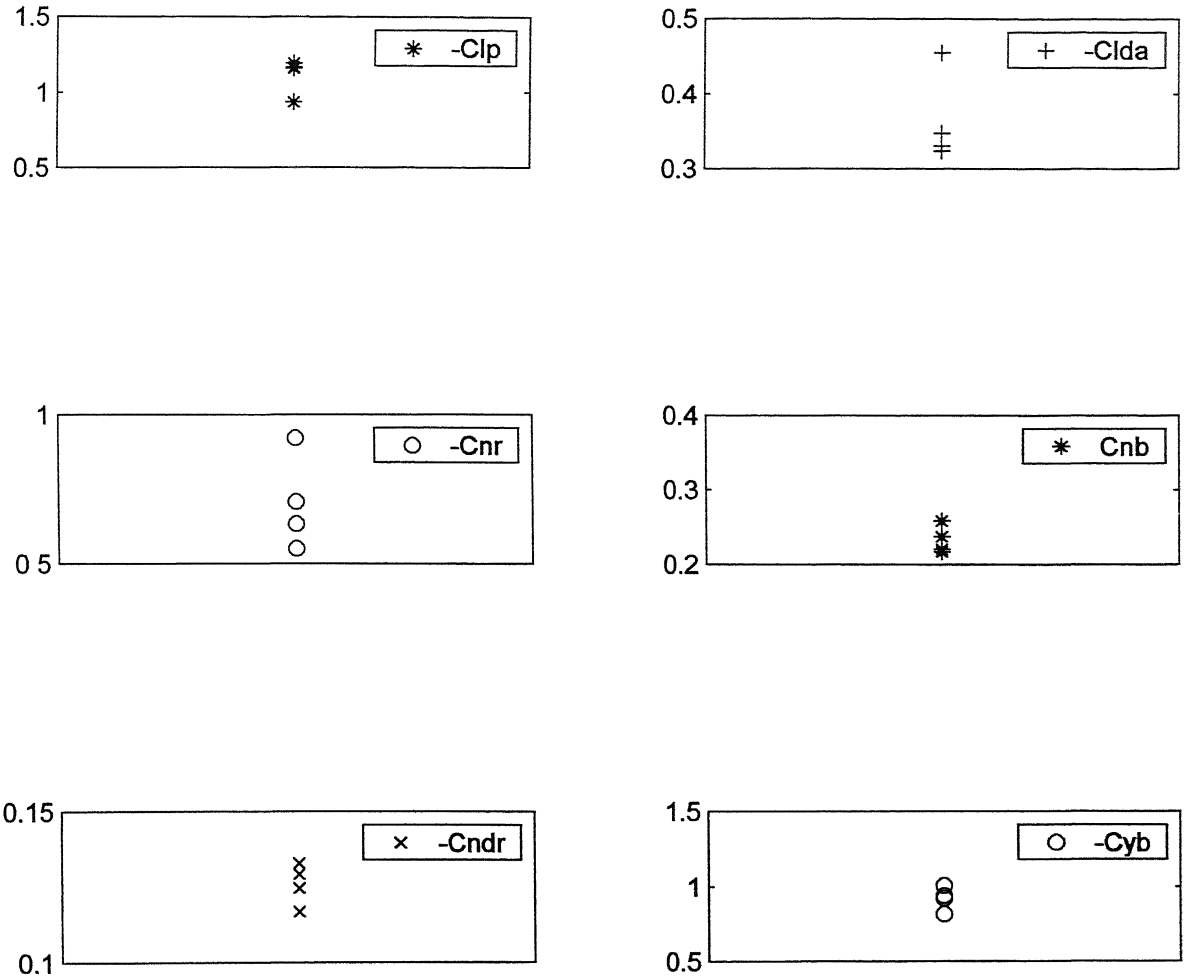

Fig. 3.32 Plot Showing The Distribution Of The Parameters Estimated Using The Delta Method From The Raw Flight Data

Table 3.1 Parameter Estimates From Simulated Data For Longitudinal Motion

Parameter (Per Radian)	True Value	Estimates for V_t = 160 KIAS			
		NO NOISE	**5% NOISE**	**10% NOISE**	**15% NOISE**
$C_{L\alpha}$	4 9	4 8841 (0 0476)*	4 8239 (0 0914)	4 9258 (0.0291)	4.9583 (0 0928)
C_{Lq}	10 0	9 7981 (0 0053)	8.7800 (0.0170)	10 4331 (0.0035)	9 0537 (0 0072)
$C_{L\delta e}$	0 4	0 4136 (0 0225)	0.3808 (0.0154)	0 4038 (0.0099)	0 3675 (0 0177)
$C_{m\alpha}$	-0 60	-0 5991 (0 0032)	-0 6090 (0 0075)	-0.5844 (0.0160)	-0.6052 (0 0107)
C_{mq}	-13.0	-12.7540 (0.0012)	-12.7868 (0.0024)	-13 4546 (0.0077)	-11 1557 (0 0035)
$C_{m\delta e}$	-0 68	-0.6753 (0 0044)	-0.6849 (0.0063)	-0 6780 (0.0182)	-0 6640 (0 0140)

* Standard Deviation

Table 3.2a Parameter Estimates from Raw Flight Data Using Delta Method of FFNN for FLT3

Parameter (Per Radian)	FLT3/TP2 (V_i = 160 KIAS)	FLT3/TP13 (V_i = 180 KIAS)
$C_{L\alpha}$	3 8822 (0.5481)*	4.0894 (0.4596)
C_{Lq}	46 8668 (0 3942)	15 67932 (0 2836)
$C_{L\delta e}$	-0 6139 (0 9352)	-0 8556 (0 4080)
$C_{m\alpha}$	-0.4689 (0 1410)	-0 4178 (0.0867)
C_{mq}	-13 3999 (0.0413)	-15 5018 (0 0270)
$C_{m\delta e}$	-0.8649 (0.1676)	-0 8028 (0 0514)

* Standard Deviation

Table 3.2b Parameter Estimates from Raw Flight Data Using Delta Method of FFNN for FLT4

Parameters (Per Radian)	Estimated Parameters					
	V_i = 160 KIAS		V_i = 180 KIAS		V_i = 220 KIAS	
	FLT4/TP1	FLT4/TP2	FLT4/TP7	FLT4/TP8	FLT4/TP14	FLT4/TP15
$C_{L\alpha}$	4.0315 (0.5841)*	3.5286 (0.4986)	4.0538 (0.5258)	4.2679 (0.5045)	4.2349 (0.2674)	4.1688 (0.3853)
C_{Lq}	-4.4228 (0.1560)	8.4112 (0.6954)	19.1345 (0.2818)	21.3603 (0.1537)	33.4108 (0.3254)	-164.9325 (0.2874)
$C_{L\delta e}$	-1 0360 (0.1576)	0.1017 (0.4208)	-1.1353 (0.1898)	-1.0966 (0.2740)	-0.9425 (0.1361)	-1.7926 (0.2559)
$C_{m\alpha}$	-0.4575 (0.0918)	-0.4146 (0.0370)	-0.4278 (0.0776)	-0.3017 (0.0763)	-0.3948 (0.1089)	-0.3984 (0.0905)
C_{mq}	-11.8338 (0.0308)	-12.9635 (0.0105)	-9.9484 (0.0192)	-11.7315 (0.0418)	-8.8664 (0.0554)	-11.8404 (0.0290)
$C_{m\delta e}$	-0.6659 (0 0623)	-0.7258 (0.0601)	-0.5907 (0.0958)	-0.6738 (0.0523)	-0.5392 (0.1778)	-0.5556 (0.0321)

*Standard Deviation

Table 3.3a Parameter Estimates from Raw Flight Data Using MLE Method for FLT3

Parameter (Per Radian)	FLT3/TP2 (V_i = 160 KIAS)	FLT3/TP13 (V_i = 180 KIAS)
$C_{L\alpha}$	4 1610 (0 2978)*	4 6630 (0 5932)
C_{Lq}	117 3570 (20 0271)	241 2067 (23 5703)
$C_{L\delta e}$	2 1487 (0 5618)	4 6854 (0 7942)
$C_{m\alpha}$	-0 5469 (0 01936)	-0.5766 (0 0364)
C_{mq}	-12 0034 (1 2316)	-12.5565 (1 9991)
$C_{m\delta e}$	-0 8063 (0 03669)	-0 7519 (0.0399)

* Cramer Rao Bounds

Table 3.3b Parameter Estimates from Raw Flight Data Using MLE Method for FLT4

Parameters (Per Radian)	Estimated Parameters					
	V_i = 160 KIAS		V_i = 180 KIAS		V_i = 220 KIAS	
	FLT4/TP1	FLT4/TP2	FLT4/TP7	FLT4/TP8	FLT4/TP14	FLT4/TP15
$C_{L\alpha}$	3.0323 (0.5342)*	3 3498 (0.2736)	4.1470 (0.3805)	4.4009 (0.4005)	4.3089 (0.5734)	4.6888 (0.1622)
C_{Lq}	92.0340 (35.1748)	61.2018 (16.7365)	8.1656 (30.1511)	-0.7120 (38.6795)	-33.0609 (43.1463)	5.3840 (15.2477)
$C_{L\delta e}$	-1.3717 (0.7773)	1 1173 (0.3621)	-1.5487 (0.7018)	-0.1264 (0.7371)	-2.5254 (0.9482)	-0.6695 (0.2637)
$C_{m\alpha}$	-0.4786 (0.0303)	-0.5106 (0 0157)	-0.4101 (0.0186)	-0.3645 (0.0196)	-0.4693 (0.0275)	-0.3337 (0.0078)
C_{mq}	-12 9971 (1.8550)	-10 3704 (0.9138)	-12.2168 (1.3698)	-16.1278 (1.8551)	-8.2094 (2.0564)	-17.6743 (0.7868)
$C_{m\delta e}$	-0 6718 (0.0362)	-0.7225 (0.0244)	-0.6879 (0.0291)	-0.7167 (0.0409)	-0.5764 (0.0410)	-0.6888 (0.0168)

*Cramer Rao Bounds

Table 3.4 Estimates of Parameters C_{Lo} and C_{mo} from Raw Flight Data (Longitudinal Motion)

Parameter	Test Points		
	FLT3/TP2 (V_I = 160 KIAS)	FLT3/TP13 (V_I = 180 KIAS)	FLT4/TP14 (V_I = 220 KIAS)
C_{Lo}	0.1602	0.1178	0.0255
C_{mo}	0.0067	0.0263	0.0152

Table 3.5a Parameter Estimates from Corrected Flight Data Using Delta Method of FFNN for FLT3

Parameter (Per Radian)	FLT3/TP2 (V_i = 160 KIAS)	FLT3/TP13 (V_i = 180 KIAS)
$C_{L\alpha}$	4 0101 (0 6019)*	3.9773 (0 2218)
C_{Lq}	-119 0009 (0 3928)	-245 8390 (0 2731)
$C_{L\delta e}$	-2 2421 (0 7699)	-2.7677 (0 7701)
$C_{m\alpha}$	-0 3684 (0.0451)	-0 3693 (0.1226)
C_{mq}	-14 1881 (0.0125)	-15.9615 (0 0201)
$C_{m\delta e}$	-0.7843 (0 0836)	-0.7824 (0.0767)

* Standard Deviation

Table 3.5b Parameter Estimates from Corrected Flight Data Using Delta Method of FFNN for FLT4

Parameters	Estimated Parameters					
	V_i = 160 KIAS		V_i = 180 KIAS		V_i = 220 KIAS	
	FLT4/TP1	FLT4/TP2	FLT4/TP7	FLT4/TP8	FLT4/TP14	FLT4/TP15
$C_{L\alpha}$	3 9771 (0.5696)*	3.6265 (0.5502)	3.9591 (0.6031)	3.9457 (0.4768)	4 0128 (0.5414)	4.1885 (0.5699)
C_{Lq}	-91.6920 (0.2968)	-121.348 (0.3769)	-169.258 (0.6516)	-150.211 (0 2489)	-126.1590 (0.4613)	-120.447 (0.1464)
$C_{L\delta e}$	-1.8121 (0.2525)	-0.6605 (1.4762)	-2.0517 (0.6930)	-1.6120 (0.7649)	-2.1410 (0.2065)	-0.9724 (0.3360)
$C_{m\alpha}$	-0 3524 (0 0975)	-0.3447 (0.0278)	-0.3023 (0.0585)	-0 2463 (0 0941)	-0.3059 (0.0529)	-0.3410 (0.0898)
C_{mq}	-14.9427 (0.0418)	-15.2054 (0.0053)	-9.9065 (0.0133)	-11.3851 (0.0386)	-9.1861 (0 0070)	-12.4383 (0.0440)
$C_{m\delta e}$	-0.7397 (0.0935)	-0.7299 (0.0572)	-0.5797 (0.0528)	-0.6133 (0 0977)	-0.5754 (0.0511)	-0.5526 (0.0653)

*Standard Deviation

Table 3.6a Parameter Estimates from Corrected Flight Data Using MLE Method for FLT3

Parameter (Per Radian)	FLT3/TP2 (V_i = 160 KIAS)	FLT3/TP13 (V_i = 180 KIAS)
$C_{L\alpha}$	4.1527 (0 4227)*	4 3309 (0 3060)
C_{Lq}	-25 6215 (34 2281)	4 3663 (28 9447)
$C_{L\delta e}$	2 5199 (1 0732)	4 9117 (0 7745)
$C_{m\alpha}$	-0 4012 (0 0171)	-0.3379 (0 0119)
C_{mq}	-12.2771 (1 5311)	-14.5814 (1 2183)
$C_{m\delta e}$	-0 8202 (0 0393)	-0 7771 (0 0262)

* Cramer Rao Bounds

Table 3.6b Parameter Estimates from Corrected Flight Data Using MLE Method for FLT4

Parameters	Estimated Parameters					
	V_i = 160 KIAS		V_i = 180 KIAS		V_i = 220 KIAS	
	FLT4/TP1	FLT4/TP2	FLT4/TP7	FLT4/TP8	FLT4/TP14	FLT4/TP15
$C_{L\alpha}$	2.5457 (0.5176)*	3.3539 (0.2764)	4.0731 (0.3876)	4.0638 (0.4680)	4.5975 (0.7153)	5.2662 (0.5025)
C_{Lq}	18 9475 (38.3206)	-41.3614 (21 5061)	-136 032 (39.9195)	23.3044 (41 2101)	-331.742 (81.9075)	-302.2495 (72.1770)
$C_{L\delta e}$	-0.7376 (0 7326)	0.9846 (0.5009)	-2.2189 (0.9258)	0.0269 (0.7929)	-4.2933 (1.6929)	-2.6445 (1.4310)
$C_{m\alpha}$	-0 4061 (0.0259)	-0 4181 (0.0128)	-0.3155 (0.0146)	-0 3909 (0.0236)	-0.3518 (0.0243)	-0.2615 (0.0157)
C_{mq}	-12 0530 (1.7880)	-11.1397 (0.9603)	-12.3961 (1.3975)	-13.5502 (1 9995)	-10.4634 (2.6737)	-17.2019 (1.8072)
$C_{m\delta e}$	-0.6263 (0.0392)	-0.7433 (0.0251)	-0.6876 (0.0299)	-0.6472 (0.0420)	-0.6100 (0.0503)	-0.6706 (0.0285)

*Cramer Rao Bounds

Table 3.7 Estimates of C_{Lo} and C_{mo} from Corrected Flight Data (Longitudinal Motion)

Parameter	Test Points		
	FLT3/TP2 (V_I = 160 KIAS)	FLT3/TP13 (V_I = 180 KIAS)	FLT4/TP14 (V_I = 220 KIAS)
C_{Lo}	0.1192	0.0751	-0.0064
C_{mo}	0.0023	0.0078	0.0172

Table 3.8 Parameter Estimates From Simulated Data (Lateral-directional Motion) Using MLE Method

Parameter	True Values of Parameters	Starting Guess Values	Estimates
C_{lp}	-1 2032	-0 6016	-1 2032 (1 0946x10^{-6})*
C_{lr}	0 1893	0 1867	0 1893 (2.6677x10^{-7})
$C_{l\beta}$	-0 1444	-0 1108	-0 1444 (1 1420x10^{-7})
$C_{l\delta r}$	0 0318	0 0363	0 0318 (1 3400x10^{-8})
C_{np}	-0 2101	-0.2347	-0 2101 (1 4870x10^{-6})
C_{nr}	-0 8050	-1.1188	-0 8050 (3 5481x10^{-7})
$C_{n\beta}$	0 1927	0 2189	0.1927 (1.5513x10^{-7})
$C_{n\delta r}$	-0 1649	-0.1405	-0.1649 (1.8218x10^{-8})
C_{yp}	0 9903	1.0771	0.9903 (7.2330x10^{-5})
C_{yr}	1 5937	1.2233	1.5937 (1.7336x10^{-5})
$C_{y\beta}$	-0.7726	-0.7691	-0.7726 (7 5400x10^{-6})
$C_{y\delta r}$	0 3016	0 2983	0.3016 (8.6147x10^{-7})

*Cramer Rao Bounds

Table 3.9 Parameter Estimates from Raw Flight Data using Delta Method of FFNN (Lateral-Directional Motion)

Parameter	Estimates			
	FLT5/TP1_5 (V_t = 160 KIAS)	FLT5/TP9_14 (V_t = 180 KIAS)	FLT5/TP17_22 (V_t = 200 KIAS)	FLT5/TP24_28 (V_t = 220 KIAS)
C_{lp}	-1.1646 (0 1832)*	-1.1585 (0 2845)	-1 1935 (0 0856)	-0.9354 (0.1898)
C_{lr}	0 4269 (0 2550)	0 1143 (0 3794)	0 3841 (0 0507)	0.3484 (0.0834)
$C_{l\beta}$	-0 1658 (0 0445)	-0.1132 (0 0800)	-0 1873 (0 0346)	-0.1285 (0.0206)
$C_{l\delta a}$	-0 4542 (0 0879)	-0.3236 (0.0875)	-0.3473 (0 0460)	-0 3302 (0.0437)
$C_{l\delta r}$	0.0227 (0 0430)	0.0564 (0 0910)	0 0339 (0.0088)	0.0307 (0 0083)
C_{np}	-0 2481 (0 0908)	-0.1812 (0 0971)	-0.1937 (0 0494)	-0.1280 (0.0633)
C_{nr}	-0 9207 (0.2688)	-0 7074 (0.0460)	-0.6328 (0.0828)	-0.5505 (0.2022)
$C_{n\beta}$	0.2376 (0 0408)	0.2588 (0.0263)	0 2173 (0.0263)	0.2205 (0.0179)
$C_{n\delta a}$	-0.0730 (0.0293)	-0.0509 (0.0361)	-0.0343 (0.0244)	-0.0640 (0.0400)
$C_{n\delta r}$	-0 1293 (0.0423)	-0.1247 (0.0157)	-0.1330 (0.0077)	-0.1168 (0.0407)
C_{yp}	3.0455 (1.3590)	0.7622 (0.2334)	1.0884 (0.3803)	0.3726 (0.1989)
C_{yr}	3.9751 (0.8872)	0.9599 (0.6629)	1 4527 (1 2308)	2.0186 (0.5459)
$C_{y\beta}$	-0.8169 (0.0919)	-1.0063 (0.0756)	-0.9227 (0.0835)	-0.9406 (0.0580)
$C_{y\delta a}$	0.8754 (0.3232)	0.3081 (0.0890)	0.2527 (0.1015)	0.1210 (0.0902)
$C_{y\delta r}$	0.3633 (0.1249)	0.1314 (0.1473)	0.3144 (0 0789)	0.3161 (0.0892)

* Standard Deviation

Table 3.10 Estimates of Parameters C_{lo} , C_{no} and C_{yo} for Raw Flight Data (Lateral and Directional Motion)

Parameter	Test Points			
	FLT5/TP1_5 (V_i = 160 KIAS)	FLT5/TP9_14 (V_i = 180 KIAS)	FLT5/TP17_22 (V_i = 200 KIAS)	FLT5/TP24_28 (V_I = 220 KIAS)
C_{lo}	-0.0086	-0.0100	-0.0136	-0.0079
C_{no}	0.0114	0.0154	0.0130	0.0132
C_{yo}	-0.0631	-0.0788	-0.0723	-0.0722

Table 3.11 Parameter Estimates from Corrected Flight Data using Delta Method of FFNN (Lateral-Directional Motion)

Parameter	Estimates			
	FLT5/TP1_5 (V_i = 160 KIAS)	FLT5/TP9_14 (V_i = 180 KIAS)	FLT5/TP17_22 (V_i = 200 KIAS)	FLT5/TP24_28 (V_i = 220 KIAS)
C_{lp}	-1 2032 (0 1925)*	-0.9370 (0.0858)	-1 0820 (0 0802)	-1.0928 (0.0746)
C_{lr}	0 1893 (0 0717)	0.0648 (0 2318)	0 2703 (0 1889)	0 2497 (0.1578)
$C_{l\beta}$	-0 1444 (0.0559)	-0 1214 (0.0658)	-0 1299 (0 0271)	-0.1137 (0.0109)
$C_{l\delta a}$	-0 3674 (0 0573)	-0 3913 (0 0813)	-0 3213 (0.0575)	-0.3348 (0.0634)
$C_{l\delta r}$	0 0318 (0.0295)	0.0497 (0.0626)	0 0367 (0 0066)	-0.0029 (0.0197)
C_{np}	-0 2101 (0 0586)	-0 2618 (0.0414)	-0.2290 (0 0654)	-0.1274 (0.0955)
C_{nr}	-0 8050 (0.0975)	-0.7993 (0.0898)	-0.6380 (0 1254)	-0.5783 (0.3960)
$C_{n\beta}$	0 1927 (0 0341)	0.2417 (0 0374)	0 1858 (0 0454)	0.1764 (0.0355)
$C_{n\delta a}$	-0.0374 (0.0457)	-0.0621 (0.0200)	-0.0614 (0.0304)	-0.0130 (0.0461)
$C_{n\delta r}$	-0.1649 (0.0206)	-0.1608 (0.0537)	-0.1437 (0.0289)	-0.0584 (0.0538)
C_{yp}	0 9903 (0.4962)	0.5539 (0.4837)	0.7841 (0.1205)	0.6700 (0.5315)
C_{yr}	1.5937 (1.3165)	1.0330 (1.0157)	2.1450 (0.4641)	1.5405 (0.8601)
$C_{y\beta}$	-0.7726 (0.0866)	-0.8529 (0.0804)	-0 7864 (0 0961)	-0.8064 (0.0809)
$C_{y\delta a}$	0.5976 (0.1816)	0.4375 (0.1415)	0 4255 (0 0929)	0.2461 (0.1095)
$C_{y\delta r}$	0.3016 (0.2391)	0.2981 (0.1655)	0 3616 (0.1097)	0.4173 (0.1319)

* Standard Deviation

Table 3.12 Estimates of Parameters C_{lo} , C_{no} and C_{yo} for The Corrected Flight Data (Lateral-Directional Motion)

Parameter	Test Points			
	FLT5/TP1_5 (V_i = 160 KIAS)	FLT5/TP9_14 (V_i = 180 KIAS)	FLT5/TP17_22 (V_i = 200 KIAS)	FLT5/TP24_28 (V_i = 220 KIAS)
C_{lo}	-0.0020	-0.0039	-6.3368×10^{-4}	0.0014
C_{no}	9.2389×10^{-4}	7.3766×10^{-4}	-0.0019	-0.0017
C_{yo}	0.1233	0.0935	0.0930	0.0835

CHAPTER 4

CONCLUSIONS AND RECOMMENDATIONS

4.1 CONCLUSIONS

In the present work, the Delta method using FFNNs has been used to estimate the stability and control derivatives from the real flight data, pertaining to longitudinal and lateral-directional dynamics. The Delta method has been used to extract the parameters from the raw as well as the corrected flight data. The results of the parameter estimates obtained from the Delta method in each case, show good consistency with low standard deviation. Further, a close match is obtained between the estimated and actual aerodynamic coefficients as well as between the estimated and measured responses. This implies that the Delta method estimates are fairly accurate. The Delta method has been found to be a simple and straight forward method that can be set up very quickly. Moreover, unlike the conventional output error methods (ML), the Delta method does not require any knowledge of the initial guess values of the parameters. Further, the output error methods will require integration of system equations of motion. This step is bypassed in the Delta method. This is a distinct advantage of the Delta method. In fact, it can be used to give a quick look at the values of the parameters, if so be desired. Subsequently, with little additional fine tuning of the network, reasonably good estimates can be obtained, as seen in the present work. This method has been proven to be a robust method, which can extract parameters even from the raw flight data using the measured values of the motion variables that are not corrected for bias and scale factor errors.

4.2 RECOMMENDATIONS

Based on the experience gathered during the present work, a few recommendations are suggested for future work:

1. For the parameter estimation for lateral-directional motion, instead of giving separate δa and δr inputs, a combined input should be tested, wherein the δr input is given first and following 1-2 second delay the δa input should be given.

2. The data analysis in the present work for the Delta method (on real flight data) was done only in the time domain. It would be of great interest, to see how the results compare. with the same analysis being done in the frequency domain.

3. The different architectures of FFNN in the present work were obtained by using a few functions/features of the Matlab Neural Network Toolbox. This aspect can be investigated in greater detail by using all the different functions to see the improvements if any, in the results.

4. The criterion used for freezing the optimal FFNN architecture during training phase was the minimum training MSE criterion. Other criteria could be investigated which may possibly lead to better training and hence improved prediction capability of the FFNN.

5. Future projects, along the lines of the present work, could be jointly undertaken by IIT Kanpur and ASTE, AF, Bangalore to explore the high angle of attack regime, as well as for parameter estimation of open loop unstable aircraft.

REFERENCES

1 Seckel, E and Morris, J J , "The Stability Derivatives of the Navion Aircraft Estimated by Various Methods and Derived from Flight Test Data," FAA-RD-71-6

2 Seckel, E , "Stability and Control of Airplanes and Helicopters, Academic Press, New York, 1964

3 Hoak, D E and Ellision, D E., "USAF Stability and Control DATCOM; Air Force Flight Dynamics Laboratory, Wright Patterson Airforce Base, Ohio, 1960, revised 1975

4. Shinbrot, M., "A Least Square Curve Fitting Method with Applications to the Calculation of Stability Coefficients from Transient Response Data," NACA TN-2341.

5. Iliff, K. W., "Parameter Estimation for Flight Vehicle," Journal of Guidance, Control and Dynamics, Vol. 12, No. 5, 1989, pp. 609-622.

6. Maine, R. E., and Iliff, K.W., "Identification of Dynamic Systems: - Application to Aircraft- part 1: Output Error Approach, " AGARD AG-300, Vol. 3, part 1, Dec. 1986.

7. Jategoankar, R. V., and Thielecke, F., "Evaluation of Parameter Estimation Methods for Unstable Aircraft," Journal of Aircraft, Vol. 31, No. 3, 1993, pp. 510-519.

8. Peter G Hamel and Jategaonkar, R. V , "The Evolution of Flight Vehicle System Identification," AGARD, DLR, Germany, 8-10, May, 1995

9 Doherr, K.F , Hamel, P , and Jategaonkar, R V , "Identification of Aerodynamic Model of the DLR research Aircraft ATTAS from Flight-Test Data," DLR, Sep 1990

10 Hornik, K , Stinchcombe, M , and White, H , "Multi Layer Feed Forward Networks are Universal Approximators," Neural Networks, Vol 2, No 5, 1989, pp 359-366.

11 Hess, R A , "On the Use of Back Propagation with Feed Forward Neural Networks for Aerodynamic Estimation Problem," AIAA Paper 93-3638, Aug. 1993

12 Linse, D. J., and Stengel, R. F., "Identification of Aerodynamic Coefficients Using Computational Neural Networks," Journal of Guidance, Control, and Dynamics, Vol. 16, No. 6, 1993, pp. 1018-1025.

13. Youseff, H. M., "Estimation of Aerodynamic Coefficients Using Neural Networks," AIAA Paper 93-3639, Aug. 1993.

14 Bassapa, and Jategaonkar, R. V., "Aspect of Feed Forward Neural Network Modeling and Its Application to Lateral-Directional Flight Data," DLR-IB 111-95/30, Braunschweig, Germany, Sept. 1995.

15. Raisinghani, S. C., Ghosh, A K., and Kalra, P. K., "Two New Techniques for Aircraft Parameter Estimation Using Neural Networks," The Aeronautical Journal, Vol. 102, No 1011, 1998, pp 25-29.

16 Raisinghani, S. C , Ghosh, A K and Kalra, P.K., "Aircraft Lateral-Directional Parameter Estimation via Neural Networks," Proceedings of 49th AGM, The Aeronautical Society of India, Jan. 16-17, 1998, pp. 6 1-6.7

17. Ghosh, A. K., Raisinghani, S. C , and Khubchandani, S., "Estimation of Aircraft Lateral-Directional Parameters Using Neural Networks," Journal of Aircraft, Vol. 35, No. 6, 1998, pp.876-881

18. Ghosh, A. K , "Aircraft Parameter Estimation From Flight Data Using Feed Forward Neural Networks," Ph. D. Thesis, IIT Kanpur, India, April 1998.

19. Khubchandani, S., "Estimation of Lateral-Directional Parameters from Flight Data Using Neural Networks, " M. Tech Thesis, IIT Kanpur, India, January 1997.

20. Chintala, S. R., "Effects of Measurement Errors on Parameter Estimation Via Neural Networks," M.Tech Thesis, IIT, Kanpur,India,December 1998.

21 Mehra, R. K., "Optimal Inputs For Linear System Identification," IEEE Transactions on Automatic Control, June 1974.

22 Mehra, R K., and Stepner, D E., "Optimal Inputs For Aircraft Parameters Identification," International Conference on Systems and Control, Coimbatore, India, August 1973

23 Gupta, N K and Halls, W E Jr , "Input design For Identification of Aircraft Stability and Control Coefficients," Technical Report, Systems Control, Inc, Palo Alto, California, March 1974

24 Roskam, J., "Methods for Estimating Stability and Control Derivatives for Conventional Subsonic Airplanes," Roskam Aviation and Engineering Corporation, 1973.

25 Saraswathi, L and Prabhu, M., "Estimation of Stability and Control Derivatives From Flight Data of Kiran Aircraft," NAL Report No: PD-FC-9706, India, Nov. 1997.

26. Meinsky, M. L. and Papert, S. A , "Perceptron, " MIT Press, Cambride, M A, 1969.

27. Haykins, S., "Neural Networks - A Comprehensive Foundation," McMaster University, Macmillan College Publishing Company, New York, 1994.

28 Hopfield, J J , "Neural Networks and Physical Systems with Emergent Collective Computational Abilities," Proceedings of the National Academy of Sciences, Vol 79, 1982, pp. 2254-2558

APPENDIX 'A'

FEED FORWARD NEURAL NETWORK

Artificial Neural Network can be described as an attempt by researchers to mimic the functioning of the human brain Meinsky and Papert[26] carried out a rigorous analysis of the perceptron and pointed out certain limitations of neuron models, the publication of these results brought the research in this area to a halt. Later, the basic idea of back propagation propounded by Werbos[27], and work of Hopfield[28] revived interest in neural networks. Presently, research on neural network is being actively pursued in many disciplines, ranging from neurobiology and physiology to engineering sciences

An artificial neural network (ANN) has a parallel and distributed processing structure and consists of processing elements called neurons. These neurons are interconnected with weighted unidirectional connections. Each neuron is composed of multiple inputs, one output, local memory and activation function. The inputs carry the weighted output of the directly connected neurons. The incoming information of a neuron is processed by the associated activation function (such as a sigmoidal function). The output is then distributed to other neurons as inputs. A variety of ANN configurations has been developed. One of the most popular ANN configurations is the feed forward neural network (FFNN) shown in Fig A.1.

Typically, the FFNN is made up of source nodes that constitute the input layer, and one or more hidden layer, and an output layer. The input signal gets propagated through the network in a forward direction, on a layer by layer basis. Each node in the

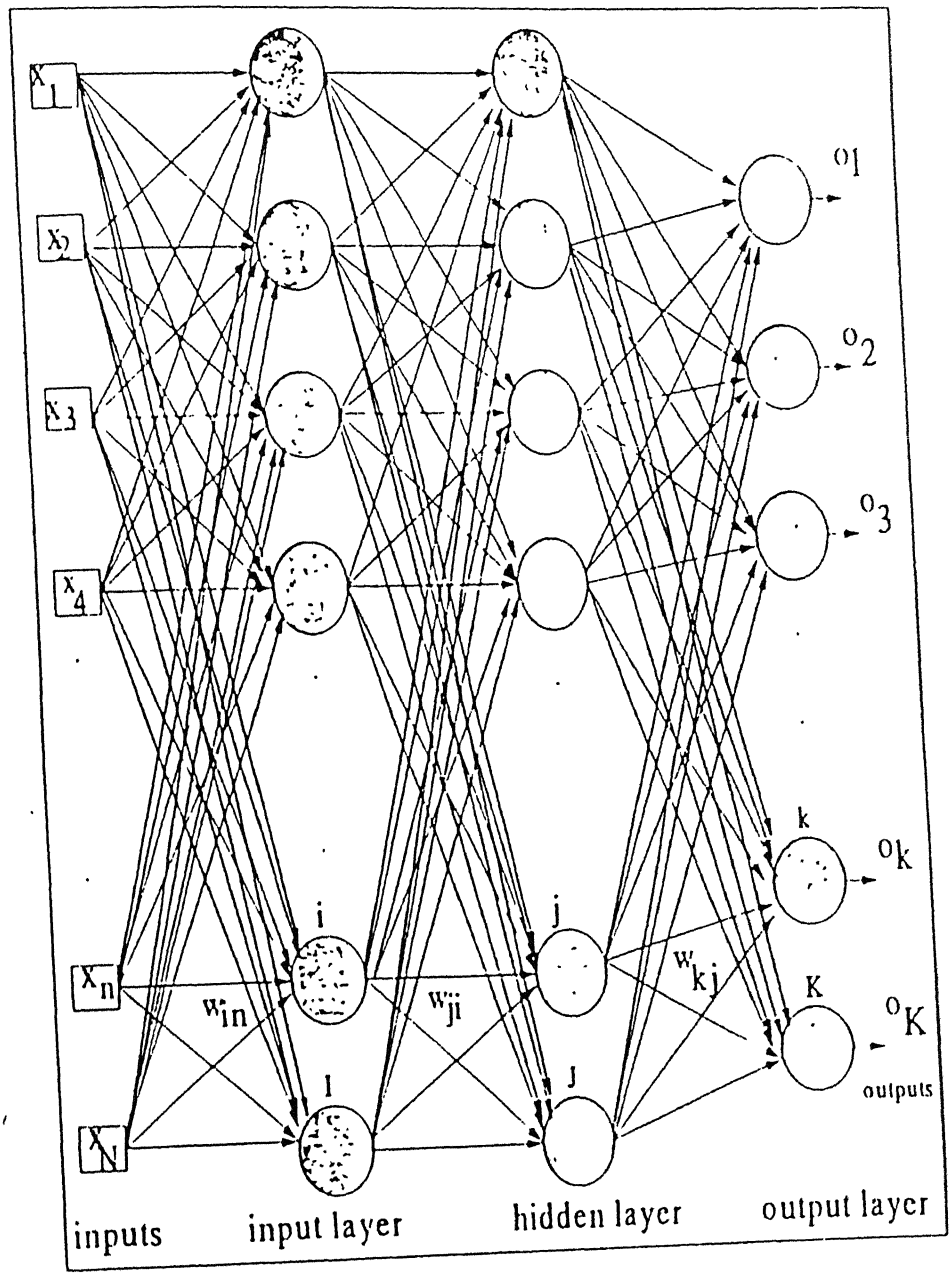

Fig. A.1 Schematic Representation of Feed Forward Neural Network

layer (input or hidden) is connected to each node in the next layer (either the hidden or the output) through the connective weight Every node in the input layer and the hidden layer is biased

A Feed Forward Neural Network has three distinct characteristics.

i) Each neuron performs aggregation of its input and this aggregated information is passed through the nonlinear activation function One of the most commonly used activation function, the sigmoidal (logistic) function is defined as

$$Y_i = \frac{1}{1+\exp(-x_1/\lambda)} \qquad \text{(A1)}$$

where x_i is the net internal activity level of neuron i, Y_i is the output of the neuron and λ is the logistic gain function

ii) The network contains one or more layers of hidden neurons that are not part of either the input or the output layer. These are not part of either the input or the output layer. These hidden neurons are primarily responsible for learning complex phenomena by progressively extracting more meaningful characteristics from the input pattern.

iii) The neurons in the architecture are progressively connected to the neurons of the next layers through connective weights. Although the model of the system to be approximated is, to a large extent, encoded in these weights, there is no direct relationship between the weights and parameters to the system to be modeled.

FFNNs have been applied successfully to model complex physical phenomena by training them in a supervised manner with a popular algorithm known as the back-propagation algorithm (BPA)[27]. The formulation of back-propagation algorithm provided a computationally efficient method for training of FFNN. Fundamentally, the BPA

consists of a forward and a backward pass through the different layers of the network. During the forward pass, the input vector is applied to the nodes of the network and its effect propagates through the network layer by layer The connective weights are all kept fixed during the forward pass On the other hand, in the backward pass, the weights are updated in accordance with the error correction rule Specifically, the actual response of the network is subtracted from the desired response to produce an error signal This error signal is then propagated backward against the direction of the connective weight-hence the name 'back-propagation algorithm'.

Back-propagation is a specific technique for implementing gradient descent in weight space for feed forward neural network In a practical application of back-propagation algorithm, learning is achieved from the many presentations of a specific training example to the FFNN. For a given training set, back-propagation learning may proceed in Pattern mode or Batch mode In pattern mode of back-propagation learning, the network weights are updated sequentially as the training data set is being presented Then the net weight change, averaged over the training set of pattern, is used to update the network weights. On the other hand, in the batch mode, weight updating is performed after presentation of all the training examples.

It may be pointed out that any back-propagation training algorithm is recursive in nature and it needs repetitive training sessions to achieve the required learning. There are many network parameters (also called the influence parameters or the tuning parameters) like the learning rate, the momentum constant, the number of hidden layers and the number of neurons in each of the hidden layers, number of iterations for which the training data is passed through the network, the logistic gain constant of the sigmoidal

function, etc that effect the accuracy of functional mapping between the input and the output variables

The most general network performance used is the "Mean Square Error (MSE)" function MSE measure the network's performance according to the mean of squared errors Thus MSE can be defined as

$$MSE = \frac{1}{m * n} \sum_{J=1}^{n} \sum_{i=1}^{m} [y_1(j) - x_1(j)]^2 \qquad (A\,2)$$

where y and x are respectively the desired (known) and the computed (predicted) outputs of the neural network, n is the number of data points, and m is the number of the output variables. If only one output variable is to be trained, then MSE is defined with m=1

APPENDIX B

MAXIMUM LIKELIHOOD METHOD (MLE)

In order to provide a comparative study for the efficacy and reliability of the FFNN method, the longitudinal parameters were also estimated using the conventional 'Maximum Likelihood Method' The programs were written in Matlab using the MLE algorithm The algorithm was derived as follows

Let a mathematical model of a system be represented by the following equations

$$\dot{X}(t_i) = AX(t_i) + BU(t_i) \qquad (B.1)$$

$$Z(t_1) = CX(t_i) + Gn_I \qquad (B\ 2)$$

where X is the state vector, U the control vector, Z the measured (observation) response and n_i is the noise vector respectively. The matrices A and B contain the unknown stability and control derivatives (parameters). If there is no state noise and the matrix G is known, then the maximum likelihood estimator minimizes the cost function,

$$J(\theta) = \frac{1}{2}\sum_{i=1}^{n}[Z(t_i) - \tilde{Z}_\theta(t_1)]^T (GG^T)^{-1}[Z(t_i) - \tilde{Z}_\theta(t_i)] \qquad (B.3)$$

where GG^T is the measurement noise covariance matrix and $\tilde{Z}_\theta(t_i)$ is the computed response estimate of Z at t_i for a given value of the unknown parameter vector θ. The cost function is a function of the difference between the measured and computed time histories In our case, we have taken $GG^T = 1$ for the cost function. To minimize the cost

function $J(\theta)$, we can apply the Newton-Raphson algorithm, which chooses successive estimates of the vector θ of unknown coefficients If k is the iteration number, then

$$\theta_{k+1} = \theta_k - [\nabla^2_\theta J(\hat{\theta}_k)]^{-1}[\nabla^T_\theta J(\hat{\theta}_k)] \qquad \text{(B 4)}$$

where the first gradient is defined by

$$\nabla_\theta J(\theta) = -\sum_{i=1}^{n}[Z(t_i) - \tilde{Z}_\theta(t_i)]^T (GG^T)^{-1}[\nabla_\theta \tilde{Z}_\theta(t_i)] \qquad \text{(B 5)}$$

and the second gradient is approximated by

$$\nabla^2_\theta J(\theta) = \sum_{i=1}^{n}[\nabla_\theta \tilde{Z}_\theta(t_i)]^T (GG^T)^{-1}[\nabla_\theta \tilde{Z}_\theta(t_i)] \qquad \text{(B 6)}$$

The matrix GG^T is approximated by a diagonal matrix, with the diagonal elements given by,

$$\sum_{i=1}^{n} \frac{[Z(t_i) - \tilde{Z}_\theta(t_i)]Z(t_i) - \tilde{Z}_\theta(t_i)]^T}{N}$$

where N is total number of data points. The term $\nabla_\theta \tilde{Z}_\theta(t_i)$ occurring in the first and the second gradients is evaluated by finite difference approximation for each of the sensitivity coefficients present in it. For example, to evaluate sensitivity coefficient $\frac{\partial \alpha}{\partial C_{mq}}$, the equations of motion are solved to obtain α for $C_{mq} + \Delta C_{mq}$ and $C_{mq} - \Delta C_{mq}$.

Let the respective values of α be α^+ and α^-, then we have

$$\frac{\partial \alpha}{\partial C_{mq}} = \frac{\alpha^+ - \alpha^-}{2\Delta C_{mq}}$$

The reliability of the estimated parameter in terms of the Cramer-Rao bounds is given by the square roots of the diagonal elements of $[\nabla^2_{\theta} J(\hat{\theta}_k)]^{-1}$, which is any way evaluated as part of the ML algorithm In the present work, for estimating the longitudinal parameters, the vector of unknown parameters is given by,

$$\theta = [C_{L\alpha}, C_{Lq}, C_{L\delta e}, C_{m\alpha}, C_{mq}, C_{m\delta e}]$$

with the $Z(t_i)$ and $\tilde{Z}_{\theta}(t_1)$ responses being α and qc/2u, while the control vector has δe as the input

133031

Date Slip

The book is to be returne
the date last stamped.